Handling Uncertainty with Application to Indoor Climate Control and Resource Allocation Planning

ALESSANDRA PARISIO

PhD in Information Engineering
Department of Engineering

UNIVERSITY OF SANNIO
Benevento, Italy 2009

Alessandra Parisio

Department of Engineering

University of Sannio, Benevento

July 2009

To my father Vincenzo.
In memoriam.

Sommario

La presente tesi ha per argomento il controllo stocastico, ossia il controllo di sistemi il cui stato é rappresentato da un processo stocastico. La questione fondamentale nel controllo stocastico é come incorporare l'incertezza nell'azione di controllo, quindi come *modellare* l'incertezza. Diversi approcci sono possibili, le cui prestazioni dipendono principalmente dalla specifica applicazione. In particolare, la tesi affronta due approcci molto promettenti nella gestione di eventi incerti nei problemi di controllo: l'approccio *stocastico* e l'approccio *robusto*. Entrambe le metodologie sono illustrate attraverso un'applicazione industriale. L'approccio robusto é applicato al problema del controllo dei livelli di scorta. Le quantitá immagazzinate nei buffer sono utilizzate per soddisfare una domanda esterna ed incerta, di cui non si conosce la distribuzione stocastica. La domanda é assunta non nota ma limitata da vincoli predefiniti. L'obiettivo che ci si pone é quindi trovare la politica di controllo ed i livelli di scorta iniziali tali che la domanda sia sempre soddisfatta. A tal fine é stata utilizzata la *Robust Invariant Set Theory*, una specifica teoria ampliamente usata nel controllo robusto. Il metodo di controllo proposto é applicato ad un impianto di produzione che si trova nel Sud Italia: i risultati di simulazione ne mostrano l'efficacia e l'affidabilitá. L'approccio stocastico é invece applicato al problema della climatizzazione degli edifici. L'obiettivo che ci si pone é lo sviluppo di strategie di controllo predittive al fine di una piú efficiente ed economica climatizzazione mantenendo alti livelli di comfort per gli occupanti. I disturbi sono principalmente le condizioni meteorologiche e gli occupanti l'edificio. Le incertezze sono modellate in maniera stocastica: la probabilitá di distribuzione dei disturbi puó essere approssimata ragionevolmente con una distribuzione normale e quindi identificata. Un caso di studio significativo é scelto per condurre l'analisi delle prestazioni del controllo via simulazione. Diverse strategie di controllo predittive basate sul modello dell'edificio sono confrontate, anche con un controllore industriale: i risultati di simulazione dimostrano l'efficacia e la flessibilitá del metodo di controllo proposto.

Parole chiave: Controllo predittivo basato su modello in ambito stocastico, controllo robusto, controllo ad orizzonte recessivo, controllo climatico abitativo, teoria degli insiemi robusti invarianti.

Resume

The thesis focuses on the stochastic control, i.e. control of systems involving uncertainty and whose states are represented by a stochastic process. The basic idea in stochastic control is how to incorporate uncertainty in the control action, i.e. how to *model* it. Several approaches are applicable, whose performances mainly depend on the specific application. In particular, the thesis deals with two attractive approaches to handling uncertainty in the control problem: the *stochastic approach* and the *robust approach*. Both these methods are illustrated through an industrial application. The robust approach is applied to classical problem of multistorage system control. An external uncertain demand is satisfied by using items stored in buffers. The demand, whose probability distribution is unknown, is assumed to be unknown but bounded inside given constraint sets. The *Robust Invariant Set Theory*, a specific theory broadly used in robust control, is exploited to find a control law and the initial buffer levels guaranteeing that an unknown bounded demand is always satisfied. The proposed control method is applied to a manufacturing plant located in South Italy: simulation results prove its efficacy and the reliability.
The stochastic approach is employed in the building climate control. The goal is to develop predictive control strategies to save energy in indoor climate control while maintaining high user comfort. The disturbances mainly consist of the weather and the people occupying the building. Uncertainties are modeled in a stochastic fashion: the disturbances probability distribution can be approximated well as a normal distribution and then identified. One industrial relevant case study was selected to carry out an in-depth simulation analysis of control performances. Several predictive control strategies based on the building model were compared, to an industry-standard controller as well: simulation results prove the efficacy and the tunability of the proposed control method.

Keywords: Stochastic Model Predictive Control, Robust Control, Receding Hori-

zon Control, Building Climate Control, Robust Invariant Set Theory.

List of publications

Journal Papers

[1] F. Borrelli, C. Del Vecchio and A. Parisio, "Robust Invariant Sets for Constrained Storage Systems", accepted as Brief Paper for *Automatica*, October 2009.

Conference Papers

[1] D. Gyalistras, A. Fischlin, M. Morari, C. Jones, F. Oldewurtel, A. Parisio, T. Frank, S. Carl, V. Dorer, B. Lehmann, K. Wirth, P. Steiner, F. Schubiger, V. Stauch, J. Tödtli, C. Gähler, M. Gwerder , "Saving Energy by Improved Building Control", *Abstracts Book of the Annual Meeting of The Alliance for Global Sustainability: Urban Futures: the Challenge of Sustainability*, January 2009.

[2] F. Borrelli, C. Del Vecchio and A. Parisio, "Robust Invariant Set Theory Applied to Buffer-Level Control in Manufacturing Systems", *47th IEEE Conference on Decision and Control*, December 2008.

[3] O. Barbarisi, C. Del Vecchio and A. Parisio, "Hybrid Model for Crane Scheduling", *17th IFAC World Congress*, July 2008.

[4] O. Barbarisi, C. Del Vecchio and A. Parisio, "Crane Control with Time-Based and Position Constraints", 46th IEEE Conference on Decision and Control, December 2007.

[5] O. Barbarisi, C. Del Vecchio and A. Parisio, "Multiple Crane Control with Tasks Deadlines and Priority Constraints", *European Control Conference*, July 2007.

[6] O. Barbarisi, C. Del Vecchio, G. Palmieri and A. Parisio, "A Software Simulator For Manufacturing Plant", *International Industrial Simulation Conference*, June 2007.

Preface

The thesis focuses on stochastic control, i.e. control of systems whose states are represented by a stochastic process. The control problem is naturally uncertain: in most of the industrial applications some of the agents acting on the system are not known, at best we have a probabilistic model of the expected outcomes of their actions. It is then desirable to reduce disturbance effects and provide robustness to the control action without increasing in complexity. Handle uncertainty and robustness have been a central theme in the development of the field of automatic control. The most common approach adopted in industry so far is simply to take the nominal behavior of uncertainty, the so-called "*certainty equivalence*" approach; it can work well in some cases, but in general it does not make the control strategy aware that the system dynamics can deviate from the nominal ones. To derive more efficient and robust control policies the uncertainty has to be incorporated in the controller, that is "*model uncertainty*". In general uncertain events are incorporated as random variables and modeled as stochastic processes: one can develop an approximate model of uncertainty and assume that the uncertain data come from this known model. Thus the uncertain probability distribution has to be identified. By doing so a *stochastic approach* to the control problem is adopted. However, when upper and lower bounds for uncertainties can be inferred from historical data or decision makers' experience more easily and with more confidence than empirical probability distributions for the same quantities, it would be preferable to adopt a deterministic approach to make a controlled system robust against uncertain events: the uncertainty is assumed to have a known range of allowed values, but no knowledge is given on which allowed values will actually be taken. This approach is referred as *robust or worst case approach*. All decisions are made accounting for the worst disturbance outcome in order to have good control performances for any disturbance realization. Clearly this can lead to an unnecessarily conservative and then expensive control action, while the stochastic approach leads to less conservative control actions. However in general stochastic

control problem is intractable to solve and requires a great amount of memory and computation time, while the robust control problem is usually tractable and less computationally demanding the the stochastic control problem. Nevertheless there are some stochastic control problems that can be solved efficiently, such as the control of systems with gaussian disturbances and quadratic criteria (LQG). As a conclusion, both the illustrated control methods have advantages and disadvantages. Which approach to apply and how to model uncertainty mainly depends on the specific application. In this thesis a stochastic control problem has been solved in indoor climate control while the robust approach has been applied to multistorage system control. In details, the following activities have been conducted during the PhD course:

- **numerical computation of robust invariant sets for multistorage systems.** Multistorage systems with control and state constraints dealing with unknown demand have been studied. Exploiting a theory broadly applied in robust control (*Robust Invariant Set Theory*) and two Matlab toolboxes (MultiParametric and InvSetBox), two kind of sets have been computed: *robust invariant sets* and *robust control invariant sets*. These sets contain the states whose trajectory will never violate the system constraints: to compute the robust invariant set a feedback control law has to be provided hence the autonomous system is considered. To compute the robust control invariant set the non-autonomous system is employed. The robust invariant sets have been computed for two commonly adopted feedback policies;

- **providing the closed form of robust invariant sets for multistorage systems.** Starting from the numerical results obtained in the previous activity and exploiting a well known algorithm, the closed form of the *robust invariant set* and of the *robust control invariant set* for the investigated system and for any system size has been provided. The obtained results allow to compute the invariant sets without resorting to any numerical computation, which could be intractable. The computed invariant sets permit to derive buffer conditions to be satisfied in order to prevent stockouts;

- **developing predictive control strategies for indoor climate control.** A stochastic model-based predictive (*Stochastic MPC*) approach has been investigated for indoor climate control that takes into account weather predictions. The control aims at increasing energy efficiency while respecting constraints resulting from desired occupant comfort. Exploiting methods and results avail-

able in literature, the stochastic control problem has been formulated, then made tractable and solved by standard solvers for linear, quadratic and conic optimization. Several approximations to speed up the optimization routine have been developed and compared.

The first two activities have been conducted at the Department of Engineering, University of Sannio in Benevento. We would gratefully acknowledge Prof. Francesco Borrelli for his essential and important contribution to the work on the robust control of multistorage systems.

The last activity have been conducted at the Automatic Control Laboratory, Swiss Federal Institute of Technology, Zürich, as part of *OptiControl* project, which aims at developing predictive control strategies to save energy in indoor climate control while maintaining high user comfort. The authors gratefully acknowledge the contributions of the OptiControl project participants, which consists of members from Siemens Building Technologies, the Building Technologies Laboratory of EMPA Dübendorf, the Federal Institute for Meterology and Climatology MeteoSwiss and the Systems Ecology Group of ETH Zurich. Swisselectric, CCEM-CH and Siemens Building Technologies are acknowledged for their financial support of the OptiControl project. In particular the authors would like to gratefully thank Prof. Manfred Morari for allowing us to visit his group at ETH in Zürich and for invaluable comments and suggestions on the results presented in this work. These visits have allowed us to establish a great working relationship with the group. In particular, we would like to deeply thank Dr. Colin Jones and Ing. Frauke Oldewurtel for sharing their knowledge and their work with us.

Finally, we would gratefully acknowledge the important role played by our tutor, Prof. Luigi Glielmo, and co-tutor, Ing. Carmen Del Vecchio for their fundamental contribution and support to our work during the PhD activities.

The organization of the thesis is the following

- chapter 1 deals with the classical problem of buffer level control. An external demand is satisfied by using items stored in buffers. The control target is to guarantee that buffers have always enough stocks to satisfy the demand. Uncertainty is modeled in a nonstochastic fashion: the demand is assumed to be unknown but bounded inside given constraint sets. These unknown-but-bounded specifications for uncertainties are quite realistic in several situations. Upper and lower bounds for production and demand can be inferred from historical data or decision makers' experience. The proposed approach has been applied to a manufacturing plant located in South Italy to show its performances;

- chapter 2 deals with the building climate control. The goal is to develop predictive control strategies to save energy in indoor climate control while maintaining high user comfort. The disturbances mainly consist of the external environment or weather and the people occupying the building. Uncertainties are modeled in a stochastic fashion: statistical analysis have shown that the disturbances probability distribution can be well approximated as a normal distribution and identified. The corresponding stochastic control problem is efficiently solved exploiting standard solvers. Several predictive control strategies based on the building model are compared to both an ideal controller and an industry-standard controller to show the performances of the proposed control method.

Contents

Chapter 1

Robust Control for Constrained Multistorage Systems

Multistorage systems represent a very important class of systems which model many real processes such as flexible manufacturing systems, communication networks, and transport systems. These dynamical systems represent processes that produce and/or transfer goods, possibly storing them temporarily in safety stocks (buffers) which supply an external demand. The final goal of a multistorage system is to satisfying any admissible demand by possibly minimizing some operational costs, such as the stocking cost. Unfortunately, many real systems work in uncertain and varying conditions. The demand is often unknown, then a stochastic process should be employed for modeling it. However the this requires stochastic information which can be unavailable. A more realistic and confident approach than building an empirical probability distributions for the uncertain quantities can be to assume a known range of allowed values for demand and production, which can be inferred from historical data or decision maker experience. Thus the uncertainties are modeled in a nonstochastic fashion by assuming them unknown but bounded inside given constraint sets. This leads to adopt a robust approach to the control problem investigated in our work. The classical problem of buffer level control is then addressed by means of robust invariant set theory for linear and switched linear systems: the target is to determine

production scheduling and item levels to be stored in buffer guaranteeing that an unknown bounded demand is always satisfied. We consider a manufacturer produces several items stored into n buffers. The external demand for items is continually supplied through stored items (make-to-stock manufacturing system). A simple model with n decoupled integrators and n additive bounded disturbances is employed. The dynamic coupling arises from bounded total production capacity and bounded total demand. Invariant set theory for linear and switched linear systems is exploited to compute robust positive invariant sets and controlled robust invariant sets for two commonly used scheduling policies. The explicit expression of the invariant sets for any arbitrary n is provided. The integrator model is further extended in order to take into account different type of constraints, setup costs and changeover times. How to use hybrid systems formalism in order to compute the corresponding robust invariant sets is part of future investigations.

1.1 Introduction

We consider multistorage systems with control and state constraints dealing with unknown demand. A manufacturer produces several items which are kept in safety stocks in order to supply an external unknown demand. Production is make-to-stock, i.e., a demand is satisfied by using items in stock while triggering a stock replenishment order. This model is generic and it corresponds to several implementations such as: *(i)* the items are distinct components assembled into a single product at a single facility (in this case, buffers connect the production line of intermediate products with the assembly line of final products), *(ii)* the items are distinct products produced at a single facility and supplying distinct demands, *(iii)* the items represent the same product manufactured and distributed at different locations, *(iv)* the items represent the same product and distinct buffers are kept for high-priority and low-priority customers. In this chapter the general term "item typology" is adopted with the following interpretation: item i is kept in the buffer x_i and has and associated demand d_i. The buffer level x_i can be increased by producing u_i and the demand d_i can be satisfied if $x_i \geq d_i$. An example of the first implementation is depicted in Figure 1.1 [31]. This kind of models are used in different contexts, such as manufac-

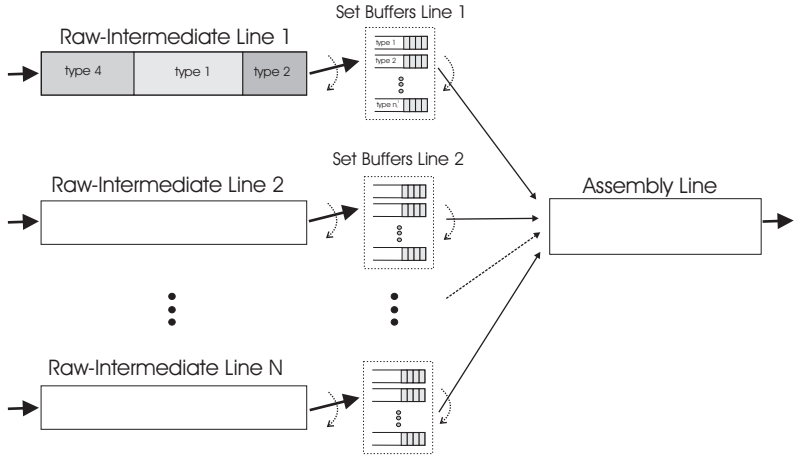

Figure 1.1: Scheme of a two-stages multiproduct batch production plant.

turing, network routing communications, logistic and traffic control, the minimization of transportation and stocking costs [11, 21, 22, 45, 69, 84, 98, 100]. For instance $x_i(t)$ can represent the energy stored at time t in the i-th battery charged by $u_i(t)$ while serving a time-varying load $d_i(t)$. Other typical applications of this kind of systems

concerns both the minimization of transportation and stocking costs [103] and the supply contract for the repeated delivery, on a long time horizon, of a given quantity of a certain commodity [109]. An appropriate inventory level has to be maintained at the delivery points at each time in order to face any demand. As the demand is usually unknown, stochastic methods has been applied to solve this kind of problems, often based on dynamic programming [21, 98, 100]. This approach requires the knowledge of stochastic information which might be not available. In this case, a worst-case approach can be used modeling the uncertainties in a different way [28–30]. The demand is assumed to be unknown-but-bounded and upper and lower bounds for production and demand are assigned (usually out of historical data as well explicitly stipulated in supply contracts). In conclusion we considered a worst case approach to the control of multistorage systems in the presence of storage and production capacity hard constraints and uncertain demand. Although our results apply to larger classes of storage systems, the language used in the chapter is typical of manufacturing process and two commonly adopted production control laws are investigated. The case study presented in the section 1.9 is also related to a manufacturing system.

1.1.1 Literature Review

A classical control problem consists of scheduling the production of each item typology in order to guarantee that buffers have enough stocks to satisfy the demand (i.e. stockout never occurs) [24, 57, 95, 113]. The buffer levels are subject to hard constraints [28–30]. Over the last decades this problem has been studied from many different angles. Computing an optimal *dynamic scheduling policy* (i.e. a policy which takes into account the current state of inventory levels before deciding which item should be produced next) is not an easy task: it requires to choice of three unknowns: which item to produce, when to start the production and for how long. Starting from a preliminary study of Zheng and Zipkin [115], in [65] the author provides the explicit form of the optimal scheduling policy for two item typologies requiring identical production times. De Vericourt and coauthors in [113] generalized the results in [65] when the two item typologies require different production times. The authors also explicitly noticed the difficulties of generalizing the results to more than two item typologies. Further extensions to the results in [113] can be found in [43] and references therein. The authors in [24, 57, 95] study the case of multiple item typologies by focusing on fixed scheduling sequence. Independently from the adopted scheduling policy, the stockouts are typically modeled either as lost demand, thus constraining bufferlevels to assume positive values, or by backordering demand and allowing bufferlevels to

take negative values corresponding to the unmet demand. In both cases the stock-out risk is *minimized* by introducing a buffershortage cost. Moreover, the scheduling policies proposed in the aforementioned works are independent on initial buffer levels and could lead to stockouts even under nominal operation. In presence of uncertain inputs, a state feedback strategy can make the system more robust.

1.2 Model and Problem Statement

A system with n buffers storing n item typologies is shown in in Figure 1.2. The

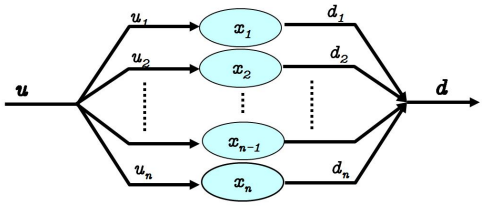

Figure 1.2: Set of Buffers. The $i-$th buffer has level x_i, outflow d_i and inflow u_i

scheme in 1.2 models also the two-stages multiproduct batch production plants depicted schematically in the Figure 1.1. The Figure 1.2 is presented here to point out the system variables $x_i(k)$, $u_i(k)$, $d_i(k)$ per each buffer type i. This kind of systems is modeled with n decoupled integrators and additive disturbances: $x_i(k+1) = x_i(k) + u_i(k) + d_i(k)$ where x_i is the level of buffer i, u_i the production rate of the i-th typology and $-d_i$ is its demand for $i = 1, \ldots, n$. Multiple item typologies can be produced during time instant k and $k+1$. This is possible by either having multiple production lines or switching the production of one line between different typologies during the sampling time. This work focuses on model (1.1)-(1.2) and studies the buffer conditions and the production laws such that for each product typology and at each time k there are items stored in the buffer sufficient o satisfy the demand (stockout never occurs). To gain insight in initial buffer level conditions we make use of robust invariant set theory [60, 73, 104] for linear and switched linear systems. The largest sets of initial buffer levels $x_i(0)$ is computed such that no-stockout ($x_i(k) \geq 0$ at all time instants k) is guaranteed for all admissible demands $d_i(k)$, $i = 1, \ldots, n$. Both the case of a generic admissible control law $u_i(k)$ (and thus compute "robust controlled invariant sets") and two specific production control laws $u_i(k) = f(x_1(k), \ldots, x_n(k))$ (and thus compute "robust invariant sets") is studied. The first production law is the *Replenish Lowest Buffer* (RLB) law: at each time instant k the system produces at the

maximum rate the item typology corresponding to the lowest buffer level. The second production law is the *Distribute Production Capacity* (DPC) law: at each time instant k the control policy starts producing the item typology with the lowest buffer level. The buffer will be filled up to the maximum demand value or up to the maximum buffer level reachable with the available production capacity. If there is a residual production capacity it will be used to replenish the second lowest buffer, and so on, until the maximum production capacity is reached or all buffers have been replenished at their maximum demand values. In RLB policies only one product typology can be produced at a time. In DPC policies more product typologies can be produced at the same time. Since the proposed control laws are piecewise linear functions, the use of hybrid system theory and tools is necessary to compute the corresponding robust invariant sets. The following discrete time model is considered

$$x(k+1) \quad = \quad x(k) + u(k) + d(k) \tag{1.1}$$

with the uniform sampling time equal to $\Delta T = t_{k+1} - t_k$. System (1.1) represents a set of n buffers where n types of items are stored. The state is $x(k) = [x_1(k), \ldots, x_n(k)] \in \mathbb{R}^n$ where $x_i(k)$ represents the level of the i-th buffer at time t_k, the positive input is $u(k) = [u_1(k), \ldots, u_n(k)] \in \mathbb{R}^n$ where $u_i(k)$ is the production rate for the i-th item typology during the sampling interval $[t_k, t_{k+1})$. The element wise negative vector $d(k) = [d_1(k), \ldots, d_n(k)] \in \mathbb{R}^n$ represents the external demand and $d_i(k)$ is the demand of the i-th typology in the sampling interval $[t_k, t_{k+1})$. A scaled model will be used, i.e., $x_i(k)$ denotes the number of products of type i stored at time instant k divided by ΔT and $u(k)$ and $d(k)$ represent production and demand rates, respectively, rather than absolute quantities. System (1.1) is subject to the following constraints for all $k \geq 0$:

$$x(k) \in \mathbb{X}^n \triangleq \{x \in \mathbb{R}^n \mid 0 \leq x_i \leq M_i \quad i = 1, \ldots, n\} \tag{1.2a}$$

$$u(k) \in \mathbb{U}^n \triangleq \{u \in \mathbb{R}^n \mid \sum_{i=1}^{n} u_i \leq P^{max}, \; 0 \leq u_i \leq p_i^{max} i = 1, \ldots, n\} \tag{1.2b}$$

$$d(k) \in \mathbb{W}^n \triangleq \{d \in \mathbb{R}^n \mid \sum_{i=1}^{n} d_i \geq -D^{max}, \; -d_i^{max} \leq d_i \leq 0 \quad i = 1, \ldots, n\} \tag{1.2c}$$

$$p_i^{max} \geq d_i^{max} \quad i = 1, \ldots, n. \tag{1.2d}$$

Constraint (1.2a) sets an upper-bound M_i to the maximum buffer capacity and it imposes that a stockout never occurs ($x_i \geq 0$), i.e. it guarantees that demand

is always satisfied. Constraint (1.2b) sets an upper-bound p_i^{max} to the production rate u_i of the i-th typology. Moreover, at any instant k the overall production can not exceed the maximum value P^{max} (which represents the maximum production capacity of the plant or machine). Constraint (1.2c) sets an upper-bound d_i^{max} to the demand $d(k)$ of the i-th typology. Moreover, at any instant k the overall demand can not exceed the maximum value D^{max}. Constraint (1.2d) guarantees that the plant production capacity for each item is greater than the maximum demand. The case $\sum_{i=1}^{n} p_i^{max} \geq P^{max} \geq D^{max} \geq 0$ is studied.

Remark 1 *In model (1.1) production and demand of all typologies at time k are synchronous. In case of one production line, switches between different typologies will occur during the sampling interval $[t_k, t_{k+1})$; these are not captured in the proposed model. Model (1.1)-(1.2) also does not include delays and setup times. Nevertheless, we will show that nonintuitive and interesting results can be obtained by studying the robust feasibility of model (1.1)-(1.2).*

For system (1.1) under constraints (1.2) and assumption (1.3), the problems we consider in our work can be stated as follows:

Problem 1 *Compute the largest set of initial buffer levels $x(0)$ such that for all admissible demands there exists a control law satisfying production constraints (1.2b) and buffer level constraints (1.2a). This set is the maximal control robust invariant set $\mathcal{C}_\infty$ (defined in Section 1.3). Hence, in this case, we are not interested in a specific production control law but we examine the initial buffer condition that guarantee that the system remain feasible for any demand. The set $\mathcal{C}_\infty$ is computed in Section 1.4.*

Problem 2 *Compute the largest set of initial buffer levels $x(0)$ such that for the RLB and DPC feedback policies, production constraints (1.2b) and buffer level constraints (1.2a) are satisfied for all admissible demands. This set is the maximal robust positive invariant set $\mathcal{O}_\infty$ for the closed loop system (defined in Section 1.3). The set $\mathcal{O}_\infty$ is computed in Section 1.5 for the RLB control law and in Section 1.5 for the DPC control law.*

Remark 2 *The first problem has been investigated in [28–30] for a larger class of multi-inventory dynamical systems. The results presented in [28–30] are more general than the one presented in Section 1.4. However, by focusing on the simpler system class (1.1), our approach allows to explicitly compute the maximal control robust invariant set $\mathcal{C}_\infty$ for arbitrary n.*

While computing the robust invariant sets described above is an interesting numerical exercise, we remark that the main contribution of this work is to provide the analytical expression for the invariant sets *for arbitrary* n. We also remark that the results of this work can be used in the design of control systems for constrained systems and applied to guaranteeing feasibility in model predictive control, since the constraints can be satisfied for all time if and only if the initial state is contained inside an invariant set.

Remark 3 *In push systems the buffer holds products waiting to be manufactured. Therefore the problem becomes the dual of the one presented in this section. The main feasibility condition consists in having each buffer level below a fixed constant and avoiding that the queue of products waiting to be manufactured grows to infinity [34, 55, 96]. The results presented in this work can be extended to push systems.*

Without loss of generality we first will assume that:

$$\begin{aligned} P^{max} &= 1 \\ D^{max} &= 1 \\ M_i &= M_j = M \quad i, j = 1, \ldots, n. \end{aligned} \tag{1.3}$$

In the Section 1.7, the simplifying assumption (1.3) is removed and system (1.1)–(1.2) is extended in order to take into account setup times. In this case, we show how to use hybrid systems formulation in order to numerically compute the corresponding robust invariant sets. In the next section a brief review on invariant set theory in provided.

1.3 Background on Robust Invariant Sets

This section has been extracted from [60, 73, 104] and provides the basic definitions and results for robust invariant sets for constrained linear systems. A comprehensive survey of papers on set invariance theory can be found in [27].
We will first introduce some basic concepts before defining the invariant sets that we wish to compute. We deal with two types of systems, namely, autonomous systems:

$$x(k+1) = f_a(x(k), w(k)), \tag{1.4}$$

and systems subject to external inputs:

$$x(k+1) = f(x(k), u(k), w(k)). \tag{1.5}$$

We will assume the origin is an equilibrium for both systems and that both systems are subject to disturbance $w(k)$ and to the constraints:

$$x(k) \in \mathbb{X},\ u(k) \in \mathbb{U},\ w(k) \in \mathbb{W}\ \forall\ k \geq 0. \tag{1.6}$$

The sets $\mathbb{X}$ and $\mathbb{U}$ and $\mathbb{W}$ are polyhedra and contain the origin in their interior. Two different types of sets are being considered: *invariant sets* and *control invariant sets*. We will first discuss invariant sets. The invariant sets are computed for autonomous systems. These types of sets are useful to answer questions such as: "For a *given* feedback controller $u = k(x)$, find the set of states whose trajectory will never violate the system constraints". The following definitions are derived from [20, 23, 27, 73, 75].

Definition 1 (Robust Positive Invariant Set) *A set $\mathcal{O}$ is said to be a robust positive invariant set for the autonomous system in* (A.2) *if*

$$x(0) \in \mathcal{O} \quad \Rightarrow \quad x(t) \in \mathcal{O}, \quad \forall w(t) \in \mathbb{W} \text{ and } \forall t \in \mathbb{N}^+$$

The set $\mathcal{O}_\infty$ is a maximal *robust positive invariant set if $0 \in \mathcal{O}_\infty$, $\mathcal{O}_\infty$ is robust positive invariant and $\mathcal{O}_\infty$ contains all robust positive invariant sets that contain the origin.*

Control invariant sets are defined for systems subject to external inputs. These types of sets are useful to answer questions such as: "Find the set of states for which *there exists* a controller such that the system constraints are never violated". The following definitions are derived from [20, 23, 27, 73, 75].

Definition 2 (Robust Control Invariant Set) *A set $\mathcal{C} \subseteq \mathbb{X}$ is said to be a robust control invariant set for system* (A.3) *if for every*

$$x(k) \in \mathcal{C}\ \Rightarrow \exists u(k) \in \mathbb{U} |\ f(x(k), u(k), w(k)) \subseteq \mathcal{C} \quad \forall w(k) \in \mathbb{W}$$

The set $\mathcal{C}_\infty$ is said to be the maximal *robust control invariant if it is robust control invariant and contains all robust control invariant sets contained in $\mathbb{X}$.*

The following algorithm provides a procedure for computing the maximal robust control invariant subset if system (A.3) is considered or the maximal positive invariant subset if system (A.2) is considered [13, 20, 73]. We first need the following definition. The set

$$\mathrm{Pre}_f(\mathcal{S}, \mathbb{W}) \triangleq \{x \in \mathbb{X} \mid \exists u \in \mathbb{U} \text{ s.t. } f(x, u, w) \subseteq \mathcal{S}\ \forall\ w \in \mathbb{W}\} \tag{1.7}$$

defines the set of system (A.3) states which can be robustly driven into the target set $\mathcal{S}$ in one time step. Similarly, for the autonomous system (A.2), we use $\mathrm{Pre}_{f_a}(\mathcal{S})$ to denote the set of the states that robustly evolves to $\mathcal{S} \subseteq \mathbb{X}^0$ in one step:

$$\mathrm{Pre}_{f_a}(\mathcal{S}, \mathbb{W}) \triangleq \{x \in \mathbb{X}^0 \mid f_a(x, w) \in \mathcal{S},\ \forall w \in \mathbb{W}\}. \tag{1.8}$$

Algorithm 1.3.1 (Computation of $\mathcal{C}_\infty$ ($\mathcal{O}_\infty$))

1. $\Omega_0 = \mathbb{X}$
2. $\Omega_{k+1} = \mathrm{Pre}_f(\Omega_k, \mathbb{W})$ *(*$\Omega_{k+1} = \mathrm{Pre}_{f_a}(\Omega_k, \mathbb{W})$*)*
3. *If* $\Omega_{k+1} = \Omega_k$ *then* $\mathcal{C}_\infty \leftarrow \Omega_{k+1}$ *(*$\mathcal{O}_\infty \leftarrow \Omega_{k+1}$*) return; Else, set* $k = k + 1$ *and goto 2.*

Algorithm 1.3.1 generates the set sequence $\{\Omega_k\}$ satisfying $\Omega_{k+1} \subseteq \Omega_k, \forall k \in \mathbb{N}$ and it terminates if $\Omega_{k+1} = \Omega_k$ so that Ω_k is the maximal robust positive invariant set $\mathcal{O}_\infty$ if system (A.2) is considered or Ω_k is the maximal robust control invariant set $\mathcal{C}_\infty$ if system (A.3) is considered. We refer the reader to [13, 20, 73] for details on the finite time termination of Algorithm 1.3.1. For practical implementation of Algorithm 1.3.1, it is necessary to develop a procedure for computing the one-step set $\mathrm{Pre}_f(\Omega_k, \mathbb{W})$. Given two sets $\Omega \subset \mathbb{R}^n$ and $\Phi \subset \mathbb{R}^n$, the Pontryagin difference $\Omega \sim \Phi$ and the Minkowski sum $\Omega \oplus \Phi$ are two set-theoretic concepts, which are useful in developing such algorithm. We refer the reader to [60, 73] for their definitions. The Pontryagin difference can be computed for polytopes by solving a sequence of LPs [75] as follows. Define the $\mathcal{P}$ and $\mathcal{Q}$ as

$$\mathcal{P} = \{y \in \mathbb{R}^n \mid P^y y \leq P^b\}, \quad \mathcal{Q} = \{z \in \mathbb{R}^n \mid Q^z z \leq Q^b\}, \tag{1.9}$$

then

$$\mathcal{W} = \mathcal{P} \ominus \mathcal{Q} \tag{1.10a}$$

$$= \{x \in \mathbb{R}^n \mid P^y x \leq P^b - H(P^y, \mathcal{Q})\} \tag{1.10b}$$

where the i-th element of $H(P^y, \mathcal{Q})$ is

$$H_i(P^y, \mathcal{Q}) \triangleq \max_{x \in \mathcal{Q}} P_i^y x \tag{1.11}$$

and P_i^y is the i-th row of the matrix P^y. The implementation of the Minkowski sum via projection will be used in this work and is described below. Consider the two

polyhedra $\mathcal{P}$ and $\mathcal{Q}$, then

$$\begin{aligned} W &= P \oplus Q \\ &= \left\{ x \in \mathbb{R}^n \mid x = y + z,\ P^y y \leq P^b,\ Q^z z \leq Q^b,\ y, z \in \mathbb{R}^n \right\} \\ &= \left\{ x \in \mathbb{R}^n \mid \exists y \in \mathbb{R}^n,\ \text{subj. to } P^y y \leq P^b,\ Q^z (x - y) \leq Q^b \right\} \\ &= \left\{ x \in \mathbb{R}^n \mid \exists y \in \mathbb{R}^n,\ \text{subj. to } \begin{bmatrix} 0 & P^y \\ Q^z & -Q^z \end{bmatrix} \begin{bmatrix} x \\ y \end{bmatrix} \leq \begin{bmatrix} P^b \\ Q^b \end{bmatrix} \right\} \\ &= \text{Proj}_x \left(\left\{ [x^T y^T] \in \mathbb{R}^{n+n} \mid \begin{bmatrix} 0 & P^y \\ Q^z & -Q^z \end{bmatrix} \begin{bmatrix} x \\ y \end{bmatrix} \leq \begin{bmatrix} P^b \\ Q^b \end{bmatrix} \right\} \right). \end{aligned} \tag{1.12}$$

where $\text{Proj}_x(\mathcal{X})$ denotes the projection of the set $\mathcal{X}$ on the x space. By using the elementary operations above one can compute the one-step set $\text{Pre}_f(\Omega_k, \mathbb{W})$ and $\text{Pre}_{f_a}(\Omega_k, \mathbb{W})$ for linear systems as follows. Assume system (A.3) to be linear, i.e., $x(k+1) = Ax(k) + Bu(k) + w(k)$. Then, the one-step robust set can be immediately computed by first computing the Pontryagin difference $\Omega \ominus \mathbb{W}$ and then the Minkowski sum as follows:

$$\text{Pre}_f(\Omega, \mathbb{W}) = A^{-1}((\Omega \ominus \mathbb{W}) \oplus (-B\mathbb{U})) \tag{1.13}$$

Algorithm 1.3.1 is also used to compute the maximal robust positive invariant set $\mathcal{O}_\infty$ for the system (A.2): it generates the set sequence $\{\Omega_k\}$ satisfying $\Omega_{k+1} \subseteq \Omega_k, \forall k \in \mathbb{N}$ and it terminates if $\Omega_{k+1} = \Omega_k$ so that Ω_k is the maximal robust positive invariant set $\mathcal{O}_\infty$ for the autonomous PWA system. Then the one-step set $\text{Pre}_{f_a}(\Omega_k, \mathbb{W})$ has to be computed for implementing the Algorithm 1.3.1. In the Appendix A a brief review of invariant sets and the computation of $\text{Pre}_{f_a}(\Omega_k, \mathbb{W})$ for piecewise affine systems is provided. We point out that the computation of $\text{Pre}_{f_a}(\Omega_k, \mathbb{W})$ when applied in Algorithm 1.3.1 for PWA systems can explode computationally.

1.4 Computation of the Maximal Robust Control Invariant Set

In this section the Problem 1 is studied. The objective is to compute the maximal robust control invariant set for system (1.1) subject to constraints (1.2)-(1.3) for arbitrary n. We denote by I^n the identity matrix of dimension n, by $\mathbf{0^n}$ a zeros column vector of dimension n and by $\mathbf{1^n}$ a ones column vector of dimension n. Given two n-dimensional vectors $\mathbf{u} = [u_1, \ldots, u_n]$ and $\mathbf{v} = [v_1, \ldots, v_n]$, we denote by $\text{HR}(\mathbf{u}, \mathbf{v})$ the set $\text{HR}(\mathbf{u}, \mathbf{v}) = \{x \in \mathbb{R}^n \mid u_i \leq x_i \leq v_i \ \ i = 1, \ldots, n\}$. Given the set $L^n = \{1, 2, \ldots, n\}$ we denote by $\text{group}(f, n)$ the set composed of all the subsets $L^n_{f,i}$ of L^n of dimension

f: group$(f,n) = \left\{L^n_{f,1}, \ldots, L^n_{f,n_f}\right\}$ with $n_f = \begin{pmatrix} n \\ f \end{pmatrix}$. As an example group$(2,3) = \{\{1,2\},\{1,3\},\{2,3\}\}$ and $L^3_{2,1} = \{1,2\}$. The following theorem provides the explicit form of the maximal robust control invariant set for arbitrary n.

Theorem 1 *The maximal robust control invariant set $\mathcal{C}_\infty$ for system (1.1) subject to constraints (1.2) is*

$$\begin{array}{l} \mathcal{C}_\infty = \{x \in \mathbb{R}^n | 0 \le x_i \le M,\ i = 1, \ldots, n, \\ \sum_{j \in L^n_{f,i}} x_j \ge \ \sum_{j \in L^n_{f,i}} d^{max}_j - 1, L^n_{f,i} \in \mathit{group}(f,n), \\ i = 1, \ldots, n_f, \quad f = 2, \ldots, n\} \end{array} \tag{1.14}$$

*Proof:*We follow the Algorithm 1.3.1 for computing $\mathcal{C}_\infty$.

- Step 0. $\Omega_0 = \mathrm{HR}(\mathbf{0}, \mathbf{M})$
- Step 1. $\Omega_0 \ominus \mathbb{W} = \mathrm{HR}(\mathbf{d^{max}}, \mathbf{M})$. $\Omega_1 = \mathrm{Pre}(\Omega_0, \mathbb{W}^n) = A^{-1}((\Omega_0 \ominus I^n\mathbb{W}^n) \oplus (-I^n\mathbb{U}^n)) = \mathrm{HR}(\mathbf{d^{max}}, \mathbf{M}) \oplus (-\mathbb{U}^n)$. By using equation (1.12) Ω_1 can be computed as follows

$$\mathcal{M} = \left\{ [x^{nT}\ y^{nT}] \in \mathbb{R}^{2n} \mid \begin{bmatrix} 0 & I^n \\ 0 & -I^n \\ I^n & -I^n \\ -\mathbf{1}^{nT} & \mathbf{1}^{nT} \\ -I^n & I^n \end{bmatrix} \begin{bmatrix} x \\ y \end{bmatrix} \le \begin{bmatrix} M\mathbf{1}^n \\ -d^{max} \\ \mathbf{0}^n \\ P^{max} \\ p^{max} \end{bmatrix} \right\} \tag{1.15}$$

$$\Omega_1 = \mathrm{Proj}_{x^n}\left(\mathcal{M}\right).$$

where $p^{max} = [p^{max}_1(k), \ldots, p^{max}_n(k)] \in \mathbb{R}^n$ By using Fourier-Motzkin procedure (see [73]), it can be proven by direct computation that the projection in (1.15) can be written as:

$$\begin{array}{l} \Omega_1 = \{x^n \in \mathbb{R}^n \mid x_i \le M,\ i = 1, \ldots, n, \\ \qquad \sum_{j \in L^n_{f,i}} x_j \ge \ \sum_{j \in L^n_{f,i}} d^{max}_j - P^{max}, \\ \qquad L^n_{f,i} \in \mathrm{group}(f,n), i = 1, \ldots, n_f, \quad f = 1, \ldots, n\} \end{array} \tag{1.16}$$

- Step 2. By using (1.10) and (1.11), then

$$\begin{array}{l} \Omega_1 \ominus \mathbb{W}^n = \{x^n \in \mathbb{R}^n \mid x_i \le M,\ i = 1, \ldots, n, \\ \sum_{j \in L^n_{f,i}} x_j \ge \ \sum_{j \in L^n_{f,i}} d^{max}_j, \\ L^n_{f,i} \in \mathrm{group}(f,n), i = 1, \ldots, n_f, \quad f = 1, \ldots, n\}. \end{array} \tag{1.17}$$

In the set $\Omega_1 \ominus \mathbb{W}^n$the constraints $\sum_{j\in L^n_{f,i}} x_j \geq \sum_{j\in L^n_{f,i}} d^{max}_j$, $\forall\ L^n_{f,i} \in \text{group}(f,n)$ are redundant for $f = 2,\ldots,n$, $i = 1,\ldots,n_f$, Therefore $\Omega_1 \ominus \mathbb{W} = \text{HR}(\mathbf{d^{max}}, \mathbf{M}) = \Omega_0 \ominus \mathbb{W}$ and thus the proof is completed.

We remark that in [30] the authors have proven that Algorithm 1.3.1 converges in one iteration for a larger class of systems. □Theorem 1 shows that for the buffer model (1.1)-(1.3) the maximal robust control invariant set can be computed explicitly for arbitrary n without resorting to the Algorithm 1.3.1. The explicit form (1.14) of the maximal robust control invariant set provides an interesting insight which is shown next through an example. Let $n = 3$ and $p^{max}_i = p^{max}_j = d^{max}_i = d^{max}_j = 1$ the invariant set for system (1.1) subject to constraints (1.2)-(1.3) is so composed: *(i)* every buffer level is greater or equal to 0 and smaller or equal to M, *(ii)* the sum of any two buffer levels is greater or equal to 1, *(iii)* the sum of all three buffer levels is greater or equal to 2. The above set of constraints guarantee the existence of a control law $u(k) = f(x(k))$ which does not lead to stockout for any feasible demand profile. We remark that the system variables are normalized to the maximum production rate. More examples can be found in Section 1.8. In the next two sections we will cope with the Problem 2, i.e. the computation of the maximal robust positive invariant set $\mathcal{O}_\infty$ both under the RLB policy and under the DPC control law.

1.5 Computation of Maximal Robust Positive Invariant Set under the RLB Feedback Policy

Consider system (1.1) subject to the constraints (1.2)-(1.3) and define the RLB control law for $i = 1,\ldots,n$, as follows:

$$u_i(k) = \begin{cases} p^{max}_i & \text{if} \quad (x_i(k) \leq x_j(k)\ \forall j \neq i) \text{ and } (x_i(k) \leq M - p^{max}_i) \\ & \quad \text{and } \sum_{l=1}^{i-1} u_l(k) = 0 \\ 0 & \text{otherwise.} \end{cases} \tag{1.18}$$

The RLB control law works as follows: at each time instant k the system produces at the maximum rate the product typology corresponding to the lowest buffer level i, unless $x(k)$ is greater than $M - p^{max}_i$.

Remark 4 *The constraint $\sum_{l=1}^{i-1} u_l(k) = 0$ in the control law (1.18) is introduced in order to uniquely define the control law in case there are several buffers at the same minimum level. Any other ordering can be used.*

The maximal robust positive invariant set $\mathcal{O}_\infty$ for system (1.1) subject to constraints (1.2) under the control law (1.18) can be computed numerically for a fixed n. Numerical tests (reported in Example (4)) show that the set $\mathcal{O}_\infty$ might be non-convex and difficult to write in explicit form for arbitrary n. However, a closed form solution can be found under the following assumption:

$$p_i^{max} = d_i^{max} = 1 \ \forall \ i = 1, \dots, n \tag{1.19}$$

The control law (1.18) with assumption (1.19) becomes:

$$u_i(k) = \begin{cases} 1 & \text{if} \quad (x_i(k) \leq x_j(k) \ \forall j \neq i) \ and \ (x_i(k) \leq M-1) \\ 0 & \text{otherwise} \end{cases} \tag{1.20}$$

Under the control law (1.20) system (1.1) is given by:

$$\begin{array}{l} x_i(k+1) = \begin{cases} x_i(k) + 1 + d_i(k) & \text{if} \quad (x_i(k) \leq x_j(k) \ \forall j \neq i) \\ & \qquad \text{and} \ \ (x_i(k) \leq M-1) \\ x_i(k) + d_i(k) & \text{otherwise} \end{cases} \\ i = 1, \dots, n \end{array} \tag{1.21}$$

The following theorem provides a closed form solution for maximal robust positive invariant set for system (1.21) for arbitrary n.

Theorem 2 *The maximal robust positive invariant set $\mathcal{O}_\infty$ for system (1.1) with $n \geq 2$ subject to constraints (1.2)-(1.3) under the control law (1.20) is:*

$$\begin{array}{rl} \mathcal{O}_\infty = & \{x \in \mathbb{R}^n \mid x_i \leq M, \ i = 1, \dots, n, \\ & \sum_{j \in L^n_{f,i}} x_j \geq \alpha_f, \ L^n_{f,i} \in group(f, n), \\ & i = 1, \dots, n_f, \ f = 1, \dots, n\} \end{array} \tag{1.22}$$

where α_k for $k = 3, \dots, n$ is defined recursively as follows:

$$\alpha_k = (\alpha_{k-1} + 1)k/(k-1), \ \alpha_2 = 2, \ \alpha_1 = 0. \tag{1.23}$$

*Proof:*We prove Theorem 2 by using *(i)* induction arguments, *(ii)* the Algorithm 1.3.1 and *(iii)* the procedure outlined in Section 1.3 for computing $\mathcal{O}_\infty$ for PWA systems. It is immediate to prove that the set $\mathcal{O}_\infty$ is constrained by $x_i \leq M$. A simple inspection shows that the control law (1.20) for all $x \in \text{HR}(\mathbf{0}^n, M\mathbf{1}^n)$ will never drive the integrators outside the level M for all possible disturbances. Therefore, next we consider the set (1.22) and focus only on the constraints $x_i \geq 0$ and $\sum_{j \in L^n_{f,i}} x_j \geq \alpha_f, \quad L^n_{f,i} \in \text{group}(f, n)$. We compute the set $\mathcal{O}_\infty$ for $n = 2$, $n = 3$ and then

for $n = i + 1$ assuming that $\mathcal{O}_\infty$ is described by (1.22)-(1.23) for $n = i$. Also, as mentioned in Remark 4 we prefer to work with the multi-valued system (1.21) rather than with one of its possible single-valued and discontinuous implementation. The results will not change but the exposition will be simplified. The maximal robust positive invariant set $\mathcal{O}_\infty$ for system (1.1) subject to constraints (1.2) under the control law (1.20) for n=2 is:

$$\mathcal{O}_\infty = \{x \in \mathbb{R}^2 \mid x_k \leq M,\ x_1 \geq 0,\ x_2 \geq 0,\ x_1 + x_2 \geq 2\}. \tag{1.24}$$

The proof is by construction as follows:

Step 0. $\Omega_0 = \mathrm{HR}(\mathbf{0}^2, M\mathbf{1}^2)$.

Step 1. $\Omega_0 \ominus \mathbb{W}^2 = \mathrm{HR}(\mathbf{1}^2, M\mathbf{1}^2)$. $\Omega_1 = \mathrm{Pre}_{f_a}(\Omega_0, \mathbb{W}^2) = \bigcup_{(y,j)\in\{1\}\times\{1,2\}} \mathcal{S}^+_{y,j}$, where $\mathcal{S}^+_{1,1} \triangleq \{x \in \mathbb{X}^2 \mid x + \begin{bmatrix} 1 \\ 0 \end{bmatrix} \in \mathrm{HR}(\mathbf{1}, \mathbf{M}),\ x_1 \leq x_2\}$ and $\mathcal{S}^+_{1,2} \triangleq \{x \in \mathbb{X}^2 \mid x + \begin{bmatrix} 0 \\ 1 \end{bmatrix} \in \mathrm{HR}(\mathbf{1}, \mathbf{M}),\ x_2 \leq x_1\}$. By computing $\mathcal{S}_{1,1}$ and $\mathcal{S}_{1,2}$ we obtain

$$\begin{aligned} \Omega_1 = \ \mathrm{Pre}_{f_a}(\Omega_0, \mathbb{W}^2) = \mathrm{HR}\left(\begin{bmatrix} 0 \\ 1 \end{bmatrix}, \begin{bmatrix} M-1 \\ M \end{bmatrix}\right) \bigcup \\ \mathrm{HR}\left(\begin{bmatrix} 1 \\ 0 \end{bmatrix}, \begin{bmatrix} M \\ M-1 \end{bmatrix}\right) \end{aligned} \tag{1.25}$$

Step 2. $\Omega_1 \ominus \mathbb{W}^2 = \left[\bigcup_{y=1,\ldots,3}(\Phi_y \oplus (-\mathbb{W}^2))\right]^c$ where $\bigcup_{y=1,\ldots,3} \Phi_y = \Omega_1^c$. By direct computation $\Phi_1 = \{x \in \mathbb{R}^2 |\ x_1 < 0\}$, $\Phi_2 = \{x \in \mathbb{R}^2 \mid x_2 < 0\}$, $\Phi_3 = \{x \in \mathbb{R}^2 \mid x_1 < 1,\ x_2 < 1\}$. Rewrite $\Omega_1 \ominus \mathbb{W}^2$ as $\Omega_1 \ominus \mathbb{W}^2 = \left[\bigcup_{y=1,\ldots,3}(\Phi_y \oplus (-\mathbb{W}^2))\right]^c = \bigcap_{y=1,\ldots,3}(\Phi_y \oplus (-\mathbb{W}^2))^c = \bigcap_{y=1,\ldots,3} \mathcal{S}^*_y$. By direct computation: $\Phi_1 \oplus (-\mathbb{W}^2) = \{x \in \mathbb{R}^2 \mid x_1 < 1\}$, $\Phi_2 \oplus (-\mathbb{W}^2) = \{x \in \mathbb{R}^2 \mid x_2 < 1\}$ and $(\Phi_3 \oplus (-\mathbb{W}^2))$ is computed by projecting the set

$$\Phi_3 \oplus (-\mathbb{W}^2) = \mathrm{Proj}_x\left(\left\{[x^T\ y^T] \in \mathbb{R}^{2+2} \mid \begin{bmatrix} 0 & I^2 \\ -I^2 & I^2 \\ \mathbf{1}^{2^T} & -\mathbf{1}^{2^T} \end{bmatrix} \begin{bmatrix} x \\ y \end{bmatrix} \leq \begin{bmatrix} \mathbf{1}^2 \\ \mathbf{0}^2 \\ 1 \end{bmatrix} \right\}\right). \tag{1.26}$$

The Fourier-Motzkin procedure for computing the projection in (1.26) yields:

$$\Phi_3 \oplus (-\mathbb{W}^2) = \{x \in \mathbb{R}^2 \mid x_1 < 2,\ x_2 < 2,\ x_1 + x_2 < 3, \} \tag{1.27}$$

Therefore, $\mathcal{S}_1^* = \{x \in \mathbb{R}^2 \mid x_1 \geq 1\}$, $\mathcal{S}_2^* = \{x \in \mathbb{R}^2 \mid x_2 \geq 1\}$, $\mathcal{S}_3^* = \{x \in \mathbb{R}^2 \mid x_1 \geq 2\} \cup \{x \in \mathbb{R}^2 \mid x_2 \geq 2\} \cup \{x \in \mathbb{R}^2 \mid x_1 + x_2 \geq 3\}$. In conclusion by direct computation we obtain $\Omega_1 \ominus \mathbb{W}^2 = \bigcap_{y=1,\ldots,3} \mathcal{S}_y^* = \{x \in \mathbb{R}^2 \mid x_1 \geq 1,\ x_2 \geq 1,\ x_1 + x_2 \geq 3,\}$ (note that the constraints "≥ 2" are redundant). $\Omega_2 = \bigcup_{(y,j)\in\{1\}\times\{1,2\}} \mathcal{S}_{y,j}^+$, where $\mathcal{S}_{1,1}^+ \triangleq \{x \in \mathbb{X}^2 \mid\ x + \begin{bmatrix} 1 \\ 0 \end{bmatrix} \in \Omega_1 \ominus \mathbb{W}^2,\ x_1 - x_2 \leq 0\}$ and $\mathcal{S}_{1,2}^+ \triangleq \{x \in \mathbb{X}^2 \mid\ x + \begin{bmatrix} 0 \\ 1 \end{bmatrix} \in \Omega_1 \ominus \mathbb{W}^2,\ x_2 - x_1 \leq 0\}$. By explicitly computing $\mathcal{S}_{1,1}$ and $\mathcal{S}_{1,2}$ we obtain $\mathcal{S}_{1,1}^+ = \{x \in \mathbb{R}^2 \mid x_1 \geq 0,\ x_2 \geq 1,\ x_1 + x_2 \geq 2,\ \ x_1 - x_2 \leq 0\}$, $\mathcal{S}_{1,2}^+ = \{x_1 \geq 1,\ x_2 \geq 0,\ x_1 + x_2 \geq 2,\ x_2 - x_1 \leq 0\}$, and therefore $\Omega_2 = \{x_1 \geq 0,\ x_2 \geq 0,\ x_1 + x_2 \geq 2\}$.

Step 3. $\Omega_2 \ominus \mathbb{W}^2 = \left[\bigcup_{y=1,\ldots,3}(\Phi_y \oplus (-\mathbb{W}^2))\right]^c$ where $\bigcup_{y=1,\ldots,3} \Phi_y = \Omega_2^c$. By direct computation $\Phi_1 = \{x \in \mathbb{R}^2 |\ x_1 < 0\}$, $\Phi_2 = \{x \in \mathbb{R}^2 \mid x_2 < 0\}$, $\Phi_3 = \{x \in \mathbb{R}^2 \mid x_1 + x_2 < 2\}$. Rewrite $\Omega_2 \ominus \mathbb{W}^2$ as $\Omega_2 \ominus \mathbb{W}^2 = \left[\bigcup_{y=1,\ldots,3}(\Phi_y \oplus (-\mathbb{W}^2))\right]^c = \bigcap_{y=1,\ldots,3}(\Phi_y \oplus (-\mathbb{W}^2))^c = \bigcap_{y=1,\ldots,3} \mathcal{S}_y^*$. By direct computation: $(\Phi_1 \oplus (-\mathbb{W}^2)) = \{x \in \mathbb{R}^2 \mid x_1 < 1\}$, $(\Phi_2 \oplus (-\mathbb{W}^2)) = \{x \in \mathbb{R}^2 \mid x_2 < 1\}$ and $(\Phi_3 \oplus (-\mathbb{W}^2))$ is computed by using the Fourier-Motzkin procedure for:

$$\mathrm{Proj}_x\left(\left\{[x^T y^T] \in \mathbb{R}^{2+2} \mid \begin{bmatrix} 0 & 1^{2^T} \\ -I^2 & I^2 \\ \mathbf{1}^{2^T} & -\mathbf{1}^{2^T} \end{bmatrix} \begin{bmatrix} x \\ y \end{bmatrix} \leq \begin{bmatrix} 2 \\ \mathbf{0}^2 \\ 1 \end{bmatrix} \right\}\right). \tag{1.28}$$

the projection in (1.28) yields:

$$\Phi_3 \oplus (-\mathbb{W}^2) = \{x \in \mathbb{R}^2 \mid x_1 + x_2 < 3,\} \tag{1.29}$$

Therefore $\mathcal{S}_1^* = \{x \in \mathbb{R}^2 \mid x_1 \geq 1\}$, $\mathcal{S}_2^* = \{x \in \mathbb{R}^2 \mid x_2 \geq 1\}$ $\mathcal{S}_3^* = \{x \in \mathbb{R}^2 \mid x_1 + x_2 \geq 3\}$. In conclusion by direct computation we obtain $\Omega_2 \ominus \mathbb{W}^2 = \{x \in \mathbb{R}^2 \mid x_1 \geq 1,\ x_2 \geq 1,\ x_1 + x_2 \geq 3,\}$ which equals $\Omega_1 \ominus \mathbb{W}^2$ and terminates the algorithm. It is proven that the set (1.22) with α_2 in (1.23) is $\mathcal{O}_\infty$ for $n = 2$.

The maximal robust positive invariant set $\mathcal{O}_\infty$ for system (1.1) subject to constraints (1.2) under the control law (1.20) for n=3 is:

$$\begin{aligned} \mathcal{O}_\infty = \quad & \{x \in \mathbb{R}^3 \mid x_k \leq M, x_1 \geq 0,\ x_2 \geq 0,\ x_3 \geq 0,\ x_1 + x_2 \geq 2, \\ & x_1 + x_3 \geq 2,\ x_2 + x_3 \geq 2,\ x_1 + x_2 + x_3 \geq 4.5\} \end{aligned} \tag{1.30}$$

The proof is by construction. We remark that the construction of the set $\mathcal{O}_\infty$ for $n = 3$ is not necessary for the proof, but it is included next in order to better understand the induction arguments when constructing the set $\mathcal{O}_\infty$ for $n = i + 1$.

Step 0. $\Omega_0 = \mathrm{HR}(\mathbf{0}^3, M\mathbf{1}^3)$.

Step 1. $\Omega_0 \ominus \mathbb{W}^3 = \mathrm{HR}(\mathbf{1}^3, M\mathbf{1}^3)$. $\Omega_1 = \mathrm{Pre}_{f_a}(\Omega_0, \mathbb{W}^3) = \bigcup_{(y,j)\in\{1\}\times\{1,2,3\}} \mathcal{S}^+_{y,j}$, where $\mathcal{S}^+_{1,1} \triangleq \{x \in \mathbb{X}^3 \mid x + \begin{bmatrix} 1 \\ 0 \\ 0 \end{bmatrix} \in \mathrm{HR}(\mathbf{1}^3, M\mathbf{1}^3),\ x_1 \le x_2,\ x_1 \le x_3\}$, $\mathcal{S}^+_{1,2}$ and $\mathcal{S}^+_{1,3}$ are computing considering the remaining two regions of the closed loop PWA system (1.21) for n=3. The computation of $\mathrm{Pre}_{f_a}(\Omega_0, \mathbb{W}^3)$ yields

$$\begin{aligned}\Omega_1 = \mathrm{Pre}_{f_a}(\Omega_0, \mathbb{W}^3) = \mathrm{HR}\left(\begin{bmatrix} 0 \\ 1 \\ 1 \end{bmatrix}, \begin{bmatrix} M-1 \\ M \\ M \end{bmatrix}\right) \\ \bigcup \mathrm{HR}\left(\begin{bmatrix} 1 \\ 0 \\ 1 \end{bmatrix}, \begin{bmatrix} M \\ M-1 \\ M \end{bmatrix}\right) \bigcup \mathrm{HR}\left(\begin{bmatrix} 1 \\ 1 \\ 0 \end{bmatrix}, \begin{bmatrix} M \\ M \\ M-1 \end{bmatrix}\right)\end{aligned} \tag{1.31}$$

Step 2. $\Omega_1 \ominus \mathbb{W}^2 = \left[\bigcup_{y=1,\dots,r}(\Phi_y \oplus (-\mathbb{W}^2))\right]^c$ where $\bigcup_{y=1,\dots,r} \Phi_y = \Omega_1^c$. The set Ω_1^c (the complement of Ω_1) in (1.31) is

$$\begin{aligned}\Omega_1^c = \bigcup_{i=1,2,3} \underbrace{\{x_i < 0\}}_{\text{Type I}} \bigcup_{i=1,2,3} \underbrace{\left\{\bigcap_{j\in L^3_{2,i}} x_j < 1\right\}}_{\text{Type II}} \\ \bigcup \underbrace{\{x_1 < 1,\ x_2 < 1,\ x_3 < 1\}}_{\text{Type } \mathbf{III}}.\end{aligned} \tag{1.32}$$

We observe the following: constraints of type I and type II are equivalent to the constraints (at the same iteration step) for the case $n = 2$ (Φ_1, Φ_2, Φ_3), the only difference is that constraints of type I are extended to the third dimension ($x_3 < 0$) and constraints of type II are extended to all couples: $x_1 + x_3 < 1$, $x_2 + x_3 < 1$, $x_1 + x_2 < 1$. Constraint of type III is the new type of constraint which appears when moving from $n = 2$ to $n = 3$. By definition $\bigcup_{y=1,\dots,r} \Phi_y = \Omega_1^c$ and thus, $\Phi_1 = \{x \in \mathbb{R}^3 \mid x_1 < 0\}$, $\Phi_2 = \{x \in \mathbb{R}^3 \mid x_2 < 0\}$, $\Phi_3 = \{x \in \mathbb{R}^3 \mid x_3 < 0\}$, $\Phi_4 = \{x \in \mathbb{R}^3 \mid x_1 < 1,\ x_2 < 1\}$, $\Phi_5 = \{x \in \mathbb{R}^3 \mid x_1 < 1,\ x_3 < 1\}$, $\Phi_6 = \{x \in \mathbb{R}^3 \mid x_2 < 1,\ x_3 < 1\}$, $\Phi_7 = \{x \in \mathbb{R}^3 \mid x_1 < 1,\ x_2 < 1,\ x_3 < 1\}$. From an algorithmic point of view the computation of Pontryagin differences and Minkowsky sums on the sets arising from constraints of type I and II proceed as in the case $n = 2$. As an example consider the set Φ_4 and compute $(\Phi_4 \oplus (-\mathbb{W}^3))$

by using Fourier-Motzkin procedure:

$$\Phi_4 \oplus (-\mathbb{W}^3) = \mathrm{Proj}_x\left(\left\{[x^T\ y^T] \in \mathbb{R}^{3+3} \mid \begin{bmatrix} 0\,0\,0 & 1\,0\,0 \\ 0\,0\,0 & 0\,1\,0 \\ -I^3 & I^3 \\ \mathbf{1}^{3T} & -\mathbf{1}^{3T} \end{bmatrix} \begin{bmatrix} x \\ y \end{bmatrix} \leq \begin{bmatrix} 1 \\ 1 \\ \mathbf{0}^3 \\ 1 \end{bmatrix} \right\}\right). \tag{1.33}$$

the projection in (1.33) yields:

$$\Phi_4 \oplus (-\mathbb{W}^3) = \{x \in \mathbb{R}^3 \mid x_1 < 2,\ x_2 < 2,\ x_3 < 2,\ x_1 + x_2 < 3\} \tag{1.34}$$

which corresponds to $\Phi_3 \oplus (-\mathbb{W}^3)$ for $n = 2$ in (1.27). When computing the last set $(\Phi_7 \oplus (-\mathbb{W}^3))$ by using Fourier-Motzkin procedure for

$$\Phi_7 \oplus (-\mathbb{W}^3) = \mathrm{Proj}_x\left(\left\{[x^T\ y^T] \in \mathbb{R}^{3+3} \mid \begin{bmatrix} 0 & I^3 \\ -I^3 & I^3 \\ \mathbf{1}^{3T} & -\mathbf{1}^{3T} \end{bmatrix} \begin{bmatrix} x \\ y \end{bmatrix} \leq \begin{bmatrix} \mathbf{1}^3 \\ \mathbf{0}^3 \\ 1 \end{bmatrix} \right\}\right). \tag{1.35}$$

we obtain:

$$\Phi_7 \oplus (-\mathbb{W}^3) = \{x \in \mathbb{R}^3 \mid x_i < 2\ \forall\, i,\ x_i + x_j < 3\ \forall\, i \neq j,\ x_1 + x_2 + x_3 < 4,\} \tag{1.36}$$

In summary, the computation of $\Omega_1 \ominus \mathbb{W}^3 = \bigcap_{y=1,\ldots,7} \mathcal{S}_y^*$ yields $\mathcal{S}_i^* = \{x_i \geq 1\}$ for $i = 1, 2, 3$, $\mathcal{S}_4^* = \{x_1 \geq 2\} \cup \{x_2 \geq 2\} \cup \{x_3 \geq 2\} \cup \{x_1 + x_2 \geq 3\}$, $\mathcal{S}_5^* = \{x_1 \geq 2\} \cup \{x_2 \geq 2\} \cup \{x_3 \geq 2\} \cup \{x_1 + x_3 \geq 3\}$, $\mathcal{S}_6^* = \{x_1 \geq 2\} \cup \{x_2 \geq 2\} \cup \{x_3 \geq 2\} \cup \{x_2 + x_3 \geq 3\}$, $\mathcal{S}_7^* = \{x_1 \geq 2\} \cup \{x_2 \geq 2\} \cup \{x_3 \geq 2\} \cup \{x_1 + x_2 \geq 3\} \cup \{x_2 + x_3 \geq 3\} \cup \{x_1 + x_3 \geq 3\} \cup \{x_1 + x_2 + x_3 \geq 4\}$, When computing the intersections of the sets $\mathcal{S}_i^*$ for $i = 1, \ldots, 7$ and removing redundant constraints we get: $\Omega_1 \ominus \mathbb{W}^3 = \bigcap_{y=1,\ldots,7} \mathcal{S}_y^* = \bigcup_{i,j \in \mathrm{group}(2,3)} \{x_1 \geq 1,\ x_2 \geq 1,\ x_3 \geq 1,\ x_i + x_j \geq 3,\}$ which are the equivalent of the constraints at the same step for $n = 2$ replicated for all the couples (x_i, x_j). The computation of the sets proceeds as in the case $n = 2$ computing the one-step reachable sets $\mathcal{S}_{i,j}^+$ for all sets and for all three regions of the closed loop PWA system. The set Ω_2 is not reported here.

Step 3. When computing the complement of Ω_2, $\Omega_2^c = \bigcup_{y=1,\ldots,7} \Phi_y$ we obtain the following sets: $\Phi_i = \{x_i < 0\}$ for $i = 1, 2, 3$, $\Phi_4 = \{x_1 + x_2 < 2\}$, $\Phi_5 = \{x_1 + x_3 < 2\}$, $\Phi_6 = \{x_2 + x_3 < 2\}$, $\Phi_7 = \{x_1 + x_2 < 3,\ x_1 + x_3 < 3,\ x_2 + x_3 < 3\}$, At this point the iteration on the sets $\Phi_1, \ldots, \Phi_6$ proceeds as in the case $n = 2$ generating the equivalent constraints for $\mathcal{O}_\infty$ as for $n = 2$; making sure that

type I are extended to all x_i and type II are extended to all couples, thus generating:

$$\begin{aligned}\mathcal{O}_\infty^1 = \quad & \{x \in \mathbb{R}^3 \mid x_k \leq M,\ x_1 \geq 0,\ x_2 \geq 0,\ x_3 \geq 0,\ x_1 + x_2 \geq 2, \\ & x_2 + x_3 \geq 2,\ x_1 + x_3 \geq 2\}.\end{aligned} \tag{1.37}$$

The final set will be $\mathcal{O}_\infty = \mathcal{O}_\infty^1 \bigcap \mathcal{O}_\infty^2$. The set $\mathcal{O}_\infty^2$ arises from Φ_7. In fact, we obtain

$$\Phi_7 \oplus (-\mathbb{W}^3) = \text{Proj}_x \left(\left\{ [x^T \ y^T] \in \mathbb{R}^{3+3} \mid \begin{bmatrix} 0\,0\,0 & 1\,1\,0 \\ 0\,0\,0 & 0\,1\,1 \\ 0\,0\,0 & 1\,0\,1 \\ -I^3 & I^3 \\ \mathbf{1}^{3T} & -\mathbf{1}^{3T} \end{bmatrix} \begin{bmatrix} x \\ y \end{bmatrix} \leq \begin{bmatrix} 3 \\ 3 \\ 3 \\ \mathbf{0}^3 \\ 1 \end{bmatrix} \right\} \right). \tag{1.38}$$

the projection in (1.38) yields:

$$\Phi_7 \oplus (-\mathbb{W}^3) = \{x \in \mathbb{R}^3 \mid x_i < 1 \ \forall\ i,\ x_i + x_j < 4 \ \forall\ i \neq j,\ x_1 + x_2 + x_3 < \beta_3, \} \tag{1.39}$$

where $\beta_3 = 1 + 3 \cdot 3/2$ and it is computed as follows: sum up the first three rows of (1.38) to get $2y_1 + 2y_2 + 2y_3 < 3 \cdot 3$, therefore $y_1 + y_2 + y_3 < 3 \cdot 3/2$ and from the last equation $x_1 + x_2 + x_3 < 1 + 3 \cdot 3/2$. Proceeding with the computation $\mathcal{O}_\infty$ one can notice that the constraints $x_i + x_j < 4$ in $\Phi_7 \oplus (-\mathbb{W}^3)$ are redundant. Therefore, the one-step reachability computation takes the last constraint in $\Phi_7 \oplus (-\mathbb{W}^3)$, $x_1 + x_2 + x_3 < \beta_3$ reverts it and sums it up to -1 to obtain

$$x_1 + x_2 + x_3 \geq \beta_3 - 1 = 3 \cdot 3/2 \tag{1.40}$$

Constraint (1.40) is invariant in the next iteration and constitutes $\mathcal{O}_\infty^2$. In conclusions

$$\begin{aligned}\mathcal{O}_\infty = \quad & \{x \in \mathbb{R}^3 \mid x_k \leq M,\ x_1 \geq 0,\ x_2 \geq 0,\ x_3 \geq 0,\ x_1 + x_2 \geq 2, \\ & x_2 + x_3 \geq 2,\ x_1 + x_3 \geq 2,\ x_1 + x_2 + x_3 \geq 4.5\}.\end{aligned} \tag{1.41}$$

It is proven that the set (1.22) with α_3 in (1.23) is $\mathcal{O}_\infty$ for $n = 3$.

Now we assume that $\mathcal{O}_\infty$ is defined by (1.22)-(1.23) for $n = i$ and prove that (1.22)-(1.23) holds true for $n = i + 1$. This will conclude the proof. We focus only on the main steps in order to avoid tedious sets enumeration. By using the same arguments used for the case $n = 3$, we can prove that $\mathcal{O}_\infty$ for $n = i + 1$ will be described by

two sets $\mathcal{O}_\infty = \mathcal{O}_\infty^1 \bigcap \mathcal{O}_\infty^2$. $\mathcal{O}_\infty^1$ can be immediately described by considering $\mathcal{O}_\infty$ for $n = i$:

$$\begin{aligned} \mathcal{O}_\infty = \quad & \{x \in \mathbb{R}^i \mid x_k \leq M,\ x_k \geq 0,\ k = 1, \dots, i,\ \textstyle\sum_{j \in L_{f,k}^i} x_j \geq \alpha_f, \\ & L_{f,k}^i \in \text{group}(f, i),\quad f = 2, \dots, i,\ k = 1, \dots, n_f, \} \end{aligned} \tag{1.42}$$

and replicating all the constraints with the additional dimension $i + 1$:

$$\begin{aligned} \mathcal{O}_\infty^1 = \quad & \{x \in \mathbb{R}^{i+1} \mid x_k \leq M,\ x_k \geq 0,\ k = 1, \dots, i+1,\ \textstyle\sum_{j \in L_{f,k}^{i+1}} x_j \geq \alpha_f, \\ & L_{f,k}^{i+1} \in \text{group}(f, i+1),\quad f = 2, \dots, i,\ k = 1, \dots, n_f, \} \end{aligned} \tag{1.43}$$

where α_f is defined recursively in (1.23). As for $n = 3$, the set $\mathcal{O}_\infty^2$ for $n = i + 1$ will be the outcome of the iterations on a set of the following form: $\Phi_{last} = \{x_1 + x_3 + \dots + x_{i+1} < \alpha_i + 1,\ x_2 + x_3 + \dots + x_{i+1} < \alpha_i + 1, \dots,\ x_1 + x_2 + \dots + x_i < \alpha_i + 1\}$. We remark here that for $n = 3$, last=7 and Φ_7 had constraints of the type "$\dots < 3$" which agrees with the fact that $3 = \alpha_2 + 1$. From the Minkowski sum we obtain:

$$\begin{aligned} \Phi_{last} \oplus (-\mathbb{W}^{i+1}) = \quad & \text{Proj}_x \Bigg(\Bigg\{ [x^T\ y^T] \in \mathbb{R}^{2i+2} \mid \begin{bmatrix} 0\ 0\ \cdots\ 0 & 0\ 1\ \cdots\ 1 \\ \vdots & \vdots \\ 0\ 0\ \cdots\ 0 & 1\ 1\ \cdots\ 0 \\ -I^{i+1} & I^{i+1} \\ \mathbf{1}^{i+1^T} & -\mathbf{1}^{i+1^T} \end{bmatrix} \begin{bmatrix} x \\ y \end{bmatrix} \leq \\ & \leq \begin{bmatrix} \alpha_i + 1 \\ \vdots \\ \alpha_i + 1 \\ \mathbf{0}^{i+1} \\ 1 \end{bmatrix} \Bigg\} \Bigg). \end{aligned} \tag{1.44}$$

by computing the projection (1.44) and removing redundant constraints one obtains:

$$\Phi_{last} \oplus (-\mathbb{W}^{i+1}) = \{x \in \mathbb{R}^{i+1} \mid x_i < 1\ \forall\ i,\ x_1 + x_2 + \dots + x_{i+1} < \beta_{i+1}, \} \tag{1.45}$$

where $\beta_{i+1} = \frac{i(\alpha_i+1)}{i-1} + 1$ and it is computed as follows: sum up the first $i + 1$ rows of (1.44) to get $iy_1 + iy_2 + iy_3 + \dots + iy_{i+1} < (i + 1)(\alpha_i + 1)$, therefore $y_1 + y_2 + y_3 + \dots + y_{i+1} < \frac{(i+1)(\alpha_i+1)}{i}$ and from the last equation in (1.44) $x_1 + x_2 + x_3 + \dots + x_{i+1} < 1 + \frac{(i+1)(\alpha_i+1)}{i}$. Proceeding with the computation, the one-step reachability computation takes the constraint in $x_1 + x_2 + x_3 + \dots + x_{i+1} < 1 + \frac{(i+1)(\alpha_i+1)}{i}$, reverts it and sums it up to -1 to obtain:

$$x_1 + x_2 + x_3 + \dots + x_{i+1} \geq \frac{(i + 1)(\alpha_i + 1)}{i}. \tag{1.46}$$

Constraint (1.46) is invariant in the next iteration and constitutes $\mathcal{O}_\infty^2$. In conclusions:

$$\mathcal{O}_\infty^2 = \{x \in \mathbb{R}^{i+1} \mid x_1 + x_2 + x_3 + \cdots + x_{i+1} \geq \frac{(i+1)(\alpha_i+1)}{i}\}. \tag{1.47}$$

and $\mathcal{O}_\infty = \mathcal{O}_\infty^1 \bigcap \mathcal{O}_\infty^2$ with $\mathcal{O}_\infty^1$ in (1.43) and $\mathcal{O}_\infty^2$ in (1.47) with $\alpha_{i+1} = \frac{(i+1)(\alpha_i+1)}{i}$. It is proven that the set (1.22) with α_{i+1} in (1.23) is $\mathcal{O}_\infty$ for $n = i+1$. This concludes the proof by induction.□

Remark 5 *We believe that there might be a simpler approach to proving Theorem 2 which makes use of the system symmetries and does not require the computation of intermediate sets as in the lengthy proof of Theorem 2.*

Theorem 2 shows that when the buffer model (1.1)-(1.3) is controlled by the RLB Feedback Policy in (1.18)-(1.19) the maximal robust positive invariant set can be computed explicitly for arbitrary n. A brief intuitive explanation of the idea of Fourier-Motzkin elimination is given in Appendix B. See [72] for a more detailed description of the algorithm. The explicit form (1.22)-(1.23) provides also an interesting insight illustrated next through an example. Let $n = 3$, then stockout will never occur with the RLB policy if the initial buffer levels satisfy the following conditions: *(i)* every buffer level is greater than 0, *(ii)* the sum of any two buffer levels is greater than 2, *(iii)* the sum of all three levels greater than 9/2. We remark that the system variables are normalized to the maximum production rate. By comparing $\mathcal{O}_\infty$ in (1.22)-(1.23) and $\mathcal{C}_\infty$ in (1.14) for $n = 3$ it is clear that there is room for improvement on the RLB policy, i.e., there might exist a control law which excludes stockout with lower initial buffer levels. Next we show that the DPC policy is one of those. More examples can be found in Section 1.8.

1.6 Computation of Maximal Robust Positive Invariant Set under the DPC Feedback Policy

Consider system (1.1) subject to (1.2)-(1.3). At time k let $m(k) = [m_1, \ldots, m_n]$ be the index vector of the state components in increasing order, i.e., $m_i \in [1, n]$ for $i = 1, \ldots, n$, $m_i \neq m_j$ for all $i \neq j$, and $x_{m_i} \geq x_{m_j}$ for all $j < i$. Define the following DPC control law for $i = 1, \ldots, n$:

$$u_{m_i(k)}(k) = \begin{cases} \min \{(d^{max}_{m_i(k)} - x_{m_i(k)}(k)), & \text{if } (x_{m_i(k)}(k) < d^{max}_{m_i(k)}) \text{ and} \\ \quad (P^{max} - \sum_{j=1}^{i-1} u_{m_j(k)})\} & \quad (\sum_{j=1}^{i-1} u_{m_j(k)} < P^{max}) \\ 0 & \text{otherwise} \end{cases} \tag{1.48}$$

The DPC control policy produces the item typologies whose buffer levels are less than the corresponding demand value; it starts from the lowest and it continues increasing order until the machine has production capacity. The buffer will be filled up to the maximum demand value or to the maximum buffer level reachable with the residual production capacity. The following theorem shows that the DCP policy (1.48) is the "best" policy in the sense that $\mathcal{O}_\infty = \mathcal{C}_\infty$.

Theorem 3 *The maximal robust positive invariant set for system (1.1) subject to constraints (1.2)-(1.3) under the control law (1.48) is equal to $\mathcal{C}_\infty$ in (1.14), i.e.,*

$$\begin{array}{l} \mathcal{O}_\infty = \{x \in \mathbb{R}^n | 0 \leq x_i \leq M,\ i = 1, \dots, n, \\ \sum_{j \in L^n_{f,i}} x_j \geq \ \sum_{j \in L^n_{f,i}} d_j^{max} - 1, L^n_{f,i} \in group(f, n), \\ i = 1, \dots, n_f, \quad f = 2, \dots, n\} \end{array} \tag{1.49}$$

Proof: We prove the theorem in two steps. First, we prove that $\mathcal{O}_\infty$ is a robust positive invariant set and then we prove that it is the largest one. Consider the set of buffers $x(k) \in \mathcal{O}_\infty$, let $I(k)$ be the index of all buffers in $x(k)$ smaller than the corresponding demand values, $x_i(k) < d_i^{max}$ if $i \in I(k)$. Denote by $x^p(k+1)$ the buffer levels at time $k+1$ assuming no demand, i.e. $x^p(k+1) = x(k) + u(k)$. Then, $x(k) \in \mathcal{O}_\infty$ implies that $x_i^p(k+1) = d_i^{max}$ for all $i \in I(k)$ and $d_i^{max} \leq x_i^p(k+1) \leq M$ for all $i \in \{1, \dots, n\} \setminus I(k)$. This, holds true by the fact that $\sum_{i \in I(k)} x_i(k) \geq \sum_{i \in I(k)} d_i^{max} - P^{max}$, by $\mathcal{O}_\infty$ in (1.49) and by the definition of the control law (1.48). In conclusion all buffers of $x^p(k+1)$ will be greater or equal than the corresponding demand values, (and less or equal to M). The disturbance $d(k)$ will lower the buffer levels from $x^p(k+1)$ to $x(k+1)$. However, from the assumption on the disturbance $d(k)$ (1.2c)-(1.3) and the property of $x^p(k+1)$ we immediately derive that $x(k+1) \in \mathcal{O}_\infty$. To see this, let $d(k)$ be one possible disturbance realization and $J(k)$ the index of all components of $d(k)$ different from zero. Then $\sum_{j \in J(k)} d_j(k) \geq -D_{max}$, which implies that $\sum_{j \in J(k)} d_j(k) \geq -P^{max}$. This is derived from the assumption on the disturbance $d(k)$, (1.2c), and from the constraint $-D^{max} \geq -P^{max}$. As $x_j^p(k) \geq d_j^{max}(k)$ for all j, we have proven that $\sum_{j \in J(k)} x_j^p(k) \geq \sum_{j \in J(k)} d_j^{max}$ which implies that $\sum_{j \in J(k)} x_j^p(k) + d_j(k) = \sum_{j \in J(k)} x_j(k+1) \geq \sum_{j \in J(k)} d_j^{max} - P^{max}$, that is $x(k+1) \in \mathcal{O}_\infty$. This proves that $\mathcal{O}_\infty$ in (1.49) is a robust positive invariant set. Next we prove that it is the maximal robust positive invariant set. Assume there exists a set of buffers which does not satisfy at least one of the inequalities defining $\mathcal{O}_\infty$ in (1.49), i.e., $\exists\ I(k)$ such that $\sum_{i \in I(k)} x_i(k) < \sum_{i \in I(k)} d_i^{max} - P^{max}$. In this case, by the definition of the control law (1.48) we conclude that there exists $l \in I(k)$ such that $x_l^p(k) < d_l^{max}$. The disturbance $d(k)$ with $d_l(k) = d_l^{max}$ and $d_j(k) = 0$ for all

$j \neq l$ will led to and infeasible $x(k+1)$. □

1.7 Extended Modeling

A brief discussion, on how to further extend the results presented in this article to take into account setup times is provided.

1.7.1 Control Policy Function of the Disturbance

The RLB and DPC control laws studied in this manuscript are a function of the current system state. Some manufacturing plants might have a preview on future demand (the disturbance). In this case the control laws could be function of the disturbance as well. In the simplest case (preview of one step) we could have $u = f(x, d)$. A classical example of f in such case is the extension of the DPC law (1.48):

$$u_i(k) = \begin{cases} \min\{p_i^{max}, (d_i^{max} - x_i(k) - d_i(k))\} & \text{if } (x_i(k) \leq -d_i(k)) \\ 0 & \text{otherwise} \end{cases} \tag{1.50}$$

The control policy (1.50) works as follows: at each time k it fills to the maximum disturbance quantity the buffer smaller than the its current disturbance $d_i(k)$. The computation of the maximal positive invariant set $\mathcal{O}_\infty$ for system subject to constraints (1.2) under the control law (1.50) and other classes of feedback policies function of the disturbance is a non-trivial extension of this work and is the object of our current studies.

1.7.2 Extension to Model Setup Times

The simplified system (1.1) can be extended in order to model setup times, i.e. the time required for switching the production from a product typology to a different one. In this case the system can be modeled as a switched system. In fact, at each time instant k, each buffer level has two different behaviors depending on the production choice at the previous step. If we assume one production line manufacturing one item typology per sampling interval, a simple model can be derived. Introduce a new state storing the previous input:

$$u_{\text{old}}(k+1) = I^n u(k) \tag{1.51}$$

and denote the production rate loss due to the setup time for product i by $u_{\text{loss},i}$. The following piecewise affine system models the buffer dynamics with setup-times:

$$\begin{aligned} x_i(k+1) &= \begin{cases} x_i(k) + u_i(k) + d_i(k) & if\ (u_i(k) \neq 0 \text{ and } u_{\text{old},i}(k) \neq 0) \\ & \quad \text{or } (u_i(k) = 0) \\ x_i(k) + u_i(k) - u_{\text{loss},i} + d_i(k) & otherwise \end{cases} \\ u_{\text{old}}(k+1) &= I^n u(k). \end{aligned} \tag{1.52}$$

The system (1.52) can model the buffer dynamics with setup-times if the RLB feedback policy is applied, because the RLB control law produces one item typology per sampling interval. The case of one production line manufacturing more item typologies per sampling interval with setup-times can be modeled by the following piecewise affine system:

$$x_i(k+1) = \begin{cases} x_i(k) + u_i(k) + d_i(k) & if\ (u_i(k) = 0) \\ x_i(k) + u_i(k) - u_{\text{loss},i} + d_i(k) & otherwise \end{cases} \tag{1.53}$$

The system (1.53) models the occurrence of a setup every time an item typology is produced. The number of setups is then overestimated because the model (1.53) does not capture that there is no setup when the production line starts to produce at time $k+1$ the same item typology manufactured at the end of time k. A possible way to prevent this overestimation would be, for example, to store the production order. The DPC feedback policy can be applied to system (1.53), because it can produce several item typologies per sampling interval. The DPC control law must be rewritten taking the setups into account. Define the following modified DPC control law for $i = 1, \ldots, n$:

$$u_{m_i(k)}(k) = \begin{cases} \min\ \{(d^{max}_{m_i(k)} - x_{m_i(k)}(k)), & \text{if } (x_{m_i(k)}(k) < d^{max}_{m_i(k)}) \text{ and} \\ \quad (P^{max} - \sum_{j=1}^{i-1} u_{m_j(k)})\} & (\sum_{j=1}^{i-1} u_{m_j(k)} < P^{max}) \text{ and} \\ & (u_{m_i(k)}(k) > u_{\text{loss},i}) \\ 0 & \text{otherwise} \end{cases} \tag{1.54}$$

The constraint $(u_{m_i(k)}(k) > u_{\text{loss},i})$ is added because the control input associated to item typology i is larger than zero if there is enough production rate to cope with the loss due to setup. Note that, if the loss due to setup was such that buffers cannot have enough additional in stock in order to satisfy all admissible demands, the persistent feasibility for the closed-loop system could not be guaranteed. The computation of the maximal robust control invariant set $\mathcal{C}_\infty$ for the systems described above and the design of a feasible control policy with large robust positively invariant sets is subject of future research.

1.8 Numerical Examples

Objective of this section is to compute numerically the robust invariant sets described in this paper and validate out theoretical results. All the sets in this section have been computed with the Multi-Parametric Toolbox [76], [77] and the Matlab Invariant Set Toolbox (InvSetBox) [73]. A processor, equipped with an *Intel Core Duo* processor with a clock frequency of 2.0 GHz has been used to compute the sets. The reader is refereed to the Appendix B for a more detailed explanation of invariant set computation. We consider two or three item typologies in order to be able to graphically visualize the results. The normalization $D^{max} = P^{max} = 1$ is used in all the examples. In the examples (1), (3) and (5), constraints (1.3) are used. In the examples (2), (4) and (6), we consider different upper bounds to the production and demand rates for each product typology. Throughout the examples we assume $M_i = Mi = 1, \ldots, N$ however different numerical values for M are chosen for a better visualization of the sets. The production plants are modeled by system (1.1) subject to constraints (1.2) for n=2 or n=3. To satisfy the external demand, (during the sampling time) each item typology must be produced in order to keep the buffer levels in the computed sets. A production law driving the buffer levels out the computed sets is infeasible. The numerical results show that: *(i)* the RLB and DPC feedback policies guarantee that stockout will never occur if the initial buffer levels take value into the corresponding set $\mathcal{C}_\infty$, *(ii)* the DPC feedback policy can satisfy the external demand with lower buffer levels. In this section we consider applying the above procedure for computing $\mathcal{O}_\infty$ and $\mathcal{C}_\infty$ to some numerical examples:

Example 1 (Computation of $\mathcal{C}_\infty$ under Assumption (1.19))
We compute the maximal robust control invariant set $\mathcal{C}_\infty$ for system (1.1) subject to constraints (1.3) for n=2 and n=3. $\mathcal{C}_\infty$ for n=2 is:

$$\begin{gathered} 0 \leq x_1 \leq M, \quad 0 \leq x_2 \leq M \\ x_1 + x_2 \geq 1. \end{gathered} \tag{1.55}$$

and it is depicted in Figure 1.10(a) ($M = 2$). $\mathcal{C}_\infty$ for n=3 is:

$$\begin{gathered} 0 \leq x_1 \leq M, \quad 0 \leq x_2 \leq M, \quad 0 \leq x_3 \leq M \\ x_1 + x_2 \geq 1, \quad x_1 + x_3 \geq 1, \quad x_2 + x_3 \geq 1 \\ x_1 + x_2 + x_3 \geq 2. \end{gathered} \tag{1.56}$$

and it is depicted in the Figure 1.10(b) ($M = 2$).

Example 2 (Computation of $\mathcal{C}_\infty$ for $n = 3$)
The maximal robust control invariant set $\mathcal{C}_\infty$ for system (1.1) subject to constraints (1.2) for $n = 3$, $p^{max} = [1; 1; 1]$ and $d^{max} = [0.8; 0.7; 0.4]$ is:

$$\begin{gathered} 0 \le x_1 \le M, \quad 0 \le x_2 \le M, \quad 0 \le x_3 \le M \\ x_1 + x_2 \ge 0.5, \quad x_1 + x_3 \ge 0.2, \quad x_2 + x_3 \ge 0.1 \\ x_1 + x_2 + x_3 \ge 0.9. \end{gathered} \tag{1.57}$$

and it is depicted in the Figure 1.4(a) (M=1.5). The maximal robust control invariant set $\mathcal{C}_\infty$ for system (1.1) subject to constraints (1.2) for $n = 3$ and $d^{max} = [0.5; 0.3; 1]$ is:

$$\begin{gathered} 0 \le x_1 \le M, \quad 0 \le x_2 \le M, \quad 0 \le x_3 \le M \\ x_1 + x_3 \ge 0.5, \quad x_2 + x_3 \ge 0.3 \\ x_1 + x_2 + x_3 \ge 0.8. \end{gathered} \tag{1.58}$$

and it is depicted in the Figure 1.4(b) (M=1.5).

Example 3 (Computation of $\mathcal{O}_\infty$ under RLB and Assumption (1.19))
System (1.1) subject to constraints (1.2) under the RLB control law (1.20) for $n = 3$ is rewritten as an autonomous PWA system defined over four polyhedral regions reported in the Figure 1.5(a) ($M = 5$). The maximal robust positive invariant set $\mathcal{O}_\infty$ is:

$$\begin{gathered} 0 \le x_1 \le M, \quad 0 \le x_2 \le M, \quad 0 \le x_3 \le M \\ x_1 + x_2 \ge 2, \quad x_1 + x_3 \ge 2, \quad x_2 + x_3 \ge 2 \\ x_1 + x_2 + x_3 \ge 4.5. \end{gathered} \tag{1.59}$$

and is depicted in the Figure 1.5(b) ($M = 5$).

Example 4 (Computation of $\mathcal{O}_\infty$ under the RLB Feedback Policy)
The system (1.1) subject to constraints (1.2) under the RLB control law (1.20) for $n = 2$, $p^{max} = [0.9; 0.8]$ and $d^{max} = [0.5; 0.3]$ is rewritten as an autonomous PWA system over three polyhedral regions. The corresponding maximal robust positive invariant set $\mathcal{O}_\infty$ is depicted in Figure 2.11(a) ($M = 3$). The system (1.1) subject to constraints (1.2) under the RLB control law (1.20) for $n = 3$, $p^{max} = [0.9; 0.9; 0.9]$ and $d^{max} = [0.5; 0.3; 0.1]$ is rewritten as an autonomous PWA system defined over four polyhedral regions. The corresponding maximal robust positive invariant set $\mathcal{O}_\infty$ is depicted in Figure 2.8(a) ($M = 3$).

Example 5 (Computation of $\mathcal{O}_\infty$ under DPC and Assumption (1.19))
System (1.1) subject to constraints (1.2)-(1.3) under the DPC control law (1.48)-(1.19) for $n = 3$ is rewritten as an autonomous PWA system defined over 23 regions

depicted in Figure 2.5(a) ($M = 2$). The corresponding maximal robust positive invariant set $\mathcal{O}_\infty$ is:

$$\begin{aligned} 0 \le x_1 \le M, \quad 0 \le x_2 \le M, \quad 0 \le x_3 \le M \\ x_1 + x_2 \ge 1, \quad x_1 + x_3 \ge 1, \quad x_2 + x_3 \ge 1 \\ x_1 + x_2 + x_3 \ge 2. \end{aligned} \tag{1.60}$$

and it is depicted in Figure 2.5(b) ($M = 2$).

Example 6 (Computation of $\mathcal{O}_\infty$ under the DPC Feedback Policy) *System (1.1) subject to constraints (1.2) under the DPC control law (1.48) for n=3, $p^{max} = [1; 1; 1]$ and $d^{max} = [0.5; 0.3; 1]$ is rewritten as an autonomous PWA system defined over 19 regions depicted in Figure 1.8(a) ($M = 1.5$). The corresponding maximal robust positive invariant set $\mathcal{O}_\infty$ is:*

$$\begin{aligned} 0 \le x_1 \le M, \quad 0 \le x_2 \le M, \quad 0 \le x_3 \le M \\ x_1 + x_3 \ge 0.5, \quad x_2 + x_3 \ge 0.3 \\ x_1 + x_2 + x_3 \ge 0.8. \end{aligned} \tag{1.61}$$

and it is depicted in the Figure 1.8(b) ($M = 1.5$).

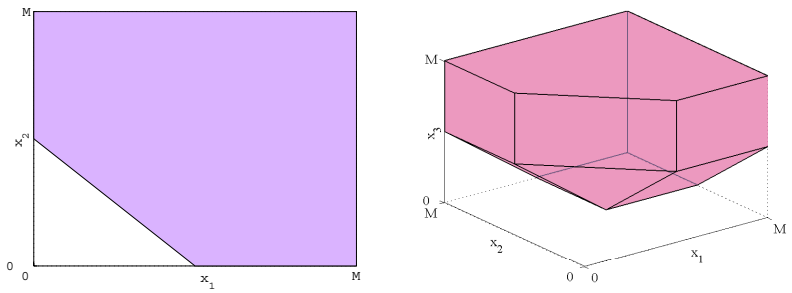

(a) n=2 (b) n=3

Figure 1.3: $\mathcal{C}_\infty$ under the Assumption (1.19).

Remark 6 *As mentioned in the Appendix B, the methods for computing the robust one-step set can be intractable for relatively for large systems. The numerical calculation of the invariant sets $\mathcal{C}_\infty$ and $\mathcal{O}_\infty$ explode computationally respectively for $n > 10$ and $n > 6$, in the sense that the invariant set computation will take days. It is useful to explicitly compute the invariant sets for arbitrary n without resorting to numerical calculations.*

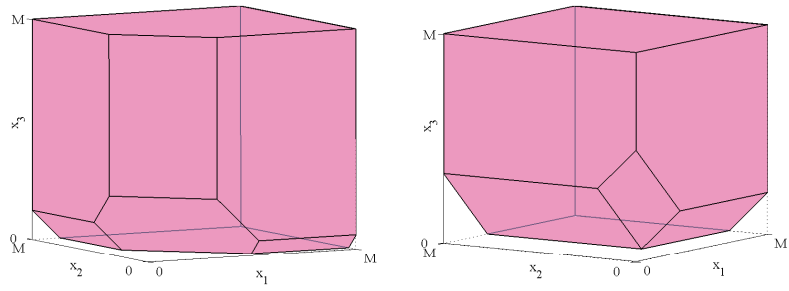

(a) d_1^{max} (b) d_2^{max}

Figure 1.4: $\mathcal{C}_\infty$ for n=3.

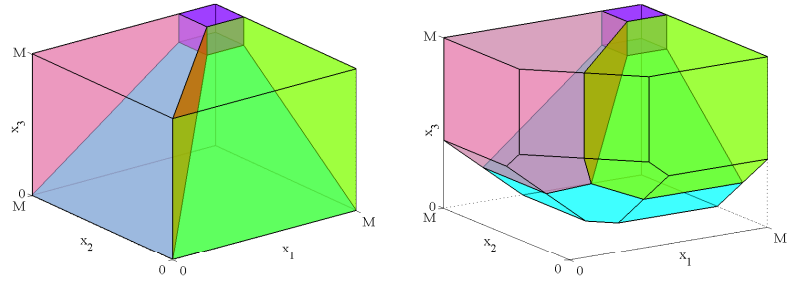

(a) S_{PWA} (b) $\mathcal{O}_\infty$

Figure 1.5: S_{PWA} and $\mathcal{O}_\infty$ under RLB and the Assumption (1.19).

In the next section a case study will show how the explicit expression of the invariant sets could be used in manufacturing.

1.9 Case Study

We consider a two-stages metal cold presswork factory located in the South of Italy. It consists of one production line and one assembly line, manufacturing 14 different item typologies (see the Figure 1.1, assuming only one production line). Then, a set of 14 buffers has to be controlled in order to prevent stockouts. Two type changes occur in one day of work; the setup time does not depend on the item typology. The maximum assembly rate d_i^{max}, as well as the maximum production rate p_i^{max} are

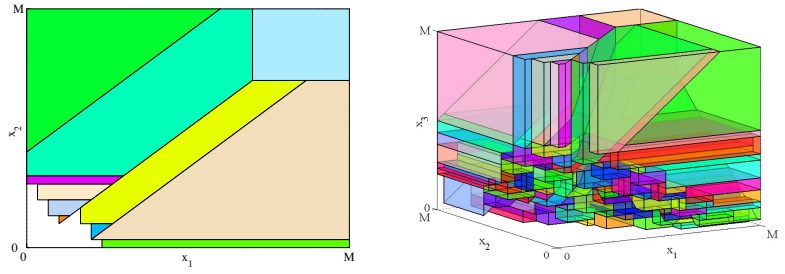

(a) n=2, p_1^{max}, d_1^{max} (b) n=3, p_2^{max}, d_2^{max}

Figure 1.6: $\mathcal{O}_\infty$ under the RLB Feedback Policy.

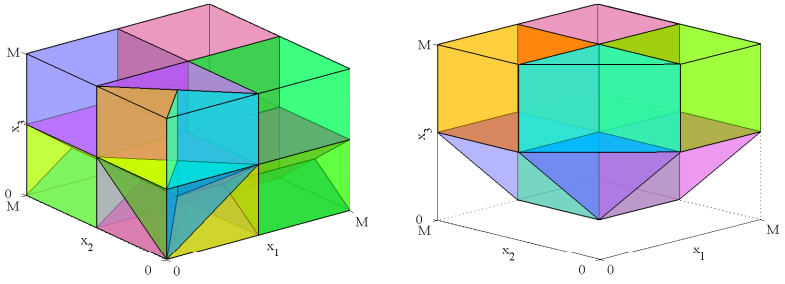

(a) S_{PWA} (b) $\mathcal{O}_\infty$

Figure 1.7: S_{PWA} and $\mathcal{O}_\infty$ under DPC and the Assumption (1.19).

known per each typology $i = 1 \dots 14$. If we don't consider setup, the overall maximum production rate P_{ns}^{max} will be equal to the maximum production rate, that is:

$$P_{ns}^{max} = \max_i \{p_i^{max}\} \quad i = 1 \dots 14$$

We have computed the production rate loss due to the setup time, denoted by p_{loss}, through a worst case assumption. The total time spent for the two daily setup is converted into a production loss rate considering the number of items that would be produced during the setup time at a production rate equal to P_{ns}^{max}:

$$p_{loss} = \frac{2 \cdot setup \;\; time \cdot P_{ns}^{max}}{24}$$

The worst case assumption consists in using P_{ns}^{max} rather than the p_i^{max} corresponding to each item typology. Hence, the effective overall daily maximum production rate

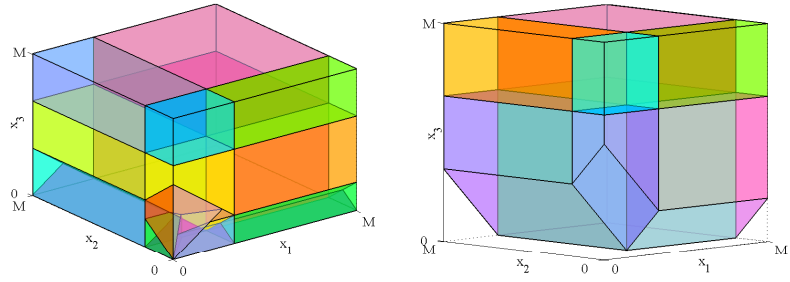

(a) S_{PWA} (b) $\mathcal{O}_\infty$

Figure 1.8: S_{PWA} and $\mathcal{O}_\infty$ under the DPC Feedback Policy.

P^{max} is computed considering the production loss due to setup, that is:

$$P^{max} = P^{max}_{ns} - p_{loss}$$

The overall daily maximum assembly request D^{max} is supposed to be equal to the overall daily maximum production capacity, according to the case $P^{max} \geq D^{max}$. Then, after normalizing all the quantities to the maximum production rate, the model (1.1) can be applied to this industrial case assuming a daily sampling time, the normalized assembly request of the typology i as the demand rate d_i and the normalized production rate of the typology i as the production rate u_i. The following data have been used:

$$\begin{aligned} d^{max} &= [0.04; 0.04; 0.05; 0.05; 0.05; 0.12; 0.12; 0.07; 0.08; 0.02; 0.03; 0.07; 0.07; 0.07] \\ p^{max} &= [0.83; 0.92; 1; 1; 1; 0.92; 0.92; 0.92; 1; 0.75; 0.75; 0.92; 0.92; 0.92] \\ D^{max} &= P^{max} = 0.81. \end{aligned}$$

We assume a simulation horizon of 50 days and a demand profile over this horizon depicted in the Figure 1.9(a). For the types 10 and 11, corresponding to the smallest maximum demand rate, the demand is supposed to be constantly equal to its maximum value. The sum of all the demand rates is equal to D^{max} at each time step. The plant model under the DPC feedback policy, which has been proved to be the "best" policy, has been simulated assuming different initial buffer states. The objective of the control policy is to be feasible, i.e. to guarantee a continuous production flow, namely to have enough additional in stock in order to satisfy all admissible assembly requests. This target can be achieved depending on the initial buffer conditions. If the initial

buffer states belong to an invariant set, the buffer dynamics will never become negative, which is the case of unmet demand. The numerical computation of the invariant set $\mathcal{O}_\infty$ for the investigated manufacturing system, which has 14 buffers, would be intractable. Exploiting the results in the Theorem 3, it is possible to detect the initial buffer levels leading to infeasibility without any computation. This is shown through an example. According to the explicit expression of the invariant set described in 1.49, the sum of all the initial buffer levels has to be greater or equal to 0.07, which means that the sum of the items stored in all the buffers at the beginning of the production period must be bigger or equal to 672. The Figure 1.10(a) shows the buffer dynamics of 12 product types corresponding to the assembly request depicted in Figure 1.9(a) and corresponding to an initial condition $x_i(0) = 0.005, \quad \forall i = 1, \dots 14$. The dynamics of the buffers for types 10 and 11 will be equal to zero because the demand rate is equal to its maximum value all the time. Note that the buffers are always nonnegative, then the feasibility of the control policy holds (the policy is "persistent" feasible). The produced item number per day is depicted in the Figure 1.9(b). The Figure 1.10(b) shows the same buffer dynamics corresponding to an initial condition $x_i(0) = 0.001, \quad \forall i = 1, \dots 14$. This initial condition does not belong to the invariant set of the system under the DPC feedback policy. Note that the number of products in the buffers becomes negative, which means that the assembly requests cannot be satisfied. The Figure 1.10(b) illustrates this infeasible case. The investigated case study describes a possible industrial application of the proposed results. The use of computed invariant set as a terminal set constraint in a receding horizon scheduling policy is currently under research.

1.10 Conclusions and Future Steps

This chapter has reported on the classical problem of buffer level control by means of robust invariant set theory for linear and switched linear systems. We have provided the analytic expression of robust positive invariant sets and controlled robust invariant sets for two common scheduling policies. The results of this paper allow to compute the invariant sets for an arbitrary number of buffers without resorting to recursive algorithms. We believe that our work may have a broad impact if developed further. For instance, it can lead to a systematic way to analyze the feasibility properties of well studied and commonly implemented scheduling control laws. Also, the application of receding horizon scheduling polices in manufacturing plants [31, 89, 108] can benefit from the proposed study. In fact, it is well known that when a receding horizon (or

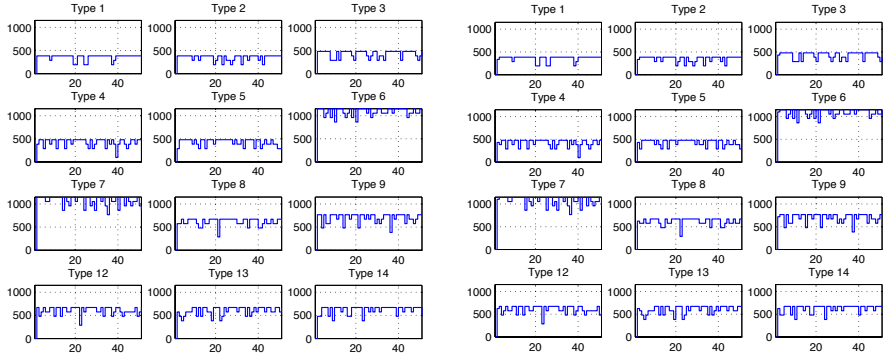

(a) Demand profile

(b) Control inputs associated to the DPC Feedback Policy

Figure 1.9: Demand profile and control inputs over 50 days.

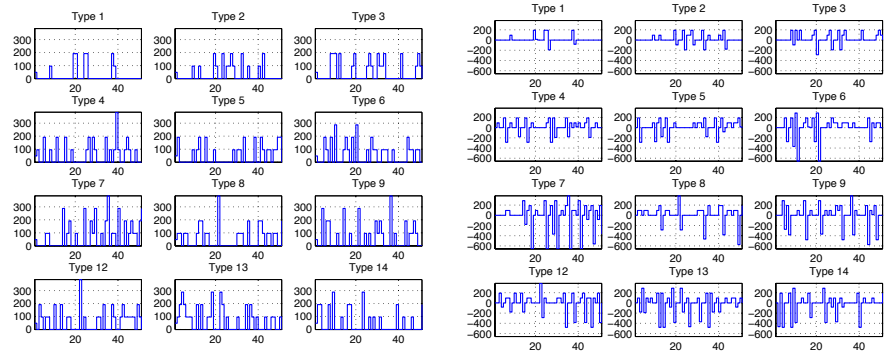

(a) without stockouts

(b) with stockouts

Figure 1.10: Buffer dynamics with stockouts over 50 days.

moving horizon) scheduling policy is used, the persistent feasibility of the closed-loop systems is hardly guaranteed [31]. The results of this chapter allow to simply compute an invariant set which can be used as a terminal set constraint in a receding horizon scheduling policy. This is a key element for guaranteeing the persistent feasibility of the closed-loop system.

Chapter 2

Stochastic Model Predictive Control for Indoor Climate Control

One of the most critical challenges facing society today is climate change and thus the need to realize massive energy savings. Since buildings account for the largest fraction in total energy use, energy efficient building climate control can have an important contribution. The work presented in this chapter is part of the *OptiControl* Project, which aims at developing predictive control strategies to save energy in indoor climate control while maintaining high user comfort. Weather forecasts are employed to achieve this target. In particular we investigate a stochastic model-based predictive approach for indoor climate control that takes into account weather predictions and thus increase energy efficiency while respecting constraints resulting from desired occupant comfort. The system model is bilinear, time-varying and with stochastic uncertainty. Model predictive strategies with time-varying and probabilistic constraints are assessed in terms of energy savings, constraint violations as well as computational requirements and compared with strategies used in today's current practice. We also describe methods to reduce the computational time without a significant performance loss. Simulation results show that Stochastic Model Predictive Control (SMPC) methods can achieve significant improvements with respect to current controllers.

2.1 Use of Weather and Occupancy Forecasts For Optimal Building Climate Control (OptiControl)

The presented work is part of the *OptiControl* Project [1], which aims at developing predictive control strategies to save energy in indoor climate control while maintaining high user comfort. The project was started in May 2007 and involves the following institutions:

- Terrestrial Systems Ecology Group, ETH Zurich, Switzerland;
- Automatic Control Laboratory, ETH Zurich, Switzerland;
- Building Technologies Laboratory, EMPA Dübendorf, Switzerland;
- Federal Office of Meteorology and Climatology (MeteoSwiss), Zurich, Switzerland;
- Building Technologies Division, Siemens Switzerland, Ltd, Zug, Switzerland.

The investigated control policies use weather and occupancy forecasts, whose benefits have been investigated in many studies 2.2.1. The most promising and interesting case studies were selected for large-scale simulations and in-depth analysis, mainly involving office buildings. The dynamic model of office buildings was identified and validated by the Building Technologies Laboratory of EMPA Dübendorf. Hourly weather data (predictions and observations) from 10 representative European measurement sites were provided by the Federal Institute for Meteorology and Climatology MeteoSwiss. The control algorithms were investigated by the Automatic Control Laboratory from ETH Zurich, which we collaborated with to developed and implemented the stochastic control strategy described in this chapter. Building models, weather data and control algorithms have been used to simulate the behavior of real buildings under different control strategies. The *OptiControl* Project activities included the development of a modeling and simulation environment, the Building Automation and Control Laboratory software (BACLab), as well as the implementation of databases containing weather and occupancy data and building system parameters. A set of performance criteria were defined to assess the proposed control solutions. A comprehensive report on the activities and results achieved in the *OptiControl* Project so far can be found in [38]. In this chapter we will focus on predictive strategies and analyze a case study.

[1] http://www.opticontrol.ethz/

2.2 Introduction

Buildings account for approximately 40% of the total energy usage in industrialized countries, of which more than 50% is electrical power [44]. The Figure 2.1 shows the total end use of energy; in residential and commercial sectors the major part of the energy consumption is in buildings. This includes energy used for controlling the indoor climate and for installed equipment [6]. Energy use and utility cost can

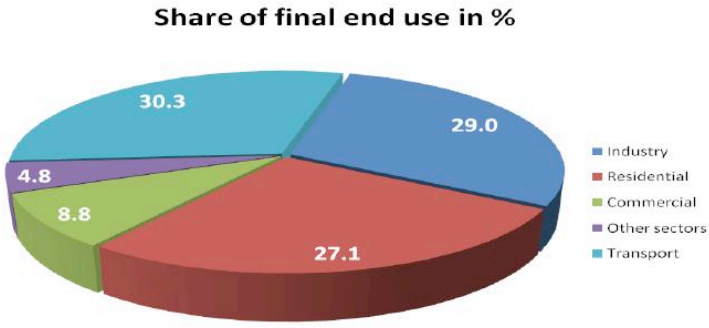

Figure 2.1: Energy consumption in different sectors [6].

be reduced by increasing the efficiency of building systems, by distributing thermal energy more efficiently while meeting the needs of users. Since a building that is built today has an expected lifetime of at least 50 to 100 years, it is urgent to investigate the existing Heating, Ventilation and Air Conditioning (HVAC) systems and to increase their energy efficiency. The use of predictive control strategies is appealing in building climate control due to several reasons, such as slow system dynamics, comfort ranges for the controlled variables defined by European standards, time-dependent costs and bounds for control actions. Initial idealized investigations have demonstrated that foreknowledge of upcoming weather conditions can significantly decrease energy consumption [64]. As building dynamics are highly affected by uncertainties, indoor climate control must cope with disturbance rejection. The disturbances mainly consist of the external environment or weather and the people occupying the building, who generate heat, CO_2 and set demands for temperature, illuminance and air quality. In this work we investigate how knowledge of the statistics of realistic weather predictions can be incorporated into a model predictive control (MPC) framework. This advanced control technique is so popular in industry mainly because of its capability to handle multivariate variable problems as well as incorporate constraints for the manipulated

and the controlled variables. The basic idea of MPC is to exploit the model of the process to predict the future evolution of the system and compute the control actions by optimizing a cost function depending on such predictions. Moreover, if the future disturbances of the controlled system are known or their distribution can be identified, a stochastic MPC can be developed in order to explicitly take into account the effect of disturbances on the future evolution of the system. A stochastic MPC strategy will be next described and applied to building climate control. Common approximations are compared through simulation.

2.2.1 Literature Review

The use of disturbance predictions (e.g. weather forecasts) for indoor climate control has been investigated in many works [9, 32, 36, 62, 64, 68, 82]. The cited papers and a more extensive bibliography can be found at the OptiControl site **http://www.opticontrol.ethz.ch/Literature.html**. In these studies the predictive strategies turn out to be more efficient and promising compared to the conventional, non predictive strategies in thermal control of buildings. In [62] the authors have developed both certainty-equivalence controllers using weather predictions and a controller based on stochastic dynamic programming for a solar domestic hot water system. The strategies are based on probability distributions derived from the weather data. The simulation results have shown that the predictive control strategies can achieve a lower energy cost compared to a non-predictive strategy. In [66–68] the use of a short-term weather predictor based on the real weather data in the control of active and passive building thermal storage inventory is explored. The predicted variables include ambient air temperature, relative humidity, global solar radiation, and solar radiation. A receding horizon policy is applied, i.e. an optimization is computed over a finite planning horizon and only the first action is executed. At the next time step the optimization is repeated over a shifted prediction horizon. It has been shown that the electrical energy savings relative to conventional building control can be significant. A predictive control strategy using a forecasting model of outdoor air temperature has been explored in [36] for intermittently heated radiant Floor Heating Systems (RHF). The control action consists of deciding when to supply the heat to the floor. In the conventional intermittent control technique the decision is based on the past experience. The experimental results show that use of the predictive control strategy could save between 10% and 12% energy during the cold winter months compared to the existing conventional control strategy. Energy savings in a predictive Integrated Room Automation (IRA) are investigated in [64]. The pro-

posed model predictive strategy manipulates passive thermal storage of the building based on predicted future disturbances (e.g. weather forecasts). Comfort bounds are provided for the room temperature. Both conventional, non-predictive strategies and the predictive control strategies are assessed using a *performance bound* as a benchmark. The performance bound is an ideal controller, i.e. no mismatch between the controlled process model and the real plant and perfectly known disturbances. The predictive control outperforms the non-predictive control because the room temperature can be kept within its comfort bounds with minimum energy, i.e. low cost energy sources are exploited as much as possible. The effect of automatic blinds and lighting control on heating and cooling requirements are studied in [32]; the authors investigate the reduction in annual primary energy requirements for indoor climate control achieved in Rome by applying automated lighting control. In the study [9] the influence of occupant behavior on energy consumption was investigated in a single room occupied by one person. The simulated occupant could manipulate six controls, such as turning on or off the heat and adjusting clothing. The simulation results have shown that occupant behavior significatively affects the energy consumption in the room. In conclusion, from the literature we can learn that potential benefits can be obtained for indoor climate control by predictive strategies as well as by including automated blinds and lighting in the control action. We focus on individual building zone or room, i.e. Integrated Room Automation (IRA) [64], in which there are both high energy sources (e.g. chillers, gas boilers, conventional radiators) and low energy methods (e.g. blind operation and evaporative cooling) for heating and cooling. This is also the practise employed in standard 382/1 [2] and 380/4 [3] of Schweizerischer Ingenieur- und Architektenverein (SIA [2]). Low cost energy sources make use of the thermal storage capacity of the building and thus are slow and heavily dependent on weather conditions. Hence the model predictive control should fit very well: if predictions of the future system evolution can be computed, low cost energy sources can be used for controlling the building and meeting the occupant requirements. The aim is to avoid the conventional expensive energy sources as much as possible in favor of the low cost ones.

2.2.2 Outline

In Section 2.3 the building model is provided and an autoregressive model for the disturbances is identified. In Section 2.4 the optimization problem taking weather uncertainties into account is formulated. Then in Sections 2.5 and 2.5.2 the proposed

[2] http://www.sia.ch/d/index.cfm

control schemes are assessed and simulation results are presented. Finally conclusions and future steps are provided in Section 2.6.

2.3 Modeling

We aim at investigating how the proposed Stochastic Model Predictive Control (SMPC) strategy taking weather uncertainty into account can increase energy efficiency in indoor climate control while respecting occupant comfort. Hence we need to develop a model of the system and to identify the uncertainty in order to employ the Model Predictive Control (MPC) technique. In the following subsections first the building model is developed, then a predictor of the error in weather forecasts is identified, finally the augmented model including both the building and the prediction error model is presented.

2.3.1 Building Model

In order to study potential energy savings we investigated a single room/zone model. As discussed in [64] and in 2.2.1, it is reasonable to estimate building-wide savings by integrating multiple zone models. The single room/zone will be represented as a simple lumped-parameter model. This means that, for example, the state for the room temperature is lumped over all floors and the whole room. The model as well as the parameter and cost estimation for a wide range of building types has been provided by the Building Technologies Laboratory of the Swiss Federal Laboratories for Materials Testing and Research (EMPA). As described in [47] and in [46], the system under investigation has the following six control inputs:

u_1 = blind position [0 : closed ... 1: open]

u_2 = electric lighting

u_3 = floor heating (positive values $\longleftrightarrow$ heating) $[W/m^2]$

u_4 = slow ceiling for cooling (positive values $\longleftrightarrow$ cooling) $[W/m^2]$

u_5 = evaporative cooling usage factor [0: off ... 1: on]

u_6 = heating power radiator (positive values $\longleftrightarrow$ heating) $[W/m^2]$

The cost of each control action is denoted as follows:

$$c = \begin{bmatrix} c_1 & c_2 & c_3 & c_4 & c_5 & c_6 \end{bmatrix}^T \quad . \tag{2.1}$$

The above costs are derived from the corresponding delivered energy, i.e. electricity energy [47]. The control inputs u_3 and u_4 are related to "slow ceilings", i.e. cooling ceilings by capillary tube systems [46]. The following eight disturbances are taken into account:

v_1 = solar gains with closed blinds $[W/m^2]$
v_2 = additional solar gains with fully open blinds $[W/m^2]$
v_3 = room illuminance by solar radiation with closed blinds [lux]
v_4 = additional room illuminance with fully open blinds [lux]
v_5 = internal heat gains by occupants $[W/m^2]$
v_6 = internal heat gains by equipment (e.g. computers) $[W/m^2]$
v_7 = outside temperature $[^oC]$
v_8 = wet bulb temperature $[^oC]$.

The wet bulb temperature depends on the outside temperature and humidity and defines the minimum temperature that may be achieved by evaporative cooling. Solar gains describe the amount of energy that is introduced to the room by solar radiation. We account for the heat gain coming into the room through solar gain and artificial lighting with closed blinds and the difference to partially or fully open blinds [46]. The goal is to use as much as possible the low cost energy sources such as u_1 and u_5 rather than the conventional heating and cooling elements such as u_6. This target is reflected in the cost function, e.g. $c_1, c_5 \ll c_6$. The controlled outputs are:

y_1 = room temperature $[^oC]$
y_2 = room illuminance [lux]
y_3 = ceiling surface temperature $[^oC]$

The system is subject to q input constraints:

$$\mathcal{U} := \{u \in \mathbb{R}^m \mid Fu \leq f\} \ , \tag{2.2}$$

and to s output constraints:

$$\mathcal{Y} := \{y \in \mathbb{R}^p \mid Gy \leq g\} \ , \tag{2.3}$$

where $F \in \mathbb{R}^{q \times m}$, $G \in \mathbb{R}^{s \times p}$, $f \in \mathbb{R}^q$ and $g \in \mathbb{R}^s$. In the investigated control problem, the set $\mathcal{U} \subset \mathbb{R}^m$ is a polytopic set describing the upper and lower bounds on the actuators, denoted by u_{max} and u_{min}. The set $\mathcal{Y} \subset \mathbb{R}^p$ is described by the upper and

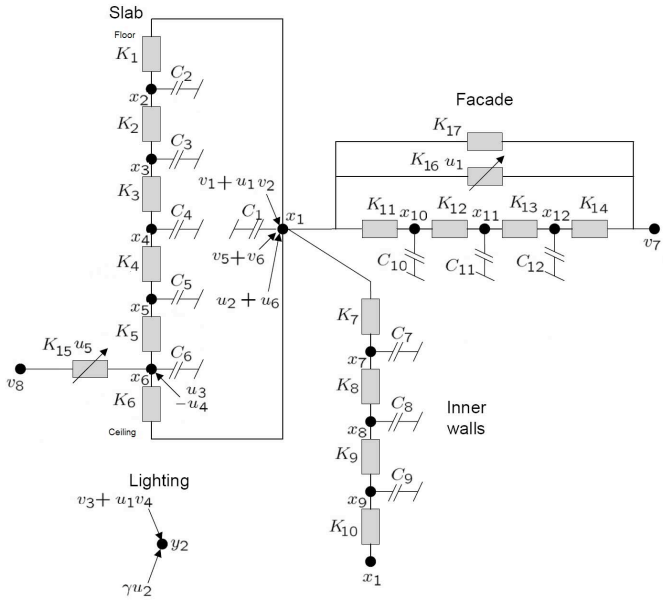

Figure 2.2: Schematic diagram of the zone (adapted from [64])

lower bounds on the outputs, denoted by y_{max} and y_{min}, therefore by thermal and illuminance comfort requirements. A schematic diagram of the lumped parameter model of the single room/zone is depicted in Figure 2.2. In the center of the figure is the room node, to the left are the slabs, at the bottom the inner walls and to the right the facade with windows. The nodes in the diagram describe the states of the system representing the temperatures at different locations. The room temperature is the state x_1, the remaining states represent the slab temperatures, floor, ceiling and the inner and outer wall temperatures. Each node i has a heat storage capacity given by C_i and the heat transmission coefficients K_i are the conductances between nodes. There are non constant parameters in the model, such as the heat transmission through the windows, which depends on the blind position. Then this heat transmission is assumed to be the sum of two terms: one constant term representing heat gain with closed blinds, the other modeling the heat gain with partially or fully opened blinds. The room illuminance is due both to natural and artificial lighting. The natural lighting depends on the solar gain coming into the room through the windows, then on the blind position as well. In the diagram, the arrow on the heat transmission coefficient block introduces a nonlinear term in the model equations, precisely a bilinear term

because the heat transmission coefficient is multiplied with the control input. The heat flux equation for each node can be derived from the Figure 2.2 directly. For example, node 6 gives:

$$C_6 \cdot \dot{x_3} = u_3 - u_4 + K_15(v_8 - x_6) \cdot u_5 + K_6(x_1 - x_6) + \ldots \\ \ldots + K_5(x_5 - x_6) \ . \tag{2.4}$$

Notice the bilinear term $K_{15}(v_8 - x_6) \cdot u_5$: the heat transfer coefficient K_{15} depends on the free cooling usage factor u_5. Notice that the external and wet bulb temperatures v_7 and v_8 are also nodes in this diagram but are taken as fixed temperature sources. The heat transfer coefficient K_{16} represents the facade insulation due to the position of the blinds and can therefore be varied by changing the blind position u_1, which results in a bilinear term in the system dynamics $u_1 K_{16}(x_1 - v_7)$ [46]. We also have a bilinear term in the equation representing the room illuminance:

$$y_2 = v_3 + u_1 \cdot v_4 + \gamma \cdot u_2 \tag{2.5}$$

where γ is a scaling factor to account for the fact that u_2 is given in terms of energy but we want to look at the illuminance. Then the room model is given as the following 12^{th}-order, stochastic discrete, time-varying, bilinear model:

$$x_{k+1} = Ax_k + B_u u_k + B_v v_k + \sum_{i=1}^{6} (B_{xu,i} x_k + B_{vu,i} v_k) u_{i,k} \tag{2.6a}$$

$$y_k = Cx_k + D_u u_k + D_v v_k + \sum_{i=1}^{6} (D_{vu,i} v_k) u_{i,k} \ . \tag{2.6b}$$

The sampling time is 1 hour. The matrices $B_{xu,i} \in \mathbb{R}^{12\times12}$, $B_{vu,i} \in \mathbb{R}^{12\times8}$ and $D_{vu,i} \in \mathbb{R}^{3\times8}$ account for the bilinear terms in states, inputs and disturbances per each input. The output, state, input and disturbance variables at each time step k are denoted respectively by $y_k \in \mathbb{R}^3$, $x_k \in \mathbb{R}^{12}$, $u_k \in \mathbb{R}^6$ and $v_k \in \mathbb{R}^8$. Therefore, for example, the i^{th} state at time k is denoted by $x_{k,i}$. As mentioned above, comfort bands are defined by placing upper and lower bounds on the outputs y. However, because buildings are not occupied at all times of the day and building standards allow for different bands during different times of the year, we have time-varying constraints on the room temperature y_1 and the room illumination y_2. These allowed comfort constraints are defined independently for each country (e.g. [12], [37]). The constraints used in this paper are defined for Switzerland and are defined based on SIA standard 382/1 [5], [1]. According to these standards, the comfort bands can be violated

from time to time. This allows to put probabilistic constraints on the outputs. The room/zone model 2.6 is nonlinear, which leads to a nonlinear MPC problem. Since nonlinear MPC problems can be extremely difficult to solve because it might involve a non-convex optimization, we will resort to the Sequential Linear Programming (SLP) method to address this issue. The SLP technique consists of iteratively linearizing the objective and constraints around the current optimal point by a Taylor series expansion until a convergence criterion is met. For applying the SLP technique to the indoor climate control, we need to iteratively linearize the nonlinear equality constraints deriving from the building model. The disturbance variables involved in the bilinear terms are assumed to be equal to available forecasts. The resulting subproblems will be provided in the next subsections; they can be approximated and recast to tractable optimization problems. The basic formulation of SLP algorithm is described in the Appendix C. We will next develop the weather uncertainty model.

Remark 7 *In the OptiControl Report [38] several building variants are investigated, considering also the indoor air quality and more control inputs, such as mechanical ventilation, which provides the room with fresh air. The interested reader can find further details on the modeling of building in [46]. The building system variants have been defined and discussed in [47]. A large-scale simulation study has been carried out to select cases with the highest saving potential, whose results are presented in [49].*

2.3.2 Augmented Model for Disturbance Rejection

We need the weather predictions over the future horizon to apply an MPC algorithm. Weather forecasts from MeteoSwiss are available, thus, for any disturbance v_j, an estimate $\hat{v_j}$ of the future disturbances v_j, $j = 1 \dots 8$ is available to the controller over some finite horizon. However the predictions are uncertain. Define at each time k:

$$v_k = \hat{v}_k + \tilde{v}_k, \tag{2.7}$$

where $\hat{v}$ is a random error. We account for this uncertainty by treating the error in the prediction as the output of a linear system driven by a gaussian noise. An autoregressive model is identified to predict the error in weather forecasts at time $k + 1$ based on the previous output. Thus the following linear stochastic process models the error in prediction:

$$\tilde{v}_{k+1} = H\tilde{v}_k + Kw_k, \qquad w_k \sim \mathcal{N}(0, I_8) \ . \tag{2.8}$$

The residuals are assumed to be normally distributed with zero mean and covariance KK^T, hence they can be expressed in terms of a standard normal variable w_k. Look-

ing at the eight disturbances defined in the previous section, there are four that are linearly dependent on solar gain v_1 (i.e. v_2, v_3 and v_4). Furthermore, the outside temperature and wet bulb temperature have a quite smoothly evolution, while the solar gain has a high variability. The uncertainty in outside and wet bulb temperatures is much smaller, then it has a negligible effect on the room compared to the solar radiation [53]. This is due to the high thermal insulation of the facade and to accurate temperature estimates, further corrected by a Kalman filter; we refer the reader to [53] for further details. Therefore this helps to obtain temperature and wet bulb temperature forecasts more accurate compared to solar gain predictions. As a consequence, in this initial study it is sufficient to consider the uncertainty only in the solar radiation prediction. So the matrices FH and K in the error model 2.8 are simply scalars. To make the control design include information about measured disturbances, the zone model is augmented as follows:

$$\begin{aligned}\begin{bmatrix} x_{k+1} \\ \tilde{v}_{k+1} \end{bmatrix} &= \begin{bmatrix} A & B_v H \\ 0 & H \end{bmatrix} \begin{bmatrix} x_k \\ \tilde{v}_k \end{bmatrix} + \begin{bmatrix} B_v \\ 0 \end{bmatrix} \hat{v}_k + \begin{bmatrix} B_v K \\ K \end{bmatrix} w_k + \\ &+ \begin{bmatrix} B_{u,1} + B_{xu,1} x_k + B_{vu,1} \hat{v}_k & \dots & B_{u,6} + B_{xu,6} x_k + B_{vu,6} \hat{v}_k \\ 0 & \dots & 0 \end{bmatrix} u_k = \\ &= A^a \begin{bmatrix} x_k \\ \tilde{v}_k \end{bmatrix} + B_v^a \hat{v}_k + B_w^a w_k + B_k^a u_k. \end{aligned} \tag{2.9}$$

$$\begin{aligned}\begin{bmatrix} y_k \end{bmatrix} &= \begin{bmatrix} C & D_v H \end{bmatrix} \begin{bmatrix} x_k \\ \tilde{v}_k \end{bmatrix} + \begin{bmatrix} D_v \end{bmatrix} \hat{v}_k + \begin{bmatrix} D_v K \end{bmatrix} w_k + \\ &+ \begin{bmatrix} D_{u,1} + D_{vu,1} \hat{v}_k & \dots & D_{u,6} + D_{vu,6} \hat{v}_k \end{bmatrix} u_k = \\ &= C^a \begin{bmatrix} x_k \\ \tilde{v}_k \end{bmatrix} + D_v^a \hat{v}_k + D_w^a w_k + D_k^a u_k. \end{aligned}$$

where $x_k \in \mathbb{R}^n$, $y_k \in \mathbb{R}^p$. Notice that the matrices B_k^a and D_k^a are time-varying. To summarize, the model which the control strategy has to be based on has been developed.

2.3.3 Kalman Filter

The weather forecasts are updated each 12^{th} hour and the predictions look forward for 72 hours for a location situated at a weather station next to the building being controlled. Therefore we must use old predictions until new ones will be provided.

Accurate hourly measurements can be available locally from sensors on the building. We assume the measurement availability and exploit this information by applying a standard Kalman filter to the error model (2.8) in order to incorporate the latest measurements each hour. The Kalman filter is useful both to update future predictions and to locally correct the systematic error in the predictions. We apply the Kalman filter [39,71] to outside and wet bulb temperature as well. In the next section the control problem will be formulated.

2.4 Control Problem Formulation

A model-based predictive approach is exploited for the inddor climate control problem. Model predictive control strategies for stochastic systems aiming at increase energy efficiency while respecting constraints resulting from desired occupant comfort are formulated and analyzed in the following.

2.4.1 Introduction to Model Predictive Control

Model Predictive Control (MPC) is one of the most successful technologies applied in a wide variety of application areas including chemicals, food processing, automotive, and aerospace applications. At each time instant, this method uses a model and all currently available information to predict the system future evolution over a given prediction horizon and solve an open-loop constrained optimization problem. A number of future control actions is computed but only the first move is applied. At the next time step, the overall procedure is repeated over a shifted prediction horizon. In presence of disturbances, measured and predicted variables are different. A convenient way to handle uncertainties, which are involved in most real applications, is to assume that uncertainty is unknown but bounded to adopt a worst case approach, as applied in Robust MPC (e.g. [17,19,85,111]). By doing so, the uncertainty is treated as deterministic because the disturbance realizations can assume values, with equal probability, in a range determined by experience or analysis (e.g. for sensor inaccuracy). The robust approach can be unnecessarily conservative because the control action has to work well for all admissible disturbances. Moreover every uncertainty whose probability distribution has the same support would lead to identical results. Even if the robust approach can be less pessimistic through a closed-loop optimization [17], a more realistic approach can be adopted: to identify the distributions of uncertain model parameters and use these to solve a stochastic MPC problem. Further details on MPC and stochastic MPC are provided in the Appendix D. Stochastic

MPC formulations have been proposed and investigated for additive and multiplicative disturbances in [41,42,54,107,114]. The performance index is the expected value of the usual quadratic cost and the uncertain variables over the prediction horizon are described as stochastic variables with known probability distribution functions. The key point of the control problem is how to deal with uncertainty. Two different approaches will be discussed in the following subsections [51].

2.4.2 Certainty Equivalence Model Predictive Control

A simple way to deal with uncertainty in the traditional MPC framework is simply to neglect the disturbance and solve a deterministic finite-horizon optimization problem, i.e. *certainty equivalence* MPC (CE-MPC). The disturbance variables involved in the bilinear terms are assumed to be equal to available forecasts. As described in the Appendix D, the future disturbances are replaced with deterministic estimates, usually the conditional mean. In the augmented system 2.9 we model the error in prediction as a linear system driven by a gaussian disturbance, whose mean is zero and whose realizations over the prediction horizon are uncorrelated. Therefore the deterministic disturbance estimates we consider are exactly the weather forecasts. The CE-MPC problem is then based on the following deterministic system:

$$x_{k+1} = Ax_k + B_u u_k + B_v \hat{v}_k + \sum_{i=1}^{6} (B_{xu,i} x_k + B_{vu,i} \hat{v}_k) u_{i,k} \tag{2.10a}$$

$$y_k = Cx_k + D_u u_k + D_v \hat{v}_k + \sum_{i=1}^{6} (D_{vu,i} \hat{v}_k) u_{i,k} \ . \tag{2.10b}$$

The resulting deterministic formulation of Problem (4) is:

Problem 3 (Certainty Equivalence MPC)

$$\begin{aligned} &\min_{u_0,\ldots,u_{N-1}} \sum_{k=0}^{N-1} c^T u_k \\ s.t. \\ &\quad \textit{system dynamics } (2.10) \\ &\quad Gy_k \leq g \qquad k = 1,\ldots,N \\ &\quad Fu_k \leq f \qquad k = 0,\ldots,N-1 \end{aligned} \tag{2.11}$$

Since the future values of disturbances are exactly as predicted, there is no future uncertainty in the controller and there are no robustness guarantees in this case.

Practical experience has demonstrated that it is often possible to achieve good performance nonetheless. That is the reason for investigating the CE-MPC in the indoor climate control.

2.4.3 Stochastic Model Predictive Control

In this section the stochastic MPC problem based on the augmented model 2.9 is formulated. The control law applied at time k is the function $u_k(\cdot) : \mathbb{R}^n \mapsto \mathcal{U}$ and y_k is the system output at time k when the state is x_0 at time 0. We choose to minimize the expected value of the non renewable primary energy cost (NRPE) distribution over the prediction horizon N. We must solve a finite horizon stochastic optimal control problem with probabilistic constraints on the outputs over a planning horizon of length N:

Problem 4 (Stochastic MPC)

$$\begin{aligned} &\min_{u_0,\dots,u_{N-1}} \mathbf{E}\left[\sum_{k=0}^{N-1} c^T u_k(x_k)\right] \\ &s.t. \\ &\quad \textit{system dynamics } (2.9) \\ &\quad \mathbf{P}\left\{Gy_k \le g\right\} \ge 1-\alpha \qquad k = 1,\dots,N \\ &\quad Fu_k(x_k) \le f \qquad\quad k = 0,\dots,N-1 \end{aligned} \tag{2.12}$$

where $1-\alpha$ is the predefined probability level for constraint satisfaction, x_k is the current system state and $u_0 \in \mathcal{U}$. The constraints on the control inputs and on the manipulated variables have been defined in 2.2 and in 2.3. The probabilistic constraints included in Problem (4) are called "chance constraints". See the Appendix D and the Appendix E for further details on chance constraints and Stochastic MPC. States and outputs are stochastic variables depending on a normal disturbance. Since the cost is linear and it is an affine linear transformation of normally distributed variables, it has a normal distribution. The coefficients in the objective, as well as lower and upper bounds on inputs and outputs, have been defined in 2.1. Problem (4) contains an infinite number of convex input constraints, non-convex chance constraints on the states and requires optimization over the class of input functions $u(\cdot)$. In the following sections, we will address the problem to obtain a convex and easily solvable formulation of Problem (4): first we will investigate how to parameterize the control inputs to make Problem (4) tractable, then the non-convex probabilistic constraints in Problem (4) will be reformulated as convex, deterministic constraints.

Control Parametrization

The stochastic control problem formulated in 4 is very hard to solve; the traditional dynamic programming approach is practically intractable except for very special cases (e.g. stochastic linear-quadratic control). In control literature, several methods have been proposed to find suboptimal policies that work well in practice, among which MPC is a very effective technique. It is known that if the uncertainty is to be accounted for in the formulation of an MPC problem, it will be preferable to have a state feedback mechanism in the controller rather than open-loop input sequences, in the sense that the control policy is computed on the basis of currently available information. The controller is able to react to future disturbance realization more properly. In the *open-loop prediction MPC* the control action over the prediction horizon is only a function of the current state and not of disturbance and state realizations, while having future control inputs formulated as functions of measured states is usually called *closed-loop prediction MPC* [16,17]. Hence, in open-loop prediction MPC there won't be future state measurements and the input sequence must guarantee constraint satisfaction for all disturbances. However the open-loop approach is computationally very attractive, it might lead to infeasibility and instability problems [86, 87] and it can also result in highly conservative control behavior. The closed-loop approach is less conservative: there will be state measurements at each time instant and feedback control policies typically introduce degrees of freedom in optimization [15, 78]. Then the closed-loop prediction MPC is an attractive approach for the indoor climate control, which is highly affected by uncertainty. In closed-loop prediction MPC optimizing over arbitrary functions is however in general not tractable if constraints have to be satisfied. A popular approach to addressing this issue, which can still be quite conservative, is to "prestabilize", i.e. to compute stabilizing control laws off-line and the online computation is restricted to select one of these control laws as well as a sequence of admissible offsets to the selected control law [14,17,87]. This parametrization, unfortunately, leads to a non-convex set of feasible decision variables. Recent results given in [18, 59, 80, 110, 112] describe one approach to address this problem. The authors have proposed to parameterize the control action as an affine function of the disturbance sequence both in the case of gaussian and unknown but bounded uncertainty. This leads to a convex set of feasible decision variables. In case of norm-bounded uncertainty, this affine disturbance feedback parametrization is shown to be equivalent to the affine state feedback parametrization in [59] in the sense that is leads to the same control inputs. Equivalent parametrization has been investigated in case of stochastic disturbances in [94, 107, 110, 112]. Whereas in [112] and [107] a

second order cone program is formulated, [94] deals with a linear problem, which can be beneficial for large-scale problems. In [110], after deriving the explicit dependance of states and inputs on disturbance in case of affine state feedback parametrization, the authors show that an equivalent and tractable convex optimization problems can be obtained by a nonlinear change of variables both in a stochastic and unknown but bounded (worst-case) setting. Then the optimization in Problem (4) can be solved in a computationally efficient fashion using convex optimization methods by parameterizing the control inputs as affine functions of the past disturbance sequence as follows:

$$u_k(\mathbf{w}_k) := \sum_{j=0}^{k-1} M_{k,j} w_j + h_k, \tag{2.13}$$

where $\mathbf{w}_k = [w_0^T, \ldots, w_{k-1}^T]^T$ is the disturbance realization at time k, $M_{k,j} \in \mathbb{R}^{m \times r}$ and $h_k \in \mathbb{R}^m$, $\forall\ k = 0, \ldots, N-1$. Define

$$\mathbf{u} := \begin{bmatrix} u_0^T & u_1(\cdot)^T & \ldots & u_{N-1}^T(\cdot) \end{bmatrix}^T \quad \text{and} \tag{2.14}$$

$$\mathbf{M} := \begin{bmatrix} 0 & \ldots & \ldots & 0 \\ M_{1,0} & 0 & \ddots & 0 \\ \vdots & \ddots & \ddots & \vdots \\ M_{N-1,0} & \cdots & M_{N-1,N-2} & 0 \end{bmatrix}, \mathbf{h} := \begin{bmatrix} h_0 \\ \vdots \\ \vdots \\ h_{N-1} \end{bmatrix}.$$

where the disturbance feedback matrix $\mathbf{M} \in \mathbb{R}^{mN \times Nr}$ is a strictly block lower triangular matrix with bandwidth $N-1$, which can be written as a block matrix with each block $M_{k,j} \in \mathbb{R}^{m \times r}$ if $j < k$, otherwise $M_{k,j} = 0$ [59, 74, 110]. Then the inputs are written as $\mathbf{u} = \mathbf{M}\mathbf{w} + \mathbf{h}$.

Remark 8 *We remark that, although perfect state measurements are generally assumed available, still the proposed methods can be used in practice with an estimate of the state, obtained by an observer or a state estimator.*

By parameterizing the control policy as an affine function of the past disturbance sequence, the input constraints of Problem (4) involve uncertainty and they are required to be satisfied for all possible disturbances. The formulation (2.13) set the inputs to be an affine functions of normally distributed disturbances having an unbounded value range. This would result in input constraint violations and then infeasibility in the optimization routine unless $M = 0$. Only in the latter case the inputs can

be constrained to lie within a bounded set. A possible approach to addressing this issue is to relax the hard input constraints and restrict the constraint satisfaction to subsets with prescribed probability levels. Therefore it is necessary to define chance constraints also on the inputs, not only on the outputs. It is desirable to impose a higher probability of satisfaction on input constraints. We denote this probability level by $1 - \alpha_u$. Hence the Problem (4) can be re-written as a closed-loop prediction stochastic MPC (CLP-SMPC) as follows:

Problem 5 (Closed-Loop Prediction SMPC)

$$\begin{aligned} &\min_{\mathbf{M},\mathbf{h}} \mathbf{E}\left[\sum_{k=0}^{N-1} c^T u_k(\mathbf{w}_k)\right] \\ s.t. \\ &\quad \textit{system dynamics } (2.9) \\ &\quad \mathbf{P}\left\{Gy_k \leq g\right\} \geq 1-\alpha \qquad k = 1,\ldots,N \\ &\quad \mathbf{P}\left\{Fu_k(\mathbf{w}_k) \leq f\right\} \geq 1-\alpha_u \qquad k = 0,\ldots,N-1 \\ &\quad u_k(\mathbf{w}_k) := \sum_{j=0}^{k-1} M_{k,j} w_j + h_k \end{aligned} \tag{2.15}$$

Remark 9 *Notice that the cost function in Problem (5) has a normal distribution with expected value equal to* 0 *then it is equal to the linear cost function* $\sum_{k=0}^{N-1} c^T h_k$.

Remark 10 *We remark that the control strategy being considered is a receding horizon policy (see the Appendix D for a brief overview). We solve an optimization problem at each* k *over a horizon of length* N*, but only the first input is actually applied to the controlled system. Since we are considering affine causal controller and the first* m *rows of* $\mathbf{M}$ *are zero, the first control input* $u_0 = h_0$ *is deterministic.*

By setting the block matrix $\mathbf{M}$ to the zero matrix and optimize over only the offsets $\mathbf{h}$, we obtain the following open-loop prediction stochastic MPC (OLP-SMPC):

Problem 6 (Open-Loop Prediction Stochastic MPC)

$$
\begin{aligned}
&\min_{\mathbf{h}} \sum_{k=0}^{N-1} c^T u_k \\
&s.t. \\
&\quad \textit{system dynamics } (2.9) \\
&\quad \mathbf{P}\left\{Gy_k \leq g\right\} \geq 1-\alpha \quad k=1,\ldots,N \\
&\quad Fu_k \leq f \qquad k=0,\ldots,N-1 \\
&\quad u_k := h_k
\end{aligned}
\tag{2.16}
$$

Notice that in Problem (6) we don't need to resort to input chance constraints. As mentioned above, this approach is generally conservative, but it is also significantly less computationally demanding. The next subsection deals with the probabilistic constraints or *chance constraints*. Since they are in general non-convex, we need to investigate how to reformulate them as tractable constraints.

Chance Constraints

Once we choose the control policies, we need to deal with chance constraints for solving the Problem (5). In building climate control there is a natural tradeoff between energy usage and occupant comfort: tighter comfort bounds requires higher energy use. Since the observed weather realizations can differ from their predictions, this tradeoff cannot be given in deterministic terms and we must account for the stochastic nature of comfort satisfaction. Today's building standards require that indoor temperature be maintained within a given bound only with a prescribed probability; European standard bounds on the temperature and illuminance can be found in [2, 3, 12, 37]. This flexibility accounts for both the potential energy-saving benefits of violating constraints from time to time as well as the uncertainty involved in the weather predictions. Conditions of this form can be translated into so-called chance constraints (see the Appendix E). Chance constraints are in general non-convex and difficult to incorporate into an optimization problem since they involve the evaluation of multivariate integrals. There exists, however, a small class that is easier to deal with. In particular, it is well-known that if the disturbance is normally distributed, the functions are bi-affine in the decision variables and the disturbances are considered in the constraints, then the chance constraints can be equivalently formulated as deterministic second order cone constraints (see the Appendix D). While these constraints are convex and hence Second Order Cone Program (SOCP) can be com-

puted efficiently in theory, the investigated control problem involves a large number of variables and its solution can be very time consuming (see 2.5.2 to get an idea of computational times). For this reason, we might need approximated reformulations of the stochastic control problem to reduce the computational burden of the optimization routine. We will next provide a deterministic and convex reformulation of the chance constraints in Problem (5), then we will discuss some approximations of the resulting control problem, which reduce the computational effort of the optimization routine.

Equivalent Second Order Cone Formulation of Chance Constraints

The previous section introduced various common methods in the literature for obtaining a finite convex parametrization of the control law. In this section we examine deterministic convex reformulations of the chance constraints of Problem (5). We consider the augmented model 2.9. We focus on the probabilistic constraints of Problem (5) on y_k and on u_k parameterized as affine function of disturbances. For notational convenience, we define the output vector over the horizon length N:

$$\mathbf{y} := \begin{bmatrix} y_0^T & \cdots & y_{N-1}^T \end{bmatrix}^T$$

where $\mathbf{y} \in \mathbb{R}^{pN}$. We define in the same manner the input vector $\mathbf{u} \in \mathbb{R}^{mN}$, the disturbance vector $\mathbf{w} \in \mathbb{R}^{rN}$, and prediction vector $\hat{\mathbf{v}} \in \mathbb{R}^{rN}$ and finally the offset vector $\mathbf{h} \in \mathbb{R}^{mN}$. Furthermore we define:

$$\mathbf{C} := \begin{bmatrix} C^a \\ C^a A^a \\ C^a (A^a)^2 \\ \vdots \\ C^a (A^a)^{N-1} \end{bmatrix} \quad \mathbf{D} := \begin{bmatrix} D_0^a & \mathbf{0} & \dots & \dots & \dots & \mathbf{0} \\ C^a B_0^a & D_1^a & \mathbf{0} & \dots & \dots & \mathbf{0} \\ C^a A^a B_0^a & C^a B_1^a & D_2^a & \mathbf{0} & \dots & \mathbf{0} \\ \vdots & \vdots & \vdots & \vdots & \vdots & \vdots \\ C^a (A^a)^{N-1} B_0^a & C^a (A^a)^{N-2} B_1^a & \dots & \dots & C^a B_{N-2}^a & D_{N-1}^a \end{bmatrix}$$

$$\mathbf{D_w} := \begin{bmatrix} D_w^a & \mathbf{0} & \dots & \dots & \dots & \mathbf{0} \\ C^a B_w^a & D_w^a & \mathbf{0} & \dots & \dots & \mathbf{0} \\ C^a A^a B_w^a & C^a B_w^a & D_w^a & \mathbf{0} & \dots & \mathbf{0} \\ \vdots & \vdots & \vdots & \vdots & \vdots & \vdots \\ C^a (A^a)^{N-1} B_w^a & C^a (A^a)^{N-2} B_w^a & \dots & \dots & C^a B_w^a & D_w^a \end{bmatrix}$$

$$\mathbf{D_v} := \begin{bmatrix} D_v^a & \mathbf{0} & \dots & \dots & \dots & \mathbf{0} \\ C^a B_v^a & D_v^a & \mathbf{0} & \dots & \dots & \mathbf{0} \\ C^a A^a B_v^a & C^a B_v^a & D_v^a & \mathbf{0} & \dots & \mathbf{0} \\ \vdots & \vdots & \vdots & \vdots & \vdots & \vdots \\ C^a (A^a)^{N-1} B_v^a & C^a (A^a)^{N-2} B_v^a & \dots & \dots & C^a B_v^a & D_v^a \end{bmatrix} \tag{2.17}$$

where $\mathbf{C} \in \mathbb{R}^{pN \times n}$, $\mathbf{D} \in \mathbb{R}^{pN \times mN}$, $\mathbf{D_w} \in \mathbb{R}^{pN \times Nr}$, $\mathbf{D_v} \in \mathbb{R}^{pN \times Nr}$ and $\mathbf{0}$ is a zero matrix with appropriate dimensions. We can express the input and the output vectors over the prediction horizon and given the initial state x_0 in terms of the matrices 2.17:

$$\begin{aligned}\mathbf{u} &= \mathbf{M}\mathbf{w} \ + \mathbf{h} \\ \mathbf{y} &= \mathbf{C}x_0 + \mathbf{D}\mathbf{h} + \mathbf{D}\mathbf{M} + \mathbf{D_v}\hat{\mathbf{v}} + \mathbf{D_w}\mathbf{w}\end{aligned}$$

with $\mathbf{M}$ and $\mathbf{h}$ defined in the subsection 2.4.3. Then the probabilistic constraints on inputs and outputs in the Problem (5) can be rewritten in terms of the matrices 2.17 as follows:

$$\mathbf{P}\left\{\mathbf{F}(\mathbf{M}\mathbf{w} + \mathbf{h}) - \mathbf{f} \leq 0\right\} \geq 1 - \alpha_u \tag{2.19a}$$

$$\mathbf{P}\left\{\mathbf{G}(\mathbf{C}x_0 + \mathbf{D}\mathbf{h} + \mathbf{D}\mathbf{M}\mathbf{w} + \mathbf{D_v}\hat{\mathbf{v}} + \mathbf{D_w}\mathbf{w}) - \mathbf{g} \leq 0\right\} \geq 1 - \alpha \tag{2.19b}$$

where $\mathbf{F} := I_{N\times N} \otimes F$, $\mathbf{f} := \mathbf{1}_{N\times 1} \otimes f$, $\mathbf{g} := \mathbf{1}_{N\times 1} \otimes g$ and $\mathbf{G} := I_{N\times N} \otimes G$ ($\otimes$ is the Kronecker product). The constraints 2.19 are *joint chance constraints*, meaning that all of the inequalities have to hold simultaneously. Unfortunately joint chance constraints are in general non-convex and hard to deal with. Therefore we approximate the joint chance constraints with the following set of *separate chance constraint* [70]: this means that each inequality in 2.19 is considered separately, for $i = 1 \dots Nm, \quad j = 1 \dots Np$:

$$\begin{aligned}&\mathbf{P}\left\{\mathbf{F}_i(\mathbf{M}\mathbf{w} + \mathbf{h}) - \mathbf{f}_i \leq 0\right\} \geq 1 - \alpha_{u,i} \\ &\mathbf{P}\left\{\mathbf{G}_j(\mathbf{C}x_0 + \mathbf{D}\mathbf{h} + \mathbf{D}\mathbf{M}\mathbf{w} + \mathbf{D_v}\hat{\mathbf{v}} + \mathbf{D_w}\mathbf{w}) - \mathbf{g}_j \leq 0\right\} \geq 1 - \alpha_j\end{aligned} \tag{2.20a}$$

where $\mathbf{F}_i$ is the i^{th} row of the matrix $\mathbf{F}$, $\mathbf{G}_j$ is the j^{th} row of the matrix $\mathbf{G}$, $\mathbf{f}_i$ and $\mathbf{g}_j$ are respectively the i^{th} of the vector $\mathbf{f}$ and the j^{th} element of the vector $\mathbf{g}$. The probability levels $1 - \alpha_{u,i}$ and $1 - \alpha_j$ are specified for each individual row, as proposed in [35, 92]. This approach may be rather conservative because it does not account for the fact that the separate chance constraints can be correlated. Since $\mathbf{w}$ follows a normal distribution and the random variables in 2.20 are also normally distributed, it is possible to exploit a classic result in [99] (see the Appendix E for proof details). Therefore the separate chance constraint 2.20 can be formulated as the following equivalent deterministic constraints with $i = 1 \dots Nm, \quad j = 1 \dots Np$:

$$\Phi^{-1}(1 - \alpha_{u,i})\|\mathbf{F}_i\mathbf{M}\|_2 \leq \mathbf{f}_i - \mathbf{F}_i\mathbf{h} \tag{2.21a}$$

$$\Phi^{-1}(1 - \alpha_j)\|\mathbf{G}_j(\mathbf{D}\mathbf{M} + \mathbf{D}_w)\|_2 \leq \mathbf{g}_j - \mathbf{G}_j(\mathbf{C}x_0 + \mathbf{D}\mathbf{h} + \mathbf{D}_v\hat{\mathbf{v}}) \tag{2.21b}$$

where Φ is the standard Gaussian cumulative probability function. The inequalities (2.21) are second order cone constraints that are convex in the decision variables

M and **h**. The Problem (5) can be cast as a convex deterministic second-order cone program (SOCP) with $i = 1 \dots Nm, \quad j = 1 \dots Np$:

Problem 7 (CLP-SMPC as SOCP)

$$\begin{aligned} &\min_{\mathbf{M},\mathbf{h}} \mathbf{E}\left[\sum_{k=0}^{N-1} c^T \left(\sum_{l=0}^{k-1} M_{k,l} w_l + h_k\right)\right] \\ &s.t. \\ &\quad \Phi^{-1}(1-\alpha_{u,i})\|\mathbf{F}_i\mathbf{M}\|_2 \leq \mathbf{f}_i - \mathbf{F}_i\mathbf{h} \\ &\quad \Phi^{-1}(1-\alpha_j)\|\mathbf{G}_j(\mathbf{D}\mathbf{M}+\mathbf{D}_w)\|_2 \leq \mathbf{g}_j - \mathbf{G}_j(\mathbf{C}x_0 + \mathbf{D}\mathbf{h} + \mathbf{D}_v\hat{\mathbf{v}}) \end{aligned} \tag{2.22}$$

where the offset vector **h**, the block matrix **M** as well as each block $M_{k,l}$ have been defined in the subsection 2.4.3. Exploiting the deterministic reformulation of the chance constraints on the outputs given in 2.21, the OLP-SMPC Problem (6) can be formulated as a deterministic linear program:

Problem 8 (OLP-SMPC as LP)

$$\begin{aligned} &\min_{\mathbf{h}} \sum_{k=0}^{N-1} c^T h_k \\ &s.t. \\ &\quad Fu_k \leq f \\ &\quad \Phi^{-1}(1-\alpha_j)\|\mathbf{G}_j\mathbf{D}_w\|_2 \leq \mathbf{g}_j - \mathbf{G}_j(\mathbf{C}x_0 + \mathbf{D}\mathbf{h} + \mathbf{D}_v\hat{\mathbf{v}}) \end{aligned} \tag{2.23}$$

with $j = 1 \dots Np$.

Remark 11 *The probability levels both in Problem (7) and in Problem (8) have to be larger than* 0.5 *in order to obtain a convex optimization problem (see [70], Theorem* 2.5*).*

To summarize, if we parameterize the control input as an affine function of past disturbances that are normally distributed, then a convex deterministic formulation of the original stochastic MPC problem can be derived, which is equivalent in the case of separate chance constraints. The resulting optimization problem is a second-order cone program (SOCP), which then has to be solved at each sampling interval. Although recent results in linear conic optimization provide quite efficient algorithms for solving SOCPs also for large (but non huge) scale problems [7, 79, 90], the complexity can grow quickly with problem size. Exactly how large is 'large' is investigated through simulation in section 2.5 for the particular case study of building control.

In case the equivalent reformulation is not tractable, several approximations can be used. We will next describe some approximations to reduce the computational burden of the optimization routine.

Approximation of Stochastic Model Predictive Control

In this subsection we will discuss some possible ways to reduce the computational complexity of the equivalent deterministic Second Order Cone Problem (7). One way is to reduce the number of degrees of freedom in the optimization routine. In Problem (7) we optimize over each block $M_{k,l} \in \mathbb{R}^{m\times r}$ and each offset $h_k \in \mathbb{R}^{m\times 1}$, for $k = 0 \dots N-1$ and $l = 0 \dots k-1$. The number of optimization variables grows quadratically with the horizon length and can lead to computationally prohibitive optimization. By reducing the number of degrees of freedom in the choice of the optimal input moves other suboptimal strategies can be applied. This sort of approximations of the Problem (7) are described next. The computational issues that could result from some of the proposed approximations will be discussed as well.

M Pre-computation Fixing $\mathbf{M}$ to be a constant matrix, rather than choosing it through an optimization problem online will significantly reduce the size of the problem to be solved. There are many possible heuristics available to choose a particular $\mathbf{M}$ [14, 87], but we here take a pragmatic approach and simply solve problem CLP-SMPC for a certain number of initial states. Then we fix $\mathbf{M}$ to be the average of the resulting solutions; all subsequent optimization problems are solved by replacing $\mathbf{M}$ with the computed average. One must optimize only over the offset vector $\mathbf{h}$, thus the Problem (7) is cast as a linear program. This technique reduces significantly the computational effort, however it can lead to infeasibilities due to the fact that the bounds on the outputs are time-varying. Denote by $\mathbf{M}_c$ the constant block matrix obtained from the pre-processing step described previously. Taking $\mathbf{M}_c$ for $\mathbf{M}$ the constraints in 2.21 can be re-written as follows:

$$\mathbf{F}_i\mathbf{h} \leq \mathbf{f}_i - \Phi^{-1}(1-\alpha_{u,i})\|\mathbf{F}_i\mathbf{M}_c\|_2 \tag{2.24a}$$

$$\mathbf{G}_j\mathbf{D}\mathbf{h} \leq \mathbf{g}_j - \mathbf{G}_j(\mathbf{C}x_0 + \mathbf{D}_v\hat{\mathbf{v}}) - \Phi^{-1}(1-\alpha_j)\|\mathbf{G}_j(\mathbf{D}\mathbf{M}_c + \mathbf{D}_w)\|_2 \tag{2.24b}$$

with $i = 1 \dots Nm, \quad j = 1 \dots Np$. Clearly only $\mathbf{h}$ contains the decision variables. Since $\mathbf{f}$ and $\mathbf{g}$ contain upper and lower limits on the actuators and on the outputs, the constraints 2.24 actually both impose different upper and lower bounds on the offset vector $\mathbf{h}$. Hence it is likely to have inconsistency in the constraints 2.24 because the bounds on the outputs can vary over time. A way of addressing this issue could

be to soft input constraints and output constraints as well and to add high violation penalties in cost function (a more detailed described of soft constraints can be found in the Appendix D).

M with Banded Structure As proposed in [81], the number of decision variables can be reduced by restricting the bandwidth of the matrix $\mathbf{M}$:

$$\mathbf{M}_b := \begin{bmatrix} 0 & \dots & \dots & \dots & \dots & 0 \\ M_{1,0} & 0 & \dots & & \dots & \vdots \\ \vdots & \ddots & \dots & & \dots & \\ M_{b,0} & \cdots & M_{b,b-1} & 0 & \dots & \vdots \\ 0 & \ddots & \ddots & \ddots & & \\ \vdots & & \ddots & \ddots & \ddots & \vdots \\ 0 & \cdots & M_{N-1,b} & \dots & M_{N-1,N-2} & 0 \end{bmatrix}$$

This structure corresponds to parameterizing the control policy to be an affine function of the previous b disturbances. The CLP-SMPC problem still stays a second order cone problem but its complexity can be significantly reduced. In particular, the smaller is b, the smaller is the number of constraints and optimization variables. The Figure 2.3 shows the sparsity structure of the disturbance feedback matrix $\mathbf{M}$ for the Problem (5) with prediction horizon $N = 24$, one disturbance and different bands b, i.e. $b = 2$, $b = 8$ and a full band $b = N = 24$. The plot is produced by the Matlab SPY function, which is useful to view the distribution of the nonzero elements within a sparse matrix. Notice that the number of optimization variables contained in the matrix $\mathbf{M}$ grows from 282 to 1800 as b increases from 2 to 24. This shows clearly the rate of increase in decision variables. In the next subsection we will briefly digress on the solver employed for the optimization routine and some numerical difficulties in the computation if the control inputs.

2.4.4 Computational Aspects

Efficient solvers are available on the Matlab platform for linear, quadratic and conic optimization. We used for our experiments the MOSEK optimization toolbox for Matlab [10], a full-featured optimization package including a primal-dual interior-point algorithm for linear and conic optimization problems, which has a polynomial-time complexity [7, 8]. MOSEK is particulary efficient on large-scale and sparse problems

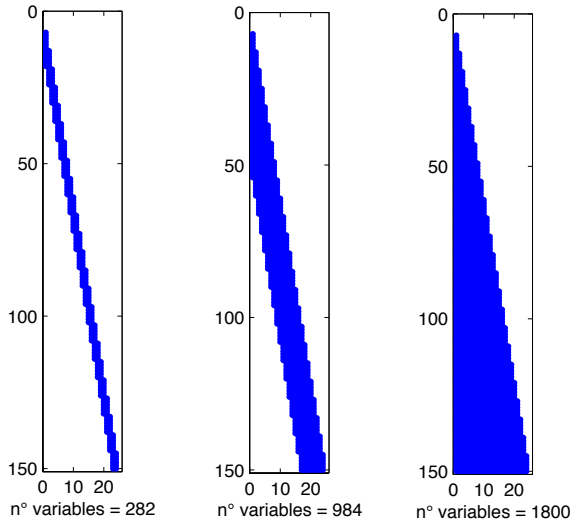

Figure 2.3: Different banded structures of $\mathbf{M}$ for the Problem (5) with prediction horizon $N = 24$ and one disturbance

as the problem we have to solve. It has a state of the art customized solver for conic optimization problems. MOSEK can be downloaded for research and evaluation purposes at **http://www.mosek.com**. Both the linear and the conic optimizer can be affected by numerical issues due to several reasons, such as:

- problems containing data with very large and very small coefficients are often hard to solve: significant digits might be truncated in calculations with finite precision, which can make calculations the optimizer rely on inaccurate;
- even well scaled problems can be numerical hard to solve if they have a certain structure making them numerical unstable.

Due to numerical finite precision, if the optimizer cannot compute a solution that has the prescribed accuracy, then it will relax the termination tolerances or apply a tiny perturbation to the problem data such that the perturbed problem has a solution. If the solution then satisfies the termination criteria, the solution is denoted near optimal [10]. In the linear case this can never occur, while this has been seen to occur often when the optimization problem involves second order cone constraints (CLP-SMPC and $\mathbf{M}_b$-SMPC strategies). In this case the interior-point optimizer must exploit a more complex and troublesome algorithm than the linear case (OLP-SMPC

and $\mathbf{M}_c$-SMPC controllers) and the optimal solutions is harder to provide (see [8] for details).

Degeneracy and Infeasibility Degeneracy might occur in linear optimization and then multiple optima will be available at each iteration of the SLP algorithm. For example, it might happen during the nighttime, when the blind position does not matter because there is no solar radiation. This can have a negative effect on bilinearity treatment and prevent the SLP algorithm C.1.1 from the convergence; it would be hard to compute a sequence of approximations converging to the original optimal solution. To avoid degeneracy in linear approximations of 7 or in OLP-SMPC Problem (8), we can perturb or "regularize" the linear program and improve the bilinearity convergence by adding a quadratic term in the objective [56], [106]. The perturbed objective function in linear approximations of 5 is:

$$\sum_{k=0}^{N-1} \left(c^T h_k + \gamma h_k^T h_k \right)$$

where γ is a positive scalar intended to be "small". It has been found that $\gamma = 10^{-3}$ is a good choice [106]. We further need to face infeasibility problems. Infeasibility can occur both in second order cone programs and in linear problems. Feasibility analysis concerns the problem of whether the chance constraint is feasible. In this case the optimization routine cannot find a feasible solution. A possible approach is to treat the output constraints as soft constraints (see the Appendix D for an overview on soft constraints). Therefore constraint violations are allowed but also penalized in the objective function in order to keep violations as small as possible. If violations are not necessary, the original problem will be solved. Notice that the objective function in the MPC problems previously formulated becomes quadratic and then the optimization problem to be solved at each SLP iteration becomes a little more complex, but still efficiently solvable.

Remark 12 *We remark that we solve a certain number of linear MPC subproblems every hour according to the Sequential Linear Programming algorithm C.1.1: each resulting subproblem to solve can be either a LP, QP or a SOCP, it depends on the original nonlinear optimization problem. The investigated methods are applied to a MPC based on a stochastic linear model; each subproblem can be efficiently solved, although the computational burden of the overall optimization procedure can be prohibitive in case of SOCP.*

In the following sections the proposed control strategies will be assessed and compared to some current controllers and to a theoretical benchmark, called *performance bound* (PB). The simulation results presented next will demonstrate the potential benefits in indoor climate control thanks to the use of stochastic predictive control.

2.5 Simulation Results

We aim at comparing the control strategies based on an MPC framework with both current practice and the defined benchmark in terms of energy savings, constraint violations and computational complexity. We will consider next a single, industrially relevant case study in detail and we will examine the performance of the above controllers on this case via simulation. We will provide the sequence of investigations for choosing the most suitable controller for the case study. We also made the assumption that the model states are observable and measured and the building model parameters are perfectly known. Before investigating the control performance, we will define the experimental setup and test the goodness of fit of the model of the error in weather predictions. The modeling and simulation software BACLab developed by the OptiControl team was employed to simulate the building dynamics under several control strategies. The simulations were performed on an *Intel Core Duo* processor with a clock frequency of 2.0 GHz.

Remark 13 *We point out that, although a one single case is not yet representative, the simulation results presented in this section are consistent with the ones shown in [50],which presents and analyzes several simulation experiments. Moreover, in this section, we mainly aim at showing how the best controller for a given case study can be selected. The simulations in [50] were carried out over a year for two sets of* 18 *meaningful selected cases involving different building attributes and different locations. Predictive and non-predictive control strategies were compared via simulation according to defined performance criteria. The comparison involved the the best possible non-predictive control strategy currently known so far (Rule-Based Controller-*4*). Looking at the simulated cases it was concluded that the stochastic predictive control can gain more in terms of a tradeoff between energy use and violations. The simulation results further suggest that the performance of SMPC controllers are robust against model parameter mismatch.*

2.5.1 Performance Criteria and Assessment Procedure

A brief description of the controllers that are investigated by the simulation analysis is provided in the followings:

- **Performance Bound (PB)**: the ideal controller used as theoretical benchmark. There are no uncertainties in the model parameters and in the system dynamics. A perfect knowledge of future weather is assumed. This ideal controller cannot be implemented in reality, it is more a concept. The performance bound is computed by solving the MPC problem considering the weather predictions as perfect, in the sense that there is no uncertainty in the predictions and a long prediction horizon (6 days);

- **Certainty Equivalence MPC (CE-MPC)**: the CE-MPC is a control strategy based on MPC. The optimization problem to solve is the deterministic Problem (3). In the controller the uncertainty is simply neglected;

- **Closed-Loop Prediction MPC (CLP-SMPC)**: the CLP-SMPC is a control strategy based on stochastic MPC. The optimization problem to solve is the Problem (7). No approximations of the feedback disturbance matrix $\mathbf{M}$ are considered;

- **Closed-Loop Prediction Stochastic MPC with $\mathbf{M}_b$ ($\mathbf{M}_b$-SMPC)**: the CLP-SMPC is a control strategy based on stochastic MPC. The optimization problem to solve is the Problem (7) with the *banded structure* approximation of the feedback disturbance matrix $\mathbf{M}$;

- **Closed-Loop Prediction Stochastic MPC with $\mathbf{M}_c$ ($\mathbf{M}_c$-SMPC)**: the CLP-SMPC is a control strategy based on stochastic MPC. The optimization problem to solve is the Problem (7) with the pre-computed and constant approximation of the block matrix $\mathbf{M}$. The chance constraints are then reformulated as approximated linear deterministic constraints. In particular, by setting the block matrix $\mathbf{M}$ to the zero matrix the open-loop prediction MPC (OLP-SMPC) is obtained;

- **Ruled-Based Controller (RBC)**: the rule-based controller is based on a non-predictive control strategy. This controller is the current practice and it is also employed by Siemens Building Technologies as well as a standard certainty equivalence MPC controller for the studied buildings. This rule-based controller decides about the position of the blinds and the operation of the evaporative

cooling based on a series of rules of the kind "if condition then action". When blind position and operation of evaporative cooling are fixed, a one step MPC with perfect weather forecast (=observed weather data of future step) is run in order to mimic an underlying PID controller. The RBC requires a simple implementation but a great tuning effort: determining a good set of rules is critical for a good performance of this controller. Clearly, by defining more complicated rules, the RBC can improve the performance. More details on rule-based control strategies can be found in [52].

The cost function represents the Non-Renewable Primary Energy (NRPE). The control target is to satisfy constraints with a minimum amount of the NRPE. In order choose the most effective controller, the assessment of the controllers described above is split in two parts:

1. first all the control strategies based on the stochastic MPC framework are investigated (CLP-SMPC, $\mathbf{M}_b$-SMPC, $\mathbf{M}_c$-SMPC, OLP-SMPC);
2. once the best formulation of the stochastic MPC has been chosen, this will be further compared to industry standard strategies as well as to certainty equivalence control.

In the assessment procedure, the control performance is analyzed considering:

- the primary energy (NRPE) usage;
- the constraint violations;
- the tunability of the investigated controller;
- the computational effort of the corresponding optimization routine.

Different probability levels of constraint satisfaction are considered to point out the tunability of the stochastic MPC. Namely it is possible to achieve a better tradeoff between energy use and constraint violations by simply tuning the parameter α, i.e. by choosing a more appropriate probability level. For example $\alpha = 0.1$ implies that the comfort levels have to be met in 90% of the cases. A higher constraint satisfaction probability results in a more conservative behavior, i.e. it provides less violations at the cost of spending more energy. However there is a limit in the achievable tradeoff between energy usage and violations because the tuning parameter α has to be less than 0.5 to obtain a solvable optimization problem. To select the most suitable control strategy for the specific application also the computational effort of the optimization

routine must be accounted for. If a control strategy results in less energy use and less violations compared to another strategy, that strategy will clearly be more efficient, but the corresponding computational burden must not be excessive. As a matter of fact, the investigated predictive control strategies exploit a receding horizon scheme and the SLP iterative procedure is applied to obtain a linear model in the optimization routine; this leads to solve one single optimization problem several times per each hour. Therefore, the assessment procedure is performed as follows:

1. compute the energy usage and the constraints violations for each controller. If the controller can be tuned, compute the energy usage and the constraints violations for some representative values of the tuning parameters;

2. if the violations are acceptable and the controller can be tuned, choose the tuning that leads to the smallest energy use.

3. if the violations are kept within standard tolerability limits, select the control strategy taking shorter computational time, even if there is a small increase in energy usage. How small is "small" can depend on the specific application.

To summarize, simulation analysis can help to address the problem to find which formulation of the stochastic MPC problem leads to the best performance in terms of energy use and occupant comfort while being sufficiently computationally tractable for the case of building climate control. We will next describe the case study and the simulation environment BACLab, which all the simulation plots and results presented in this section are obtained by.

2.5.2 Simulation Environment and Setup

A common and spread building type was selected as case study for the simulation analysis. The description of the simulation environment has been extracted from the OptiControl Two Year Report [47]. The BACLab, a MATLAB-based modeling and simulation environment developed in the OptiControl project [48], allows to simulate and investigate many realistic situations involving many different types of zones/rooms. As already mentioned, in this work we focus on Integrated Room Automation (IRA), which deals with the control of individual building zones or rooms. According to to the practice employed in design tools such as SIA 382/1 [2] and SIA 380/4 [3], the energy and air dynamical behavior is affected to a small extent by the room/zone interconnection. Therefore the overall building energy savings can

be studied by integrating multiple zone models. In the simulation environment BACLab a building type can be defined by selecting its features from the following set of room/zone attributes:

- facade orientation: North, South, South-West, South-Est;
- construction type: Heavyweight, Lightweight;
- building standard: Swiss Average, Passive House;
- window area fraction of the facade: 30% window area per facade, 80% window area per facade.

The construction type attribute is related to the internal dynamic heat capacity of the room/zone (80 $\frac{Wh}{m^2K}$ for "Heavyweight" and 36 $\frac{Wh}{m^2K}$ for "Lightweight"). The building type attribute is related to a bigger or smaller overall heat transfer coefficients both of opaque facade parts and of windows: in the "Swiss Average" standards both heat transfer coefficients are significatively larger than in the "Passive House" standard. Combining these attributes it is possible to cover many different building types. The most common building types are:

- Type 1: Passive House, Heavyweight, 80% window area per facade, either North or South orientation;
- Type 2: Heavyweight, 30% window area per facade, either North or South orientation.

Another important key factor in building classification is the number of automated control actions available in the room/zone. The number of control inputs goes from 6 to 10 and consists of automated blinds and light, both low and high heating/cooling energy sources, natural/mechanical ventilation Different comfort ranges for temperature, illuminance and CO2 concentration (given as the main indicator for air quality) are provided from European standards [2], [3], [37], [12]. For the illuminance comfort only a lower threshold (500 lux) is applied, because a manual adjustment of internal blinds is assumed on case of excess incoming solar radiation. The bounds on temperature and illuminance can be either constant or time-varying because dependent on working hours, which are determined from the occupancy schedule. We used hourly profiles from the Swiss standards [4], [5] for cellular offices. The simulation setup for the case study is reported in the following:

- system building with no ventilation action;

- hourly time step;
- daily prediction horizon $N = 24$;
- year 2007;
- zurich (MeteoSwiss);
- office building;
- south Orientation and Swiss average building type (heavyweight);
- 30% window fraction area;
- high occupancy;
- illuminance bounds occupancy dependent;
- temperature bound working hour schedule dependent;
- tuning of the stochastic controllers: the controller based on stochastic MPC were run with different values of the tuning parameter α to set different thermal and illuminance comfort levels.

The chosen building attributes belong to one of the most common and spread building types. The simulated room belongs to a passive house with large window areas in a south orientation. This is one case study to test the suitability of the proposed control strategies. The discussed control methods were applied to the time-varying building model described in (2.9), with model parameters defined by the Building Technologies Laboratory (EMPA).

2.5.3 Goodness of Fit of Weather Uncertain Model

The weather applied to the building was recorded hourly in Zurich during January 2007 and historical predictions for the weather were also made available by MeteoSwiss for the considered period. Since it is sufficient to consider the uncertainty only in the solar radiation prediction (see the subsection 2.3.2), we need to identify the parameters H and K in the error model 2.8 for the simulation horizon, i.e. January 2007, and for Zurich. For this purpose we have investigated the error in solar gain predictions from hourly solar gain measurements and predictions taken from the MeteoSwiss station at Zurich over the entire year of 2006. The investigations are carried out as follows

1. define a suitable model for the data by detecting the data pattern. For this purpose, the 1-step lag plot is exploited;
2. fit the model of data by employing an identification toolbox;
3. test the randomness of the residuals to evaluate the correctness of the model fitting the error data.

The Figure 2.4(a) depicts the 1-step lag plot come out of the empirical error in solar gain prediction (i.e. measurements-predictions over 2006 at Zurich). A lag is a fixed time displacement. Lag plots can be generated for any arbitrary lag, although the most commonly used lag is 1; for the investigated case a lag is a 1 hour time displacement. Then the Figure 2.4(a) shows the observed prediction error at time k^{th} hour given its value at time $(k-1)^{th}$ hour. The lag plot exhibits a linear pattern. This means that the data have a strong autocorrelation and further suggests that an autoregressive model might be appropriate. We have used MATLAB's Identification Toolbox to fit an autoregressive linear model of the error in solar gain predictions, obtaining $H = 0.6232$ and $K = 129.35$. One way to assess the goodness of fit is to investigate the randomness of residuals, i.e. the deviation of the observed errors from the fitted error values. The Figure 2.4(b) shows the autocorrelations for residual values at different lags up to 100; each lag is a 1 hour time displacement. We can used this plot to test that there are no time dependance in the residuals, i.e. the residuals are random. If random, such autocorrelations should be near zero for any lag [105] and the section 3 of [93]). The Figure 2.4(b) depicts the autocorrelation for forecast error identification. The red dotted lines in Figure 2.4(b) are the 99% confidence bands. Almost all of the autocorrelations fall within the 99% confidence limits (the autocorrelation at lag 0 is equal to 1 per definition). As a conclusion, the assumption of randomness of residuals is reasonable as well as the model fitting the error in solar gain predictions. Finally, it is reasonable to assume no violations in the illuminance as the user would immediately adjust the light level according to the comfort bounds. Therefore the room illuminance is corrected at each hour to mimic the user behavior [50].

2.5.4 Stochastic MPC Controller Comparison

We investigate all the control strategies based on the stochastic MPC framework (SMPCs):

- CLP-SMPC;

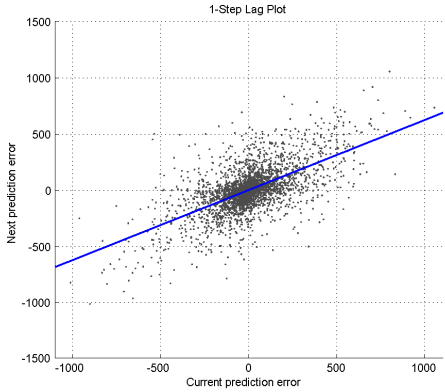

(a) 1-Step Lag Plot (hours)

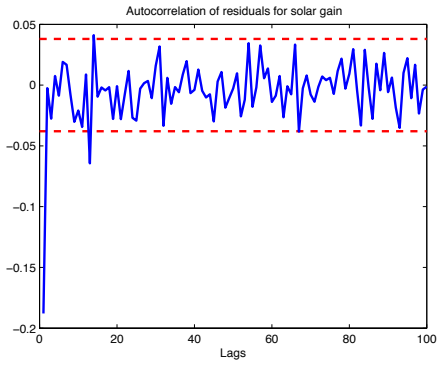

(b) Residual autocorrelation for solar radiation ($\frac{W}{m^2}$)

Figure 2.4: Lag plot and residual autocorrelation for solar radiation.

- $\mathbf{M}_b$-SMPC with $b = 2$;
- $\mathbf{M}_b$-SMPC with $b = 8$;
- $\mathbf{M}_c$-SMPC;
- OLP-SMPC.

The optimization routine was run with an hourly time step, a prediction horizon of $24h$ and for January 2007. The controllers listed above can be tuned by assigning a specific value to the parameter α; by doing so the constraint satisfaction probability is set. The prediction horizon can also be changed; usually a longer prediction horizon usually improves the controller performance, but this can come at the cost of a significative increase in computational time. Once the controller is selected, further investigations n the prediction horizon should be performed. We will next describe the procedure to set the number of optimal feedback matrices for the $\mathbf{M}_c$-SMPC controller, then the comparison among all the control strategies listed above will be provided.

$\mathbf{M}_c$-SMPC Controller Consider the $\mathbf{M}_c$-SMPC strategy: the affine disturbance feedback matrix is first optimized over a given time period ΔT, then the average over the obtained optimal feedback matrices is computed and fixed for the subsequent optimization. We carried out several tests with different time periods aiming at

investigating how the controller performance is affected by the choice of ΔT. We considered three ΔT:

1. ΔT_1 = the first week of January 2007;
2. ΔT_2 = the first day of January 2007;
3. ΔT_3 = four days of 2006, each one representative of a season.

Optimization was done with an hourly time step, a prediction horizon of $24h$ and different values of the tuning parameter ($\alpha = [0.01,\ 0.1,\ 0.2]$). For the sake of brevity, the simulation plots are not depicted. The results showed that the difference in terms of energy usage and violations relative to the ΔT with minimum energy use was at most 1%. Then it is enough to optimize over a single day, and likely over a shorter time period, to compute the fixed $\mathbf{M}_c$. In conclusion the choice of the time period ΔT seems not to affect in general significatively the controller performances.

The controllers are assessed as follows:

1. the energy usage and the constraint violations for several values of the parameter α are computed in order to properly tune each controller. The Figures 2.5, 2.7(b). and 2.6(a) are useful for this purpose;
2. the computational aspects are analyzed by exploiting the Table 2.1 and Figure 2.7(a);
3. the effect of the prediction horizon on the controller performance is investigated through the Table 2.2.

The three investigations mentioned above are discussed into detail respectively in the following three paragraphs.

The *Tuning Curve*

The Figure 2.5 compares the SMPC strategies in terms of energy use and violations with the different tuning settings: the energy usage is plotted versus the number of violations and the amount of violations respectively. The amount and the number of violations are defined as the sum of the upper and the lower bounds violations of the comfort band. The SMPCs were run with different values of the tuning parameter $\alpha = [0.001,\ 0.005,\ 0.008,\ 0.01,\ 0.05,\ 0.08,\ \ 0.1,\ 0.2]$: therefore eight values are depicted per each controller on the Figure 2.5. One can see that a smaller value of α,

which corresponds to a higher constraint satisfaction probability, has more primary energy use but fewer violations. Consider, for example, the $\mathbf{M}_c$-SMPC controller (red rotated squares): a curve can be easily drawn, going from the first red rotated square on the top right ($\alpha = 0.001$) to the last one on the bottom left ($\alpha = 0.2$). We can drawn this curve for any controller; we will refer to this curve as *tuning curve*. The stochastic MPC methods can achieve a tradeoff between energy use and probability of constraint violations by moving along the tuning curve. As expected, the control strategies optimizing over the disturbance feedback matrix $\mathbf{M}$ and then solving a second order cone problem, i.e. CLP-SMPC and $\mathbf{M}_b$-SMPC, outperform the controllers fixing $\mathbf{M}$ either to the zero matrix or to a constant matrix, i.e. $\mathbf{M}_c$-SMPC and OLP-SMPC, both in terms of energy usage and violations. The CLP-SMPC and $\mathbf{M}_b$-SMPC controllers show a larger NRPE usage than both $\mathbf{M}_c$-SMPC and OLP-SMPC, and also an increase in the amount and the number of violations. One can further see that the rotated squares corresponding to CLP-SMPC and $\mathbf{M}_b$-SMPC controllers (blue, magenta and yellow) are very close: this is more evident in Figure 2.7(b). The Figure 2.6(a) illustrates more clearly how to achieve a better tradeoff between energy use and violation by acting on the tuning parameter *alpha*: the plot shows the energy usage and the amount of violations versus the comfort level for January 2007 when the $\mathbf{M}_c$-SMPC controller is applied. Consider that $alpha = 0.1$ corresponds to a comfort level of 90%. It can be seen that if one increases the comfort level, which is equivalent to decreasing *alpha*, the energy usage will increase as well at the cost of much violation. It is preferable to select the biggest α resulting in admissible violations in order to keep the energy consumption as small as possible. The Figure 2.6(b) shows how the energy usage for the year 2007 can be reduced by decreasing the comfort level and allowing a larger and still admissible amount of violation, when $\mathbf{M}_c$-SMPC is applied. The tuning curve both of $CLP-SMPC$ and $\mathbf{M}_b$-SMPC controller, which have conic constraints, exhibits a countertrend for some α values. This behavior needs to be further investigated: from a certain point on further increase in the constraint satisfaction level seems to lead to an small increase of NRPE usage. This results could be related to active soft constraints and to some numerical problems in the underlying optimization procedure, as discussed in the subsection 2.4.4.

Conclusions The performance of CLP-SMPC, which was run with the conic constraints 2.21 without any approximation, are superior, despite a countertrend occurs for some α values. It is evident from the Figure 2.7(b) that the difference in per-

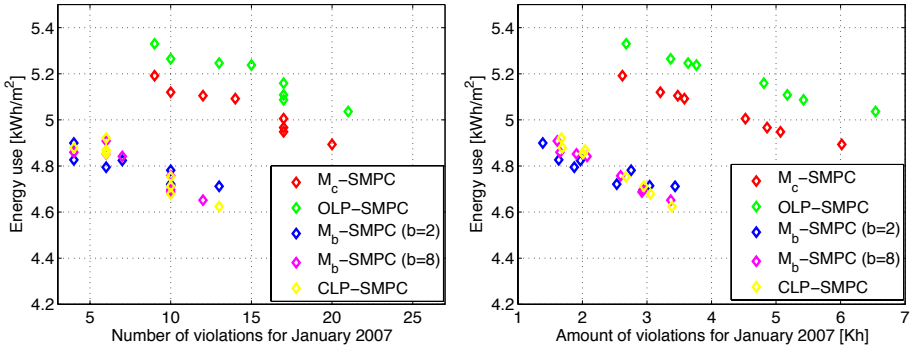

(a) NRPE versus number of violations (b) NRPE versus amount of violations

Figure 2.5: Comparison of SMPC strategies for January 2007

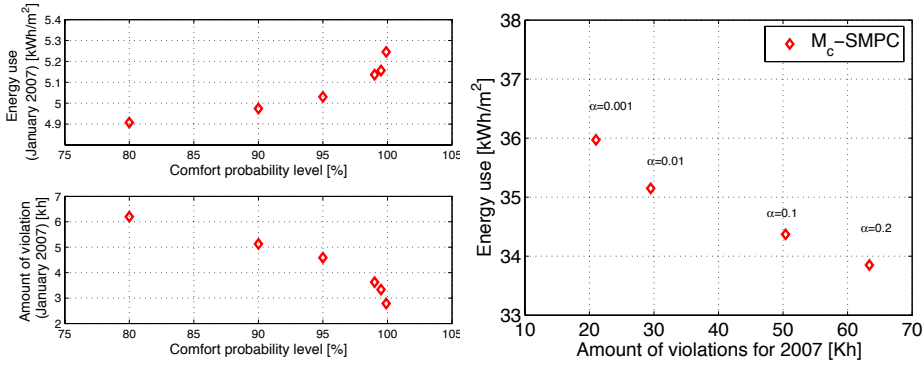

(a) Energy use and amount of violation versus comfort levels for January 2007 (b) Energy use versus amount of violation with different comfort levels for 2007

Figure 2.6: Energy use and violations versus comfort levels when the $\mathbf{M}_c$-SMPC controller is applied.

formance between CLP-SMPC and $\mathbf{M}_b$-SMPC is negligible for the case study; it would be preferable to use the controller resulting in the smallest computational burden ($\mathbf{M}_b$-SMPC with $b = 2$, as shown next). The Figure 2.5 further shows that $\mathbf{M}_c$-SMPC performs better than OLP-SMPC: in particular OLP-SMPC results in a larger NRPE usage than $\mathbf{M}_b$-SMPC, and also has a clear increase in the amount of violations. While it is easy to make a decision between CLP-SMPC and $\mathbf{M}_b$-SMPC, it is not so straightforward to select the more suitable controller among all the investi-

gated SMPC strategies. For this purpose, we need to look into the computational time taken for solving the single optimization problem underlying the SMPC controllers.

Computational Burden for Stochastic MPC Controllers

We need to investigate how different approximations might help to reduce the computational burden and the resulting cost in terms of performance. The superior performance of the control formulations based on a Second Order Cone Problem (7) comes at the cost of much larger computation time, a comparison of which is given in Table 2.1 for different prediction horizons. The conic constraints have to be converted into a specific form to obtain a convex and solvable optimization problem by introducing additional variables and linear constraints. We provide an example of the size of the modified problem in case of CLP-SMPC strategy, which has conic constraints, for $N = 24$:

- constraints number: 6237;
- variable number: 7881.

Then the CLP-SMPC controller yields a very large increase in problem size and in computational time compared to the other strategies. The Table 2.1 provides an overview of the single optimization problem underlying each controller. Applying a banded structure for the feedback disturbance matrix ($\mathbf{M}_b$-SMPC) can reduce significantly the computational burden (see the case with $b = 2$), but it is still problematic. Since each single optimization problem described in the Table 2.1 has to be solved several times per each hour, the computational burden of a SOCP can make it not applicable to an online optimization as the problem size grows. In the building case, this is especially true if a prediction horizon longer than one day is taken into account, as seen in the Table 2.1. The OLP-SMPC and $\mathbf{M}_c$-SMPC controllers are pretty much preferable from a computational point of view. Since the performance of $\mathbf{M}_c$-SMPC is superior (see the Figure 2.5), it can be considered the most suitable controller applicable to the case study. This is also shown in the Figure 2.7(a), which depicts the percentage of energy usage versus the yearly computational time for the 90% comfort level. The percentage is computed accounting for the relative difference with the performance bound (PB). A prediction horizon $N = 24$ and 3 iterations per each hour are assumed in the optimization routine. The Figure 2.7(a) shows that a higher energy consumption is the result of reduced computation time.

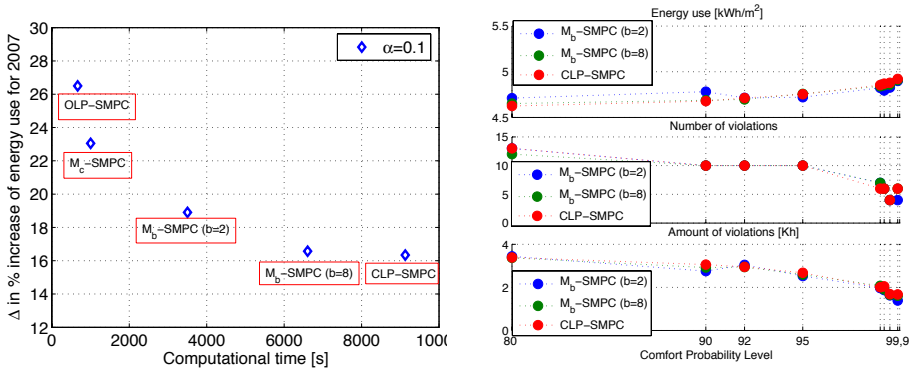

(a) Percentage of increase of energy use versus computational time for 2007

(b) Comparison of CLP-SMPC and $\mathbf{M}_b$-SMPC strategies for January 2007

Figure 2.7: Comparison of SMPC strategies for 2007

Conclusions The linear stochastic MPC formulations, OLP-SMPC and $\mathbf{M}_c$-SMPC, result in higher energy consumption with respect to the CLP-SMPC strategy, while the difference in computational time is very large; for example, the overall computational time is about 16 minutes for $\mathbf{M}_c$-SMPC and more than 2 hours for CLP-SMPC. Moreover the linear stochastic MPC formulations, OLP-SMPC and $\mathbf{M}_c$-SMPC, can result in an energy consumption comparable to the CLP-SMPC strategy if a little more violations are allowed. Therefore, the $\mathbf{M}_c$-SMPC is preferable because it outperforms OLP-SMPC in terms of energy use, while the difference in computational time is quite small.

Effect of Different Prediction Horizons

The Table 2.2 shows the performance of $\mathbf{M}_c$-SMPC with different prediction horizons. To report the computational time, only 3 iterations per each hour and January 2007 have been considered.

Conclusions Despite a longer prediction horizon usually improves the controller performance, as shown in the Table 2.2 a prediction horizon longer than $N = 24$ does not really improve the performance of the controller in this particular case because of too small differences compared to the increase in computational time (some slight countertrend is likely due to numerical problems). It is however very likely that there are other buildings, e.g. with active storage elements, where a longer prediction hori-

zon of several days might be more beneficial. This makes the $\mathbf{M}_c$-SMPC controller even more preferable.

The room temperature resulting from the application of the $\mathbf{M}_c$-SMPC and the CLP-SMPC controller is depicted to further prove that the $\mathbf{M}_c$-SMPC controller must be chosen for this case study. The Figures 2.8 show the resulting room temperature over the period of January 2007 with $\alpha = 0.1$ for CLP-SMPC (2.8(a)) and for $\mathbf{M}_c$-SMPC (2.8(b)). The room temperature evolution are very similar for both controllers. The Figure 2.12 depicts the disturbances that are acting on the building: external and wet bulb temperature, solar gains, illuminance as well as internal heat gains by occupants and equipment. One can see that the chance constraint leads to occasional violations of the temperature comfort bounds. Since the external temperature is quite low, the room temperature is kept close to the lower bounds in order to use as less high cost heating as possible. Then the violations of the lower bounds are found to be more frequent: the amount of violations is always less than $1K$ for both controllers. It can be also seen that there are no very large temperature changes, which is favorable to the occupants. The peaks in the room temperature correspond to the peaks in solar radiation. The application of the CLP-SMPC controller does not seem to significatively improve the room temperature profile with respect to $\mathbf{M}_c$-SMPC. Hence, as the computational burden of $\mathbf{M}_c$-SMPC is more attractive, this controller will be selected for the comparison with both the performance bound and the current practice. The next subsection will provide the comparison between the selected stochastic MPC controller and standard controllers via simulation for the case study.

2.5.5 Comparison with Industry Standards

Once we have selected the most favorable stochastic MPC controller, M_c-SMPC, we compare it with:

- the most typical, broadly applied state-of-the-art of Integrated Room Automation, i.e. *rule-based control* (RBC);
- the standard certainty equivalence MPC controller (CE-MPC);
- the ideal controller (PB),

to finally assess the control performance. The industry-standard rule-based controllers has been developed by Siemens Building Technologies as well as a standard certainty

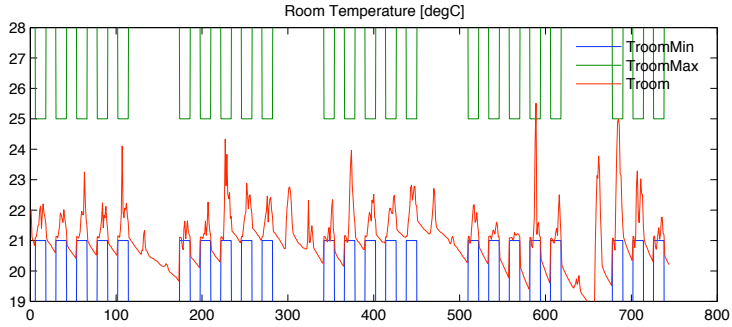

(a) CLP-SMPC with $\alpha = 0.1$

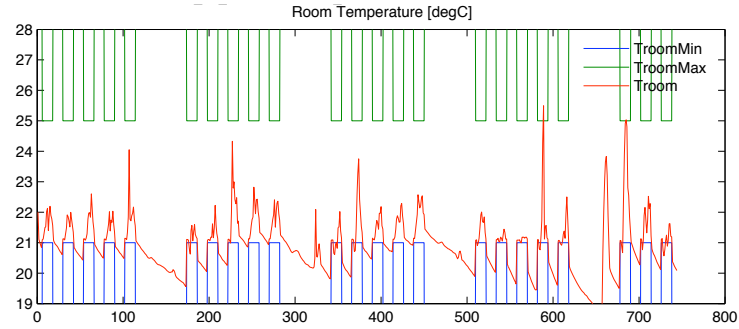

(b) $\mathbf{M}_c$-SMPC with $\alpha = 0.1$

Figure 2.8: Room temperature for January 2007

equivalence MPC controller for the studied building. The M_c-SMPC was run for different value of *alpha* to show the benefits of the tunability of the stochastic predictive controllers.

In order to evaluate the M_c-SMPC controller performance, the European standards about tolerable violations need to be considered: standard tolerable amount of violations are 20 Kh per year for the lower bound and 50 Kh for the upper bound per year, i.e. total amount of 70 Kh per year.

The following plots will show which controller meets the standards:

- the Figure 2.9: it depicts the comparison of the control strategies mentioned above in terms of energy use and violations for the year 2007. The red line in the Figure 2.5(a) is relative to the standard limit for the amount of violation (70 Kh);
- the Figure 2.10 shows the energy use versus the amount of violations of upper bounds (2.10(a)) and lower bounds (2.10(b)). The red line both in the

Figure 2.10(a) and in the Figure 2.10(b) is relative to the standard limits respectively for the upper (50 Kh) and lower bound violation (20 Kh).

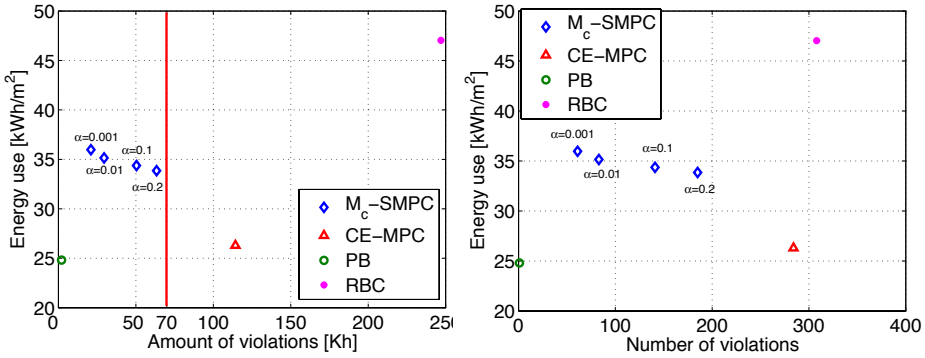

(a) NPRE versus amount of violations (b) NPRE versus number of violations

Figure 2.9: Comparison of PB, RBC, CE-MPC and M_c-SMPC for 2007

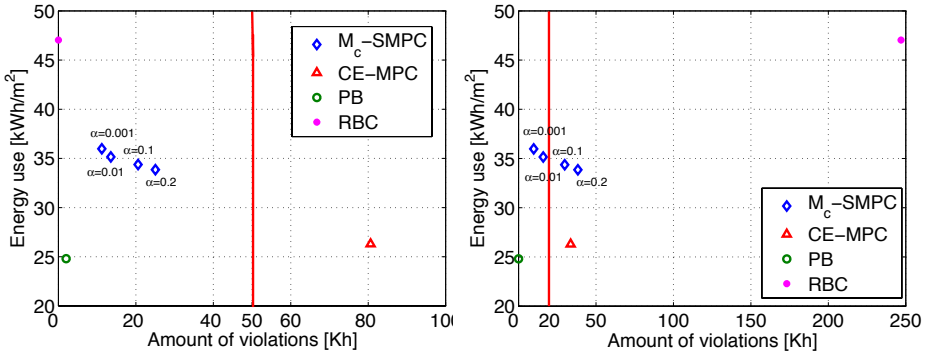

(a) NPRE versus amount of upper bound violations (b) NPRE versus amount of lower bound violations

Figure 2.10: Comparison of PB, RBC, CE-MPC and M_c-SMPC for 2007

From the above plots we can learn that:

- from the Figure 2.9: it can be seen that PB shows practically no violations and requires a very low NRPE usage. The other strategies use more energy and have violations. The RBC controller requires a very large energy use and

has much more violations both in terms of amount and number; this controller exceeds 70 Kh per year of amount of violation. Then RBC does not exhibit good performance for the case study. The CE-MPC control strategy results in a smaller NRPE usage than M_c-SMPC but also a very large increase in both the amount and the number of violations. To make a decision between CE-MPC and M_c-SMPC we have to look into the tolerability of violations. The plot shows that CE-MPC exceeds 70 Kh per year of amount of violations. The amounts of violations for M_c-SMPC are always less than 70 Kh. Further we have to check if the tolerability limits for upper and lower bounds are satisfied;

- from the Figure 2.10: it can be seen that CE-MPC exceeds both 20 Kh for the amount of lower bound violations and 50 Kh for the amount of upper bound violations. The amounts of upper bound violations for M_c-SMPC are always less than 50 Kh, but the amounts of lower bound violations exceed the limit 20 Kh for $\alpha = 0.1$ and $\alpha = 0.2$. Exploiting the tunability of M_c-SMPC controller we can adjust the comfort probability level in order to have a smaller amount of violations. By setting $\alpha = 0.01$, the M_c-SMPC controller can satisfy all the tolerability limits at the cost of a small increase in energy use (less than 1 $\frac{kWh}{m^2}$).

We will next show the resulting room temperature and control inputs under the M_c-SMPC controller for different *alpha* and the RBC controller to further prove that the $\mathbf{M}_c$-SMPC with $\alpha = 0.01$ controller must be chosen for this case study.
The Figure 2.13 depicts the disturbances that are acting on the building during the year 2007. The Figure 2.11 depicts the annual room temperature over the year 2007 for $\mathbf{M}_c$-SMPC with $\alpha = 0.001$ (2.11(a)), $\mathbf{M}_c$-SMPC with $\alpha = 0.2$ (2.11(b)) and for RBC (2.11(c)). The Figures 2.11(a) and 2.11(b) show that an increase in constraint satisfaction probability, which corresponds to a smaller α, tends to keep the room temperature more in the middle of the comfort band in order to obtain less violations; this can be seen mainly during spring and summer. The RBC controller does not achieve a good performance: the room temperature is always kept too close to the lower bound, resulting in a large amount and frequency of lower bound violations mainly in winter and fall. The Figure 2.15 shows the resulting heating and cooling control inputs over the year 2007 for $\mathbf{M}_c$-SMPC with $\alpha = 0.01$ (2.14(a)) and for RBC (2.14(b)). It can be seen that the two control inputs are never applied at the same time, as expected. Both heating and cooling are more frequently applied by the RBC controller; in particular RBC makes a large use of cooling. Despite the larger use of heating during the colder months, the room temperature is lower when the RBC controller is employed, as shown in Figures 2.11. This is likely due to the

blind control, which has a large effect on the controller performance; the $\mathbf{M}_c$-SMPC controller is able to move the blinds to an arbitrary position, while the current practice RBC allows three different positions. This is shown in the Figures 2.15(a) and 2.15(b), which depict the blind control respectively for $\mathbf{M}_c$-SMPC with $\alpha = 0.01$ and for RBC.

Remark 14 *In the OptiControl Report [52] an advanced RBC controller is described, which is based on the same rules but it can move the blinds to an arbitrary positions, as the* $\mathbf{M}_c$*-SMPC does. The simulation results depicted in the report show that the* $\mathbf{M}_c$*-SMPC controller can perform better than the advanced RBC controller as well.*

In conclusion the proposed $\mathbf{M}_c$-SMPC strategy is clearly superior compared to the industry standards.

2.6 Conclusion and Future Steps

Several predictive control strategies based on a stochastic MPC have been applied to the indoor climate control. The controllers make use of weather and internal gain prediction to compute how much energy and which low/high-energy sources are needed to keep the room temperature and illuminance in the required comfort levels. A procedure for selecting the most promising controller has been provided: first the stochastic MPC methods are compared in terms of energy use, violations and computational effort. Then the chosen controller is compared to current practice and the theoretical benchmark for assessing its performance. Different formulations of the stochastic MPC are compared with standard commercial controllers via simulations. The tested approximations of the problem were all showing that the performance loss is quite significant for the SOC formulation. However it has been proved that the approximation of the feedback disturbance matrix as a constant matrix ($\mathbf{M}_c$-SMPC controller) with a prediction horizon of $N = 24$ has very good performances both in terms of energy consumption and violations and computational time as well. The computational complexity of the control formulations based on SOCP (CLP-SMPC and $\mathbf{M}_c$-SMPC) is too high for online optimization, especially if a longer horizon is to be used to improve the controller performance. Which controller is to be applied depends mainly on the specific case, but the linear approximation $\mathbf{M}_c$-SMPC seems to be the most suitable controller to apply in most cases. In fact it has been proven to achieve a good tradeoff between the too high computational burden of the formulations based on SOCP and the larger performance loss of the formulations based on LP ($\mathbf{M}_c$-SMPC and OLP-SMPC). It has been also proved through a quantitative assessment

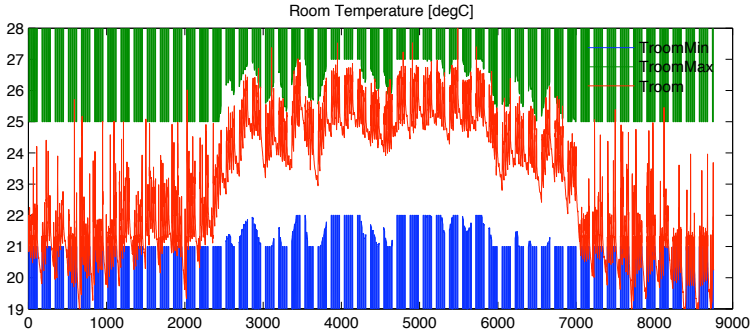

(a) M_c-SMPC with $\alpha = 0.001$

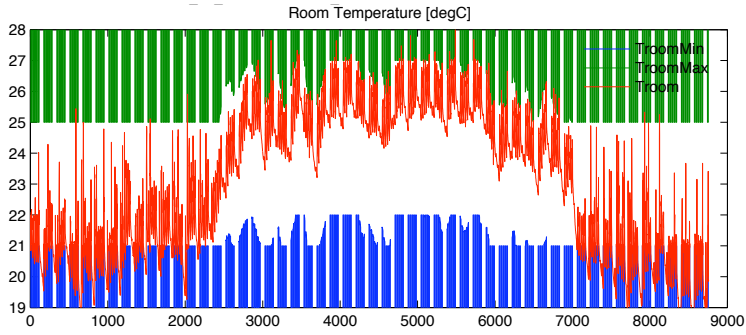

(b) M_c-SMPC with $\alpha = 0.2$

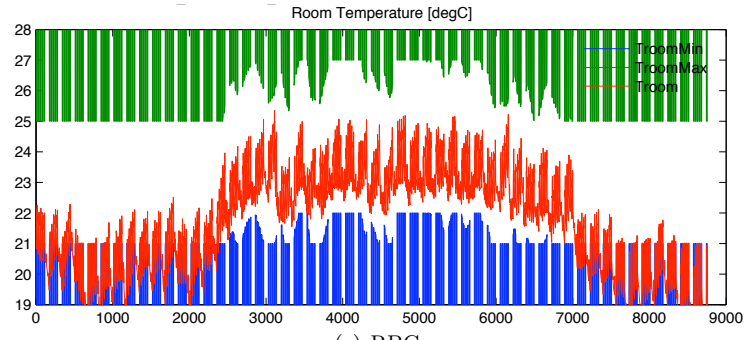

(c) RBC

Figure 2.11: Room temperature for 2007

that the stochastic MPC controller can achieve better performances in terms of a tradeoff between energy use and user comfort compared to industry controllers while respecting the European comfort standards. Our results indicate that the stochastic predictive controllers outperform the certainty equivalence MPC strategy. This also

proves that the uncertainty in the weather prediction has a significant impact and should be taken into account to improve the controller performance. Moreover SMPCs perform better than the state of the art, non-predictive rule-based controller RBC both in terms of energy use and violations. Finally, it has been proved the easy tunability of SMPCs, which involves only one parameter. The probability level of constraint violations can be changed in order to achieve a better tradeoff between energy use and violations. The OptiControl Project is an ongoing project and several future steps are going to be investigated and developed [38]:

- simplify the models used for the stochastic MPC to reduce the computational effort;
- develop a building system state estimation algorithms for the stochastic MPC strategies and also a tuning method for them.
- investigate how sensitive are the controllers to the uncertainty in the predictions and in the model parameters;
- investigate the occupancy and internal heat gain predictions;
- adapt the MPC control strategies to the commercial applications for building automation, which usually involve a hierarchical control scheme (high and low level controller). A possible approach is just to replace the high-level controller of the existing controller with the proposed control schemes;
- test the control strategies through a demonstrator.

Table 2.1: **Overview of the single optimization problems**

OLP-SMPC: quadratic cost function, linear constraints, softened outputs (QP)					
	N=24	N=36	N=48	N=60	N=72
constraint number	596	884	1172	1460	1748
variable number	225	333	441	549	657
Computational times [s]	0.30	0.40	0.50	0.64	0.76

$\mathbf{M}_c$-**SMPC**: quadratic cost function, linear constraints, softened outputs and inputs (QP)					
	N=24	N=36	N=48	N=60	N=72
constraint number	896	1328	1760	2192	2624
variable number	375	555	735	915	1095
Computational times [s]	0.45	0.67	1.05	1.58	2.36

$\mathbf{M}_b$-**SMPC** ($b = 2$): linear cost function, linear and conic constraints, softened outputs (SOCP)					
	N=24	N=36	N=48	N=60	N=72
constraint number	596	884	1172	1460	1748
variable number	507	759	1011	1263	1515
Computational times [s]	1.57	8.38	34.58	81.98	326.44

$\mathbf{M}_b$-**SMPC** ($b = 8$): linear cost function, linear and conic constraints, softened outputs (SOCP)					
	N=24	N=36	N=48	N=60	N=72
constraint number	596	884	1172	1460	1748
variable number	1209	1893	2577	3261	3945
Computational times [s]	2.96	19.89	65.42	172.49	635.21

CLP-SMPC: linear cost function, linear and conic constraints, softened outputs (SOCP)					
	N=24	N=36	N=48	N=60	N=72
constraint number	596	884	1172	1460	1748
variable number	2025	4329	7497	11529	16425
Computational times [s]	4.09	35.40	106.22	665.82	1009.72

Table 2.2: $\mathbf{M}_c - SMPC$ **with different prediction horizons for January** 2007

	N=24	**N=36**	**N=48**	**N=60**	**N=72**
Energy Use $\left[\frac{kWh}{m^2}\right]$	4.9481	5.0054	4.7307	4.8244	5.0362
Number of violations	17	19	16	15	15
Amount of violations $[Kh]$	5.0690	5.8750	4.5220	4.1120	4.2370
Computational time $[s]$	1004.4	1495.4	2343.6	3526.6	5267.5

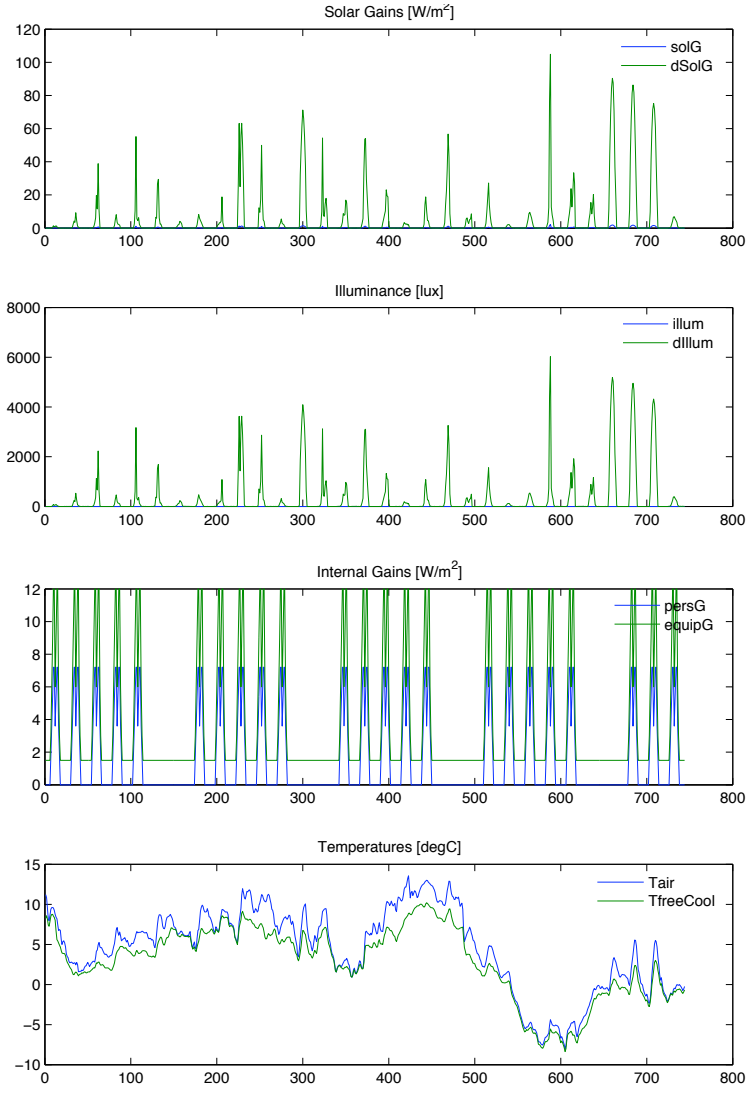

Figure 2.12: Disturbances acting on the building in January 2007

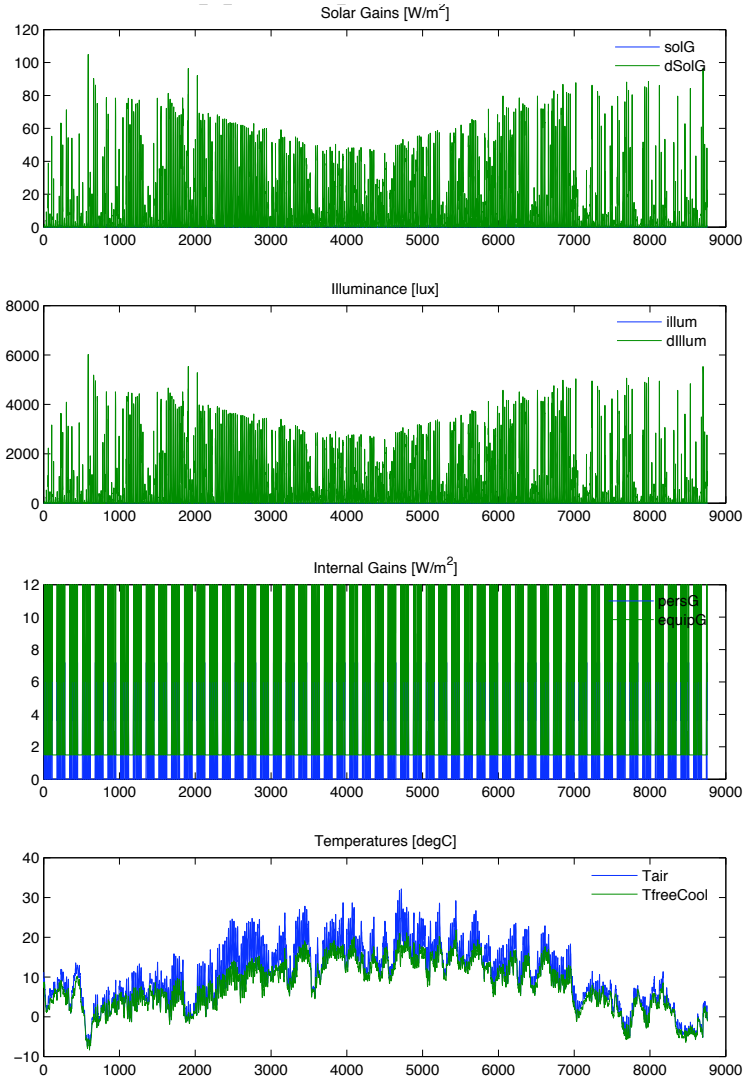

Figure 2.13: Disturbances acting on the building during 2007

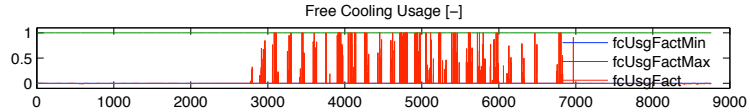

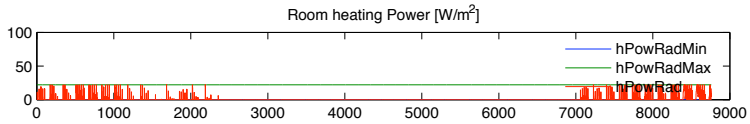

(a) M_c-SMPC with $\alpha = 0.01$

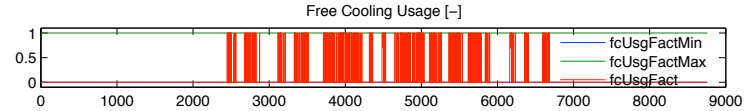

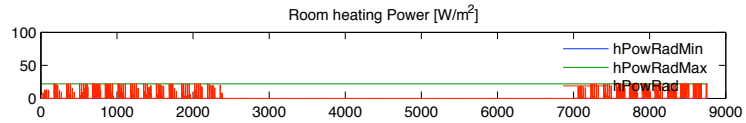

(b) RBC

Figure 2.14: Heating and cooling for 2007

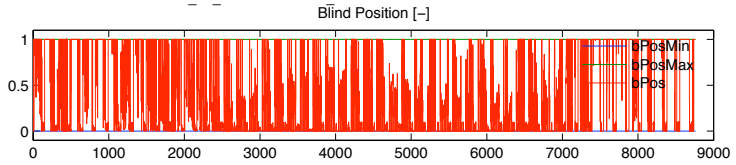

(a) M_c-SMPC with $\alpha = 0.01$

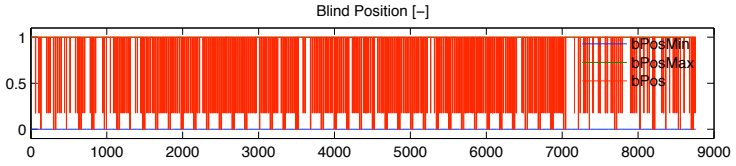

(b) RBC

Figure 2.15: Blind position for 2007

References

[1] SIA Standad 2028. Klimadaten für bauphysik, energie- und gebüdetechnik. 2008.

[2] SIA Standard 380/4. Elektrische energie im hochbau. 2006.

[3] SIA Standard 382/1. Lüftings- und klimaanlagen - allgemeine grundlagen und anforderungen. 2006.

[4] SIA Standard 384/1. Heizungsanlagen in gebäuden - grundlagen und anforderungen. 2009.

[5] SIA Standad 384.201. Heizungsanlagen in gebäuden - berechnung der normheizlast. 2005.

[6] International Energy Agency. Energy efficiency requirements in building codes. 2008.

[7] F. Alizadeh and D. Goldfarb. Second-order cone programming. *Mathematical Programming, Series B*, 95:3–51, 2002.

[8] E. D. Andersen, C. Roos, and T. Terlaky. On implementing a primal-dual interior-point method for conic quadratic optimization. *Mathematical Programming*, 95(2):249–277, 2003.

[9] R. V. Andersen, B. Olesen, and J. Toftum. Simulation of the effects of occupant behaviour on indoor climate and energy consumption. In *Proceedings of Clima 2007 WellBeing Indoors*, International Centre for Indoor Environment and Energy, Department of Mechanical Engineering, Technical university of Denmark, 2007.

[10] Mosek ApS. *The Mosek optimization tools manual*.

[11] J. E. Aronson. A survey of dynamic network flows. *Annals of Operations Research*, 20:1–66, 1989.

[12] ASHRAE. *ASHRAE Standard 55-2004 – Thermal Environmental Conditions for Human Occupancy (ANSI Approved).* ASHRAE, 2004.

[13] J. P. Aubin. *Viability theory.* Systems & Control: Foundations & Applications. Birkhaüser, 1991.

[14] A. Bemporad. Reducing conservatism in predictive control of constrained systems with disturbances. *Proc. IEEE Conference on Decision and Control*, 37:1384–1389, 1998.

[15] A. Bemporad. Reducing conservativeness in predictive control of constrained systems with disturbances. In *Proc. of 37th IEEE Conf. Decision Control*, pages 1384–1391, 1998.

[16] A. Bemporad, F. Borrelli, and M. Morari. Min-max control of constrained uncertain discrete-time linear systems. *IEEE Transations of Automatic Control*, 48(9):1600–1606, 2003.

[17] A. Bemporad and M. Morari. Robust model predictive control: a survey. In A. Garulli, A. Tesi, and A. Vicino, editors, *Robustness in Identification and Control*, number 245 in Lecture Notes in Control and Information Sciences, pages 207–226. Springer-Verlag, 1999.

[18] A. Ben-Tal, A. Goryashko, E. Guslitzer, and A. Nemirovski. Adjustable robust solutions of uncertain linear programs. *Mathematical Programming*, 99(2):351–376, 2004.

[19] A. Ben-Tal and A. Nemirovski. Robust optimization methodology and applications. *Math. Program., ser. B*, 92:453–480, 2002.

[20] D. P. Bertsekas. *Control of uncertain systems with a set–membership description of the uncertainty.* PhD thesis, MIT, 1971.

[21] D. P. Bertsekas. *Dynamic programming: deterministic and stochastic models.* Prentice Hall, Englewood Cli s, NJ, 1987.

[22] D. P. Bertsekas. *Dynamic programming and optimal control.* Athena Scientific, Belmont, Massachusetts, 1995.

[23] D. P. Bertsekas and I. B. Rhodes. On the minimax reachability of target sets and target tubes. *Automatica*, 7:233–247, 1971.

[24] D. Bertsimas and I. Ch. Paschalidis. Probabilistic service level guarantees in make-to-stock manufacturing systems. *Operations Research*, 49(1):119–133, 2001.

[25] D. Bertsimas and M. Sim. Tractable approximations to robust conic optimization problems. *Mathematical Programming*, ser. B 107:5–36, 2006.

[26] F. Blanchini. Nonquadratic Lyapunov functions for robust control. *Automatica*, 31(3):451–461, 1995.

[27] F. Blanchini. Set invariance in control — a survey. *Automatica*, 35(11):1747–1768, November 1999.

[28] F. Blanchini, S. Miani, R. Pesenti, and F. Rinaldi. Stabilization of multi-inventory systems with uncertain demand and setups. *IEEE Transactions on Robotics and Automation*, 19(1):103–116, 2003.

[29] F. Blanchini, R. Presenti, F. Rinaldi, and W. Ukovich. Feedback control of production-distribution systems with unknown demand and delays. *IEEE Transactions on Robotics and Automation, Special Issue on Automation of Manufacturing Systems*, RA-16(3):313–317, June 2000.

[30] F. Blanchini, F. Rinaldi, and W. Ukovich. A network design problem for a distribution system with uncertain demands. *SIAM Journal on Optimization*, 7(2):560–578, May 1997.

[31] F. Borrelli, P. Falcone, and C. del Vecchio. Event-based receding horizon control for two-stage multi-product production plants. *Control Engineering Practice*, 15(12):1556–1568, December 2007.

[32] D. Bourgeois, C. Reinhart, and I. Macdonald. Adding advanced behavioural models in whole building energy simulation: A study on the total energy impact of manual and automated lighting control. *Energy and Buildings*, 38:814–823, 2006.

[33] M. Cannon, P. Couchman, and B. Kouvaritakis. MPC for stochastic systems. In *Assessment and Future Directions of Nonlinear Model Predictive Control*, Lecture Notes in Control and Information Sciences, vol. 358, pages 255–268. Springer, Berlin, 2007.

[34] C. J. Chase and P. J. Ramadge. On real-time scheduling policies for flexible manufacturing systems. *IEEE Transactions on Automatic Control*, 37:491–496, 1992.

[35] F. Chen and J.-S. Song. Optimal policies for multiechelon inventory problems with markov-modulated demand. *Operations Research*, 49(2):226–234, 2001.

[36] S. H. Cho and M. Zaheer-uddin. Predictive control of intermittently operated radiant floor heating systems. *Energy and Conversion Management*, 44:1333–1342, 2003.

[37] CEN Report CR1752. Ventilation for buildings design criteria for the indoor environment, european committee for standardization. 1998.

[38] M. Gwerder (Eds.) D. Gyalistras. Use of weather and occupancy forecasts for optimal building climate control (opticontrol): Two years progress report. Technical report, Terrestrial Systems Ecology ETH Zürich, Switzerland and Building Technologies Division, Siemens Switzerland Ltd., Zug, Switzerland, 2009. http://www.opticontrol.ethz/.

[39] S. Dan. *Optimal state estimation: Kalman, H-infinity, and nonlinear approaches*. John Wiley & Sons, Inc., 2006.

[40] G. B. Dantzig. *Linear programming and extensions*. Princeton University Press, Princeton, N.J., 1963.

[41] D. M. Munoz de la Pena, A. Bemporad, and T. Alamo. Stochastic programming applied to model predictive control. In *Proc. of the 44th IEEE Conference of Decision and Control*, Dec 2005.

[42] P. Doganis, E. Aggelogiannaki, and H. Sarimveis. A model predictive control and time series forecasting framework for supply management. volume 15, Oct 2006.

[43] F. Dusonchet and M. O. Hongler. Continuous-time restless bandit and dynamic scheduling for make-to-stock production. *IEEE Transactions on Robotics and Automation*, 19(6):977–990, 2003.

[44] European Economic, Social Committee, and the Committee of the Regions. Debate europebuilding on the experience of plan d for democracy, dialogue and debate. *COM(2008) 158/4*, 2008.

[45] A. Ephremides and S. Verdú. Control and optimization methods in communication networks. *IEEE Transactions on Automatic Control*, AC-34:930–942, 1989.

[46] B. Lehmann et al. Modeling of buildings and building systems. Technical report, Terrestrial Systems Ecology ETH Zürich, Switzerland and Building Technologies Division, Siemens Switzerland Ltd., Zug, Switzerland, 2009. In [38].

[47] D. Gyalistras et al. Control problem and experimental setup. Technical report, Terrestrial Systems Ecology ETH Zürich, Switzerland and Building Technologies Division, Siemens Switzerland Ltd., Zug, Switzerland, 2009. In [38].

[48] D. Gyalistras et al. Modeling and simulation environment. Technical report, Terrestrial Systems Ecology ETH Zürich, Switzerland and Building Technologies Division, Siemens Switzerland Ltd., Zug, Switzerland, 2009. In [38].

[49] D. Gyalistras et al. Performance bounds and potential assessment. Technical report, Terrestrial Systems Ecology ETH Zürich, Switzerland and Building Technologies Division, Siemens Switzerland Ltd., Zug, Switzerland, 2009. In [38].

[50] F. Oldewurtel et al. Analysis of model predictive control strategies. Technical report, Terrestrial Systems Ecology ETH Zürich, Switzerland and Building Technologies Division, Siemens Switzerland Ltd., Zug, Switzerland, 2009. In [38].

[51] F. Oldewurtel et al. Model predictive control strategies. Technical report, Terrestrial Systems Ecology ETH Zürich, Switzerland and Building Technologies Division, Siemens Switzerland Ltd., Zug, Switzerland, 2009. http://www.opticontrol.ethz/.

[52] M. Gwerder et al. Ruled-based control strategies. Technical report, Terrestrial Systems Ecology ETH Zürich, Switzerland and Building Technologies Division, Siemens Switzerland Ltd., Zug, Switzerland, 2009. In [38].

[53] V. Stauch et al. Local weather forecasts and observations. Technical report, Terrestrial Systems Ecology ETH Zürich, Switzerland and Building Technologies Division, Siemens Switzerland Ltd., Zug, Switzerland, 2009. In [38].

[54] A. J. Felt. Stochastic linear model predictive control using nested decomposition. In *Proc. of the American Control Conference*, Denver, Colorado June 4-6, 2003.

[55] S. B. Gershwin. Design and operation of manufacturing systems: the control-point policy. *IIE Transactions*, 32:891–906, 2000.

[56] P. E. Gill, W. Murray, D. B. Ponceleon, and M. A. Saunders. Solving reduced kkt systems in barrier methods for linear and quadratic programming. Technical Report SOL 91-7, Department of Operations Research, Stanford University, CA, USA, Jul 1991. http://www.stanford.edu/group/SOL/reports/SOL-91-7.pdf.

[57] P. Glasserman. Allocating production capacity among multiple products. *Operations Research*, 44(5):724–734, 1996.

[58] C. C. Gonzaga. Path-following methods for linear programming. *SIAM Rev.*, 34:167–224, 1992.

[59] P. J. Goulart, E. C. Kerrigan, and J. M. Maciejowski. Optimization over state feedback policies for robust control with constraints. 42(4):523–533, 2006.

[60] P. Grieder. *Efficient computation of feedback controllers for constrained systems*. PhD thesis, IFA, ETHZ, 2004.

[61] R. E. Griffith and R. A. Steward. A nonlinear programming technique for the optimization of continuous processing systems. *Journal of Management Science*, 7:379–392, 1961.

[62] W. J. Grunenfelder and J. Tödtli. The use of weather predictions and dynamic programming in the contorl of solar demostic hot water systems. In *Mediterranian elettrotechnical Conference of IEEE Region 8 Conference*, Madrid, Spain, October 8-10, 1985.

[63] W. J. Grunenfelder and J. Tödtli. Model-based predictive control design: new trends and tools. In *45th IEEE Conf. on Decision and Control*, pages 6678–6683, San Diego, CA, 2006.

[64] M. Gwerder and J. Tödtli. Predictive control for integrated room automation. In *8th REHVA World Congress for Building Technologies CLIMA*, Lausanne, 2005.

[65] A. Ha. Optimal dynamic scheduling policy for a make to stock production system. *Operations Research*, 45(1):42–53, 1997.

[66] G. P. Henze, C. Felsmann, and G. Knabe. Evaluation of optimal control for active and passive building thermal storage. *International Journal of Thermal Sciences*, 43(2):173–183, 2004.

[67] G. P. Henze, C. Felsmann, and G. Knabe. Impact of forecasting accuracy on predictive optimal control of active and passive building thermal storage inventory, *International Journal of HVAC & RESEARCH*. 10(2):153–178, 2004.

[68] G. P. Henze, D. E. Kalz, S. Liu, and C. Felsmann. Experimental analysis of model-based predictive optimal control for active and passive building thermal storage inventory, *HVAC & RESEARCH*. 11(2), Apr 2005.

[69] A. Iftar and E. J. Davison. Decentralized robust control for dynamic routing of large scale networks. In *Proc. Amer. Contr. Conf.*, pages 441–446, San Diego, CA, 1990.

[70] P. Kall and J. Mayer. *Stochastic linear programming: models, theory, and computation*. Springer-Verlag, Berlin, 2005.

[71] R. E. Kalman. A new approach to linear filtering and prediction problems. *Journal of Basic Engineering*, 82(1):35–45, 1960.

[72] S. S. Keerthi and E. G. Gilbert. Computation of minimum-time feedback control laws for discrete-time systems with state-control constraints. *IEEE Transactions on Automatic Control*, 32(5):432–435, 1987.

[73] E. C. Kerrigan. *Robust constraint satisfaction: invariant sets and predictive control*. PhD thesis, University of Cambridge, Cambridge, UK, November 2000.

[74] E. C. Kerrigan and T. Alamo. A convex parameterization for solving constrained min-max problems with a quadratic cost. In *Proc. of American Control Conference*, volume 3, pages 2220–2221, 2004.

[75] I. Kolmanovsky and E. G. Gilbert. Theory and computation of disturbance invariant sets for discrete-time linear systems. *Mathematical Problems in Egineering*, 4:317–367, 1998.

[76] M. Kvasnica, P. Grieder, M. Baotić, and F.J. Christophersen. *Multi-Parametric Toolbox (MPT): User's Manual*.

[77] M. Kvasnica, P. Grieder, M. Baotić, and M. Morari. Multi Parametric Toolbox (MPT). In *Hybrid Systems: Computation and Control*, Lecture Notes in Computer Science, Volume 2993, pages 448–462, Pennsylvania, Philadelphia, March 2004. Springer Verlag. http://control.ee.ethz.ch/research/publications/publications.msql.

[78] J. H. Lee and Z. Yu. Worst-case formulations of model predictive control for systems with bounded parameters. *Automatica*, 33(5):763–781, 1997.

[79] M. S. Lobo, L. Vandenberghe S. Boyd, and H. Lebret. Applications of second-order cone programming. *Linear Algebra and Applications*, Jan 1997.

[80] J. Löfberg. Approximations of closed-loop MPC. In *Proc. of 42nd Conf. on Decision and Control*, pages 1438–1442, 2003.

[81] J. Löfberg. *Minimax approaches to robust model predictive control*. PhD thesis, Linköping University, Sweden, 2003.

[82] D. L. Loveday, J. Y. M. Cheung, and G. S. Virk. Multivariate stochastic modeling of a full-scale office zone and air conditioning plant: the potential for bems. *Building Services Engineering Research and Technology*, 16(1):17–23, 1995.

[83] J. M. Maciejowski. *Predictive control with constraints*. Prentice Hall, 2002.

[84] T. L. Magnanti and R. T. Wong. Network design and transportation planning: models and algorithms. *Transportation Science*, 18:1–55, 1984.

[85] D. Q. Mayne, S. V. Rakovic, R. Findeisen, and F. Allgöwer. Robust output feedback model predictive control of constrained linear systems. *Automatica*, 42:1217–1222, 2006.

[86] D. Q. Mayne, J. B. Rawlings, C. V. Rao, and P. O. M. Skokaert. Constrained model predictive control: stability and optimality. *Automatica*, 36(6):789–814, 2000.

[87] D. Q. Mayne, M. M. Seron, and S. V. Rakovic. Robust model predictive control of constrained linear systems with bounded disturbances. *Automatica*, 41(2):219–224, 2005.

[88] D.Q. Mayne, J.B. Rawlings, C.V. Rao, and P.O.M. Scokaert. Constrained model predictive control: stability and optimality. *Automatica*, 36(6):789–814, June 2000.

[89] L. Miao and C. G. Cassandras. Receding horizon control for a class of discrete-event systems with real-time constraints. *Transaction on Automatic Control*, 52(5):825–839, May 2007.

[90] H. D. Mittelmann. Recent developments in SDP and SOCP software. In *INFORMS Annual Meeting Pittsburgh, PA*, 2006.

[91] M. Morari and J.H. Lee. Model predictive control: past, present and future, *Computers & Chemical Engineering*. 23(4–5):667–682, 1999.

[92] A. Nemirovski and A. Shapiro. Convex approximation of chance constrained programs. *SIAM Journal on Optimization*, 17(14):969–996, Dec 2006.

[93] NIST/SEMATECH. *e-Handbook of statistical methods*. 2006. available at `http://www.itl.nist.gov/div898/handbook/`.

[94] F. Oldewurtel, C. N. Jones, and M. Morari. A tractable approximation of chance constrained stochastic MPC based on affine disturbance feedback. In *Proc. 47th IEEE Conf. on Decision and Control*, Cancun, Mexico, 2008.

[95] A. P. Perez and P. Zipkin. Dynamic scheduling rules for a multiproduct make-to-stock queue. *Operations Research*, 45(6):919–930, Nov. 1997.

[96] J. R. Perkins and P. R. Kumar. Stable, distributed, real-time scheduling of flexible manufacturing/assembly/disassemble systems. *IEEE Trans. on Automatic Control*, 34(3):139–148, 1989.

[97] A. Polanski. Lyapunov function construction by linear programming. *IEEE Trans. Automatic Control*, 42(7):1013–1016, July 1997.

[98] W. B. Powell, P. Jaillet, and A. Odoni. Stochastic and dynamic networks and routing. *Handbooks in Operations Research and Management Science*, 8, 1995.

[99] A. Prékopa. *Stochastic programming*. Kluwer Academic Publishers, Dordrecht, The Netherlands, 1995.

[100] A. Prékopa and E. Boros. On the existence of feasible flow in a stochastic transportation networks. *Annals of Operations Research*, 39:119–129, 1991.

[101] S. J. Qin and T. A. Badgwell. An overview of industrial model predictive control technology. In *Chemical Process Control - V*, volume 93, no. 316, pages 232–256. AIChe Symposium Series - American Institute of Chemical Engineers, 1997.

[102] S. J. Qina and T. A. Badgwell. A survey of industrial model predictive control technology. *Control Engineering Practice.*, 11:733–764, 2003.

[103] S. Rakovic, P. Grieder, M. Kvasnica, D. Mayne, and M. Morari. Computation of invariant sets for piecewise affine discrete time systems subject to bounded disturbances. In *IEEE Conference on Decision and Control*, Bahamas, December 2004.

[104] S. V. Rakovic. *Robust control of constrained discrete time systems: characterization and implementation*. PhD thesis, Imperial College London, London, United Kingdom, 2005.

[105] T. P. Ryan. *Modern engineering statistics*. Wiley, New York, 2007.

[106] M. A. Saunders and J. A. Tomlin. Solving regularized linear programs using barrier methods and kkt systems. In *5th SIAM Conference on Optimization*, Victoria, BC, Canada, May 20-22, 1996.

[107] A. T. Schwarm and M. Nikolaou. Chance-constrained model predictive control. *AIChE journal*, 45(8):1743–1752, Aug 1999.

[108] J. D. Schwartz and D. E. Rivera. Simulation-based optimal tuning of model predictive control policies for supply chain management using simultaneous perturbation stochastic approximation. In *Proc. American Contr. Conf.*, Minneapolis, Minnesota. USA., 2006.

[109] E. A. Silver and R. Peterson. *Decision systems for inventory management and production planning*. Wiley, New York, 1985.

[110] J. Skaf and S. Boyd. Design of affine controllers via convex optimization. *IEEE Transactions on Automatic Control*, Apr 2008. http://www.stanford.edu/boyd/papers/pdf/.

[111] R. S. Smith. Robust model predictive control of constrained linear systems. In *Proc. American Contr. Conf.*, Boston, MA, USA, 2004.

[112] D. H. van Hessem and O. H. Bosgra. A conic reformulation of model predictive control including bounded and stochastic disturbances under state and input constraints. In *Proc. of 41st IEEE Conf. on Decision and Control*, pages 4643–4648, 2002.

[113] F. De Vericourt, F. Karaesmen, and Y. Dallery. Dynamic scheduling in a make-to-stock system: a partial characterization of optimal policies. *Operations Research*, 48(5):811–819, 2000.

[114] L. Xie, P. Li, and G. Wozny. Chance constrained nonlinear model predictive control. In *Lecture Notes in Control and Information Sciences, vol. 358*, pages 295–304. Springer, Berlin, 2007.

[115] Y. Zheng and P. Zipkin. A queueing model to analyze the value of centilized inventory information. *Operations Research*, 38:296–307, 1990.

Appendix A

Background on Robust Invariant Set Theory

This appendix has been extracted from [60, 73, 104] and provides the basic definitions and results for robust invariant sets for constrained piecewise linear systems needed for computing the maximal positive robust invariant set $\mathcal{O}_\infty$ for the production laws RLB and DPC.

A.1 Robust Invariant Sets for Piecewise Affine Systems

Given the set $\mathcal{S} \subseteq \mathbb{R}^n$, $\mathcal{S}^c$ denotes its complement in $\mathbb{R}^n$.

Definition 3 (P-collection) *A set $\mathcal{C} \subseteq \mathbb{R}^n$ is called the* P-collection *(in $\mathbb{R}^n$) if it is collection of a finite number of n-dimensional polytopes, i.e.*

$$\mathcal{C} = \{\mathcal{C}_i\}_{i=1}^{N_C}, \tag{A.1}$$

where $\mathcal{C}_i := \{x \in \mathbb{R}^n \mid C_i^x x \leq C_i^b\}$, $\dim(\mathcal{C}_i) = n$, $i = 1, \ldots, N_C$, with $N_C < \infty$.

In the following a PWA systems subject to an additive disturbance $w(k)$ is defined:

$$x(k+1) = f_a(x(k), w(k)) = \tilde{A}_r x(k) + \tilde{g}_r + w(k), \tag{A.2a}$$

$$\text{if } \; x(k) \in \tilde{\mathcal{P}}_r, \; r \in \{1, 2, \ldots, R\}, \tag{A.2b}$$

$$x(k) \in \mathbb{X}, \quad w(k) \in \mathbb{W}, \quad \forall \; k \geq 0. \tag{A.2c}$$

where the active dynamic r is defined by the polyhedron $\tilde{\mathcal{P}}_r$ and R represent the number of different dynamics. The sets $\mathbb{X}$ and $\mathbb{W}$ are compact and polytopic and contain the origin in their interior. We will denote the set of states over which the PWA system (A.2) is defined as $\tilde{\mathcal{S}}_{\text{PWA}} = \bigcup_{r\in\mathcal{R}} \tilde{\mathcal{P}}_r$, where $\tilde{\mathcal{S}}_{\text{PWA}}$ is a P-Collection. We will also consider PWA systems subject to the input $u(k)$ and the disturbance $w(k)$:

$$x(k+1) = f(x(k), u(k), w(k)) = A_r x(k) + B_r u(k) + g_r + w(k), \tag{A.3a}$$

$$\text{if} \quad [x(k)^T \; u(k)^T]^T \in \mathcal{P}_r, \quad r \in \mathcal{R}, \tag{A.3b}$$

$$x(k) \in \mathbb{X}, \quad u(k) \in \mathbb{U}, \quad w(k) \in \mathbb{W}, \quad \forall\, k \geq 0. \tag{A.3c}$$

where the active dynamic r is defined by the polyhedron $\tilde{\mathcal{P}}_r$ and R represent the number of different dynamics. The sets $\mathbb{X}$ and $\mathbb{W}$ are compact and polytopic and contain the origin in their interior. The set $\text{Pre}_f(\mathcal{S})$ defines the set of system (A.3) states which can be robustly driven into the target set $\mathcal{S}$ in one time step. Similarly, for the autonomous PWA system (A.2), we use $\text{Pre}_{f_a}(\mathcal{S})$ to denote the set of the states that robustly evolves to $\mathcal{S} \subseteq \mathbb{X}^0$ in one step. The two different types of invariant sets, the *Robust Positive Invariant Set* $\mathcal{O}$ and the *Robust Control Invariant Set* $\mathcal{C} \subseteq \mathbb{X}$, are defined for PWA systems as well. The set $\mathcal{O}_\infty$ is the maximal robust invariant set of the autonomous PWA system (A.2) if $0 \in \mathcal{O}_\infty$, $\mathcal{O}_\infty$ is robust invariant and $\mathcal{O}_\infty$ contains all robust invariant sets that contain the origin. The set $\mathcal{C}_\infty$ is said to be the maximal robust control invariant set for the PWA system in (A.3) if it is robust control invariant and contains all robust control invariant sets contained in $\mathbb{X}$.

Remark 15 *The condition that $\mathcal{O}_\infty$ must contain the origin is added because PWA systems may have multiple equilibrium points and thus multiple robust invariant sets which are disconnected (i.e. $\mathcal{F}_\infty = \emptyset$). Furthermore, if these sets are used as target sets in control problems, they should only contain one equilibrium point in order to get predictable closed-loop behavior.*

Next, the computation of $\text{Pre}_{f_a}(\Omega_k, \mathbb{W})$ for PWA systems is detailed. More details can be found in [60, 73].

Computation of $\text{Pre}_{f_a}(\mathcal{S}, \mathbb{W})$

The set $\text{Pre}_{f_a}(\mathcal{S}, \mathbb{W})$ can be computed for autonomous PWA systems as described by the following Proposition.

Proposition 1 *Consider autonomous PWA system* (A.2)*. Let $\mathcal{S} \subseteq \mathbb{X}^0$ be a P-collection, then the set* $\text{Pre}_{f_a}(\mathcal{S}, \mathbb{W})$*, defined in* (1.8)*, is a P-collection.*

Proof: Since $\mathcal{S}$ is a P-collection by properties of the Pontryagin difference, $\mathcal{S}^* = \mathcal{S} \ominus \mathbb{W}$ is also a P-collection so that $\mathcal{S}^* = \bigcup_{y=1,\ldots,Y} \mathcal{S}_y^*$ for some finite integer Y. It trivially follows from the definition of $f_a(x,w)$ that $\mathrm{Pre}_{f_a}(\mathcal{S},\mathbb{W}) = \bigcup_{(y,j)\in\{1,\ldots,Y\}\times\mathcal{R}_0} \mathcal{S}_{y,j}^+$, where $\mathcal{S}_{y,j}^+ \triangleq \{x \in \mathbb{X} \mid \tilde{A}_j x + \tilde{g}_j \in \mathcal{S}_y^*\}$. Since each $\mathcal{S}_{y,j}^+$ is polyhedral, the set $\mathrm{Pre}_{f_a}(\mathcal{S},\mathbb{W})$ is a P-collection. □

In order to compute the set $\mathcal{S}^* = \bigcup_{y=1,\ldots,Y} \mathcal{S}_y^*$ the following operations need to be performed on the set $\mathcal{S} = \bigcup_{y=1,\ldots,L} \mathcal{S}_y$. First compute the complement of $\mathcal{S}$ in order to get a P-collection $\mathcal{S}^c$ of open polyhedra Φ_j, $\mathcal{S}^c = \bigcup_{y=1,\ldots,T} \Phi_y$. Then $\mathcal{S}^* = \mathcal{S} \ominus \mathbb{W} = \left[\bigcup_{y=1,\ldots,T} (\Phi_y \oplus (-\mathbb{W}))\right]^c$.

Appendix B

Robust Invariant Set Computation

Two Matlab toolboxs, the Multi-Parametric Toolbox [77], [76] and the Invariant Set Toolbox (InvSetBox) [73], has been used for the computation of the invariant sets described in the Chapter 1. They can be downloaded from the authors' Internet sites:

- http://www-control.eng.cam.ac.uk/eck21/ for the Invariant Set Toolbox
- http://control.ee.ethz.ch/ mpt/ for the the Multi-Parametric Toolbox

The toolboxes provide an implementation of the Algorithm 1.3.1 for discrete-time LTI and autonomous PWA systems and, as a consequence, of the robust one-step set computation. For this purpose, either vertex-based method or projection method such as Fourier-Motzkin elimination, used in the proof of Theorem 1, has been implemented. We refer the reader to [73] for more details and references about these methods. The basic idea of vertex-based methods is to find all the vertices of the corresponding sets and computing the convex hull of their sums. However, as the dimension of the system n grows the number of vertices increases quite rapidly compared to the number of hyperplanes required to describe the various sets. The vertex-based method can therefore become impractical for large systems. The Fourier-Motzkin elimination method is very popular because it is simple and easy to be implemented. The basic idea of Fourier elimination algorithm is to choose a variable and then to eliminate it by projection its constraints onto the rest of the system, resulting in new constraints. The projection forms a new problem with one variable fewer, but possibly more constraints. This is done recursively, until all variables but one have been eliminated.

This method might still be not efficient, because number of redundant constraints could increase exponentially in the worst case.

B.1 Computation of $\mathcal{C}_\infty$

The maximal robust control invariant set $\mathcal{C}_\infty$ described in the Chapter 1 has been numerically computed using Matlab and the Invariant Set Toolbox. The basic object of the toolbox is the n-dimensional polyhedron given in the augmented form

$$[H \quad K]$$

and converted from the standard form

$$Hx \leq K$$

to the augmented form by the function STD2AUG. The toolbox can handle the discrete-time LTI system subject to polytopic uncertainty and state disturbances:

$$x(k+1) \quad = \quad Ax(k) + Bu(k) + Ew(k) \tag{B.1}$$

subject to control and states constraints, $u(k) \in \mathbb{U}$ and $x(k) \in \mathbb{X}$, for all $k \geq 0$, and polytopic uncertainty. The sets $\mathbb{U}$ and $\mathbb{X}$ are n-dimensional polyhedron. The disturbances vary within the polytope (compact polyhedron) $\mathbb{W}$. The function KINFSET computes the maximal robust control invariant set for the system B.1, providing $\mathbb{X}$ as target set. Hence the function KINFSET is used for computing the set $\mathcal{C}_\infty$ for our model (1.1)-(1.2), where $A = B = E = I^n$ and the sets $\mathbb{U}$, $\mathbb{X}$ and $\mathbb{W}$ are those defined in the constraints 1.2.

B.2 Computation of $\mathcal{O}_\infty$

The maximal robust positive invariant set $\mathcal{O}_\infty$ described in the Chapter 1 has been numerically computed using Matlab and the Multi-Parametric Toolbox (MPT). The Multi-Parametric Toolbox is a free Matlab toolbox for design, analysis and deployment of optimal controllers for constrained linear, nonlinear and hybrid systems [77], [76]. The toolbox allows to compute the invariant sets for systems with additive and polytopic uncertainties. In particular, we are interested in computing the set $\mathcal{O}_\infty$ for autonomous PWA systems subject to an additive disturbance $w(k)$. This kind

of systems have been defined in Appendix A (see A.2). The function INFSETPWA computes the maximal robust positive invariant set for the PWA system

$$x(k+1) = A_i x(k) + f_i + w(k). \tag{B.2a}$$

where the active dynamic i is defined by the polyhedron $\mathcal{P}_i$, R represent the number of different dynamics and the additive uncertainty $w(k)$ vary within the polytope $\mathbb{W}$. As a matter of fact, given a feedback control law, the system (1.1) subject to constraints (1.2) under the control law is rewritten as an autonomous PWA system over R polyhedral regions and subject to an additive polytopic uncertainty. We will show through a simple example how to rewrite the system (1.1)-(1.2) under either the RLB or DPC feedback policy as an autonomous PWA system.

Example 7 (PWA system under the RLB Feedback Policy)
Let $n = 2$, $P^{max} = D^{max} = 1$, $d^{max} = [0.8; 0.6]$ and $p^{max} = [0.9; 0.8]$. The system (1.1)-(1.2) under the RLB feedback policy can be rewritten as follows:

$$x(k+1) = \begin{cases} x(k) + \begin{bmatrix} 0.9 \\ 0 \end{bmatrix} + d(k) & \text{if} \quad (x_1(k) \leq x_2(k)) \quad \text{and} \quad (x_1(k) \leq 2.1) \\ x(k) + \begin{bmatrix} 0 \\ 0.8 \end{bmatrix} + d(k) & \text{if} \quad (x_2(k) < x_1(k)) \quad \text{and} \quad (x_2(k) \leq 2.2) \\ x(k) + d(k) & \text{if} \quad (x_2(k) > 2.1) \quad \text{and} \quad (x_2(k) > 2.2) \end{cases} \tag{B.3}$$

The PWA system B.3 is defined over 3 regions depicted in figure B.1(a) ($M = 3$).

Example 8 (PWA system under the DPC Feedback Policy)
Let $n = 2$, $P^{max} = D^{max} = 1$, $d^{max} = [0.8; 0.6]$ and $p^{max} = [0.9; 0.8]$. The

system (1.1)-(1.2) under the DPC feedback policy can be rewritten as follows:

$$x(k+1) = \begin{cases} x(k) + \begin{bmatrix} 0.8 - x_1(k) \\ 0.2 + x_1(k) \end{bmatrix} + d(k) & \text{if } (x_1(k) \leq x_2(k)) \\ & \text{and } (x_1(k) + x_2(k) < 0.4) \\ x(k) + \begin{bmatrix} 0.4 + x_2(k) \\ 0.6 - x_2(k) \end{bmatrix} + d(k) & \text{if } (x_2(k) < x_1(k)) \\ & \text{and } (x_1(k) + x_2(k) < 0.4) \\ x(k) + \begin{bmatrix} 0.8 - x_1(k) \\ 0.6 - x_2(k) \end{bmatrix} + d(k) & \text{if } (x_1(k) < 0.8) \text{ and } (x_2(k) < 0.6) \\ & \text{and } (x_1(k) + x_2(k) \geq 0.4) \\ x(k) + \begin{bmatrix} 0.8 - x_1(k) \\ 0 \end{bmatrix} + d(k) & \text{if } (x_1(k) < 0.8) \\ & \text{and } (x_2(k) \geq 0.6) \\ x(k) + \begin{bmatrix} 0 \\ 0.6 - x_2(k) \end{bmatrix} + d(k) & \text{if } (x_1(k) \geq 0.8) \\ & \text{and } (x_2(k) < 0.6) \\ x(k) + \begin{bmatrix} 0 \\ 0 \end{bmatrix} + d(k) & \text{if } (x_1(k) \geq 0.8) \\ & \text{and } (x_2(k) \geq 0.6) \end{cases} \tag{B.4}$$

The PWA system B.4 is defined over 6 *regions depicted in figure B.1(b) (*$M = 3$*).*

Hence the function INFSETPWA is used for computing the set $\mathcal{O}_\infty$ for our model (1.1)-(1.2) under either the RLB or DPC feedback policy, once the autonomous PWA system has been derived from the original model by applying the designed control law.

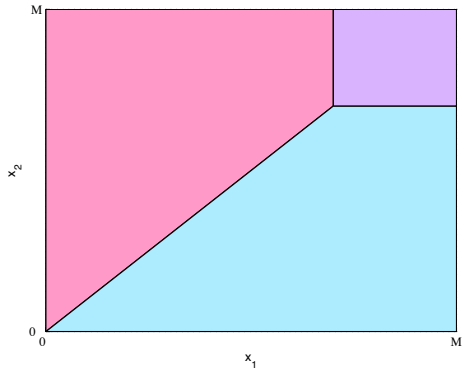

(a) RLB

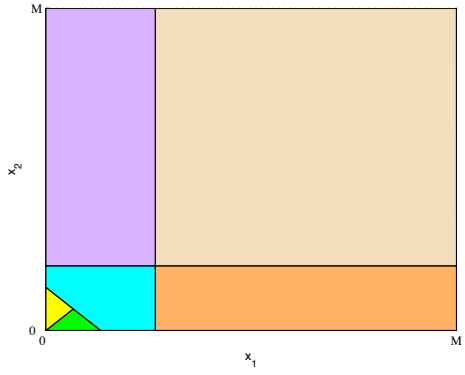

(b) DPC

Figure B.1: S_{PWA} under both RLB and DPC control laws.

Appendix C

Sequential Linear Programming

Sequential Linear Programming (SLP) is a popular standard method for solving nonlinearly constrained optimization problems. This method uses linear programming as a search technique. SLP consists of linearizing the objective and constraints around a starting point by a Taylor series expansion. The resulting linear programming subproblem is then efficiently solved by standard methods such as the Simplex (see [40]) or the Interior-Point methods (see [58]). The procedure is repeated by linearizing the nonlinear problem around the new point. A sequence of approximations is computed this way, hopefully converging to the solution of the original problem. The method is easy to implement and requires only 1^{st} order derivatives. The basic formulation of SLP algorithm is described next.

C.1 Basic SLP Algorithm

Consider a generic constrained optimization problem:

$$\begin{aligned} &\min_x f(x) \\ &s.t. \\ &g_i(x) \geq 0 \quad \forall i = 1 \dots n_g \end{aligned} \tag{C.1}$$

Algorithm C.1.1 (Algorithm SLP)

1. *Choose a starting point* x_0. *Set* $k = 0$.

2. *Terminate if x_k satisfies the convergence condition or if $k > k_{max}$, where k_{max} is the maximum iteration number.*

3. *Obtain linear approximations around x_k using 1^{st} order Taylor expansion of f and g. Then solve the LP_k problem:*

$$\begin{aligned} &\min_x f(x_k) + \Delta x^T \nabla f(x_k) \\ &s.t. \\ &g_i(x_k) + \Delta x^T \nabla g_i(x_k) \geq 0 \quad \forall i = 1 \dots n_g \end{aligned} \tag{C.2}$$

   Denote the solution by x_k.

4. *Set $k = k + 1$ and goto 2.*

For a detailed description of this method we refer the reader to [61].

Appendix D

Background on Linear Model Predictive Control

This appendix has been extracted from [83], [63], [102], [88], [17], [91], [101], [33] and provides the basic definitions and results on Model Predictive Control (MPC) we have applied in indoor climate control. The system model is a critical piece of the MPC controller. Several types of models can be considered in MPC schemes. We will focus on linear system model, which is the most common model type. This is the only one that will result in a convex and easily solvable optimization problem.

D.1 MPC and Receding Horizon Policy

Model predictive control is a technique that has been successfully applied in many constrained deterministic optimal control problems. MPC is also referred as Receding Horizon Control (RHC). The receding horizon strategy introduces a feedback mechanism and helps to reduce the effect of uncertainty due to model mismatch, model parameter errors, external disturbances. Figure D.1 illustrates the basic idea of RHC. The fixed horizon optimization leads to a control sequence $\{u_k \dots u_{k+N}\}$, which begins at the current time k and ends at some future time $k+N$. Something unexpected may happen to the system at some time over the future interval $\{u_k \dots u_{k+N}\}$. The receding horizon strategy copes with this issue:

- At time k and for the current state x_k, solve an optimal control problem over a fixed future interval $[k, k+N]$.

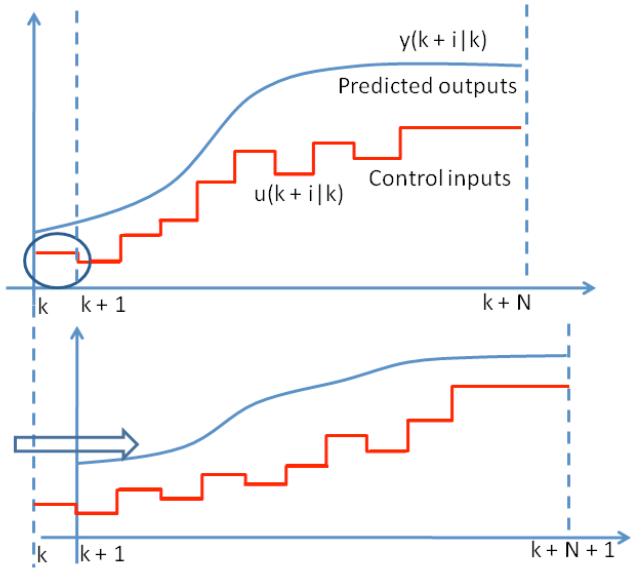

Figure D.1: Receding horizon control strategy.

- Apply only the first step in the resulting optimal control sequence.
- Measure the state reached at time $k+1$.
- Repeat the fixed horizon optimization at time $k+1$ over the future interval $[k+1, k+N+1]$, starting from the current state x_{k+1}.

D.2 Linear MPC

Consider the linear discrete-time prediction model:

$$\begin{aligned} x_{k+1} &= Ax_k + Bu_k \\ y_k &= Cx_k \end{aligned} \tag{D.1}$$

where $x_k \in \mathbb{R}^n$ is the state, $u_k \in \mathbb{R}^m$ is the input and $y_k \in \mathbb{R}^p$ the output at time k. In the classical MPC framework, at each time instant k the following finite-horizon optimization problem is solved for the current state x:

Problem 9 (Linear MPC)

$$\min_{u_{k|k},\dots,u_{k+N-1|k}} f(x_{k+N|k}) + \sum_{i=0}^{N-1} l(x_{k+i|k}, u_{k+i|k})$$

$$\begin{aligned} &s.t. \\ &\quad system \quad dynamics\ (D.1) \\ &\quad x_{k|k} = x \\ &\quad y_{min} \leq y_{k+i|k} \leq y_{max} \qquad i = 1, \dots, N \\ &\quad u_{min} \leq u_{k+i|k} \leq u_{max} \qquad i = 0, \dots, N-1 \end{aligned} \tag{D.2}$$

where N is the prediction horizon and $[u_{k|k}, \dots, u_{k+N-1|k}] \in \mathbb{R}^{Nm}$ is the sequence of decision variables to be optimized. The prediction of x_{k+i} and y_{k+i} made at time k are denoted respectively by $x_{k+i|k}$ and $y_{k+i|k}$, inputs The upper and lower bounds in the component-wise inequalities D.2 and D.2 define the constraints on inputs and outputs. Several common cost functions are in use, the majority of which are convex, which results in simple optimization problems to solve. Typical choices for f and l are quadratic functions of the form:

$$\begin{aligned} f(x_{k+N|k}) =& x_{k+N|k}^T P x_{k+N|k} \\ l(x_{k+i|k}, u_{k+i|k}) =& x_{k+i|k}^T Q x_{k+i|k} + u_{k+i|k}^T R u_{k+i|k} \qquad i = 0, \dots, N-1 \end{aligned} \tag{D.3}$$

where P and Q are semidefinite positive matrices and R is a definite positive matrix. The relative weighting between the states and the inputs provide a trade-off between regulation quality and input energy. More generally f and l are of the form:

$$\begin{aligned} f(x_{k+N|k}) =& \|P x_{k+N|k}\|_p \\ l(x_{k+i|k}, u_{k+i|k}) =& \|Q x_{k+i|k}\|_p + \|R u_{k+i|k}\|_p \end{aligned} \tag{D.4}$$

where the p-norm can be equal to $1, 2, \dots, \infty$. The stability of the closed loop system will be guaranteed by choosing the structure of the cost function such that the optimal cost forms a Lyapunov function ([26, 97]). In practice, this requirement is generally relaxed for stable systems with slow dynamics, such as buildings, such that it is possible to focus on performance when the cast has to be selected.

D.2.1 Linear MPC with Soft Constraints

In the MPC framework, infeasibility might occur when the hard-constrained optimization problem is solved. A strategy for dealing with the possibility of infeasibility

is to "soft" the constraints by adding new nonnegative variables to the problem, called "slack variables". The size of the slack variables correspond to the size of the associated constraints (see [83]). It is desirable that the solution to the soft constrained MPC problem be the same as the solution to the original hard constrained MPC problem, if the latter is feasible. Therefore, the slack variables are nonzero only when the boundaries described by the original "hard" constraints have to be crossed and they must be heavily penalized in the cost function in order to keep violations as small as possible. Hence the violation penalty is some order of magnitude larger than the input and output weights. Usually a quadratic penalty for constraint violations is added in the cost, hence a quadratic program with a larger number of decision variables is to be solved. The input constraints cannot be softened due to physical limitations of the actuators. The optimization problem 9 solved at each time step in MPC scheme with soft constraints is the following:

Problem 10 (Linear MPC with Soft Constraints)

$$\min_{\varepsilon, u_{k|k}, \ldots, u_{k+N-1|k}} f(x_{k+N|k}) + \sum_{i=0}^{N-1} l(x_{k+i|k}, u_{k+i|k}) + \rho \|\varepsilon\|^2$$

$$\begin{aligned} &s.t. \\ &\quad system \quad dynamics \ (D.1) \\ &\quad x_{k|k} = x \\ &\quad y_{min} - \varepsilon \leq y_{k+i|k} \leq y_{max} + \varepsilon \qquad i = 1, \ldots, N \\ &\quad u_{min} \leq u_{k+i|k} \leq u_{max} \qquad i = 0, \ldots, N-1 \end{aligned} \tag{D.5}$$

The slack variable are denoted by ε and the cost of violations is ρ. The term $\rho\|\varepsilon\|^2$ is added to penalize violations of the original hard constrains in the cost function.

D.3 Stochastic Linear MPC

Consider the linear stochastic discrete-time prediction model:

$$\begin{aligned} x_{k+1} &= Ax_k + Bu_k + B_w w_k \\ y_k &= Cx_k + D_w w_k \end{aligned} \tag{D.6}$$

where $x(k) \in \mathbb{R}^n$ is the state and $x(k) \in \mathbb{R}^m$ is the input at time k. The disturbance at time k is denoted by w_k. As the model involves uncertainty, process output predictions, as well as states, are also uncertain. This would result in output constraint violations in 9 and then infeasibility in the optimization routine. Two possible strategies for facing stochastic models in the MPC framework will be illustrated next.

D.3.1 Certainty Equivalence MPC

A straightforward way for facing stochastic models in the MPC framework is to make the control action neglect the uncertainty and to solve the *certainty equivalence* MPC (CE-MPC) problem at every time k, where the future disturbances are replaced with deterministic estimates. The current and future disturbances $[w_k, \ldots, w_{k+N-1}]$ are predicted given the state information available at time k. The simplest choice is the conditional mean, i.e. $\mathbf{E}[w_k|w_0, \ldots, w_{k-1}]$. We denote the disturbance predictions over the prediction horizon N by $[\hat{w}_{k|k}, \ldots, \hat{w}_{k+N-1|k}]$. Then the CE-MPC optimization problem to be solved at every time instant is the deterministic problem 9 where the dynamic constraints are replaced with:

$$\begin{aligned} x_{k+1} &= Ax_k + Bu_k + B_w\hat{w}_k \\ y_k &= Cx_k + D_w\hat{w}_k \end{aligned} \tag{D.7}$$

Therefore the future values of disturbances are exactly as predicted, there is no future uncertainty in the controller. Despite this rough approximation, CE-MPC might work well in some cases (see [110]).

D.3.2 Chance Constrained MPC

A more realistic strategy to cope with the infeasibility problem illustrated above is to consider "feasible" a solution such that all random inequalities are satisfied for restricted subsets with prescribed probability levels (see [99]). The performance index is the expected value of the usual cost function. The constraints on outputs can be formulated as probabilistic constraints, called "chance constraints". The resulting optimization problem to be solved in the stochastic MPC scheme is:

Problem 11 (Linear Chance Constrained MPC)

$$\begin{aligned} &\min_{u_{k|k},\ldots,u_{k+N-1|k}} \mathbf{E}\left[f(x_{k+N|k}) + \sum_{i=0}^{N-1} l(x_{k+i|k}, u_{k+i|k}) \right] \\ &s.t. \\ &\quad \textit{system} \quad \textit{dynamics } (D.7) \\ &\quad \mathbf{P}\left\{ y_{min} \leq y_{k+i|k} \leq y_{max} \right\} \geq 1-\alpha \qquad i = 1, \ldots, N \\ &\quad u_{min} \leq u_{k+i|k} \leq u_{max} \qquad i = 0, \ldots, N-1 \end{aligned} \tag{D.8}$$

where $1-\alpha$ is the predefined level of confidence. These models ensure that a loss may occur with a small probability without providing any control when a loss occurs.

The optimization problem 11 is nonconvex in general, because the sets described by the probabilistic constraints in Problem 11 are nonconvex in general. The main challenge lies in the computation of the multivariate integration os the density function of the uncertain variables. Most of the approaches try to avoid the "exact" numerical integration and either to relax the probabilistic constraints or to find a deterministic equivalent if exists. Since any affine linear transformation of normally distributed variables has a multivariate normal distribution, if the random variables have a multivariate normal distribution, the optimization problem 11 will be convex. The interested reader is referred to [25, 92, 99] for an overview. Exploit a classical results by Prékopa, a deterministic equivalent formulation of chance constraints will be provided in the appendix E.

Appendix E

Chance Constrained Linear Stochastic Programs

This appendix has been extracted from [70, 99] and introduces a well known method in the literature for obtaining a deterministic reformulation of the chance constraint. Consider the following optimization problem:

$$\begin{aligned} & \min_x c^T x \\ s.t. & \\ & G(w)x - g(w) \geq 0 \\ & x \in \mathcal{X} \end{aligned} \tag{E.1}$$

where $x \in \mathbb{R}^n$ is the vector of decision variables, $\mathcal{X}$ is a polyhedral set, $G(w) : \mathbb{R}^r \mapsto \mathbb{R}^{s \times n}$ and $g(w) : \mathbb{R}^r \mapsto \mathbb{R}^s$ are functions of the random vector $w : \Omega \mapsto \mathbb{R}^r$. In the Stochastic Linear Programming an affine linear dependance on the random variable is assumed:

$$\begin{aligned} G(w) &= G + \sum_{j=1}^{r} G_j w_j \\ g(w) &= g + \sum_{j=1}^{r} g_j w_j \end{aligned} \tag{E.2}$$

where $G, G_j \in \mathbb{R}^{s \times n}$ and $g, g_j \in \mathbb{R}^s$ are respectively deterministic matrices and vectors. Therefore the constraints in E.1 can be regarded as an affine linear combination of random vectors. We can act on the constraint distribution through the decision

variables, which are the coefficients in the linear combination. The stochastic constraints in E.1 may be also written in a row-wise form:

$$G_i^T(w)x - g_i(w) \geq 0 \quad i = 0, \dots s \tag{E.3}$$

The chance constrained version of the problem E.1 involves probabilistic constraints of the form:

$$\mathbf{P}\left\{G(w)x - g(w) \geq 0\right\} \geq 1 - \alpha \tag{E.4}$$

where $1 - \alpha$ is the prescribed probability level. The constraint E.4 is called a *joint chance constraint*, meaning that all of the s inequalities have to hold simultaneously. It can be necessary to consider separately the s inequalities in E.3 both because joint chance constraints are in general non-convex in x and because this could be required by the specific application. As a consequence, define the *separate chance constraint*:

$$\mathbf{P}\left\{G_i^T(w)x - g_i(w) \geq 0\right\} \geq 1 - \alpha_i \quad i = 0, \dots s \tag{E.5}$$

where the probability levels $1 - \alpha_i$ are specified for each individual rows.

E.1 Deterministic Equivalent of Chance Constraints

If we assume that each $(n+1)$-dimensional vector $[G_i(\mathbf{w})\ g_i(\mathbf{w})]^T, \quad i = 0, \dots s$ has a multivariate normal distribution, the random variables in E.3 are also normally distributed. Define for $i = 0, \dots s$:

$$G_i(\mathbf{w}) \sim \mathcal{N}(\bar{\mu}_i, \Sigma_i \Sigma_i^T)$$
$$g_i(\mathbf{w}) \sim \mathcal{N}(\mu_i, \sigma_i^2)$$

Each constraint $G_i^T(w)x - g_i(w)$ can be rewritten as:

$$\tilde{w}^T(\Sigma_i^T x - \sigma_i) + \bar{\mu}_i^T x - \mu_i \tag{E.6}$$

We obtain from E.6 via standardization:

$$\begin{aligned}
&\mathbf{P}\left\{G_i^T(w)x - g_i(w) \geq 0\right\} = 1 - \mathbf{P}\left\{G_i^T(w)x - g_i(w) \leq 0\right\} = \\
&= 1 - \mathbf{P}\left\{\frac{G_i^T(w)x - g_i(w) - \bar{\mu}_i^T x + \mu_i}{\|\Sigma_i^T x - \sigma_i\|} \leq \frac{-\bar{\mu}_i^T x + \mu_i}{\|\Sigma_i^T x - \sigma_i\|}\right\} = \\
&= 1 - \Phi\left(\frac{-\bar{\mu}_i^T x + \mu_i}{\|\Sigma_i^T x - \sigma_i\|}\right) = \Phi\left(\frac{\bar{\mu}_i^T x - \mu_i}{\|\Sigma_i^T x - \sigma_i\|}\right)
\end{aligned}$$

where Φ is the standard cumulative distribution function. In conclusion a separate chance constraint of the form described above can be reformulated as a deterministic

second order cone (SOC) constraint:

$$\mathbf{P}\left\{G_i^T(w)x - g_i(w) \geq 0\right\} \geq 1-\alpha \Leftrightarrow \Phi^{-1}(1-\alpha)\|\Sigma_i^T x - \sigma_i\|_2 - \bar{\mu}_i^T x \leq -\mu_i$$
$$\mathbf{P}\left\{G_i^T(w)x - g_i(w) \leq 0\right\} \geq 1-\alpha \Leftrightarrow \Phi^{-1}(1-\alpha)\|\Sigma_i^T x - \sigma_i\|_2 + \bar{\mu}_i^T x \leq \mu_i$$

If $(1-\alpha) > 0.5$ the sets described by the chance constraints are convex, otherwise they are non-convex (see [70], Theorem 2.5).

List of Figures

List of Tables